International Journal of
Young Scientist Research

Vol 5, No2, Dec 2021
ISSN: 2588- 5111

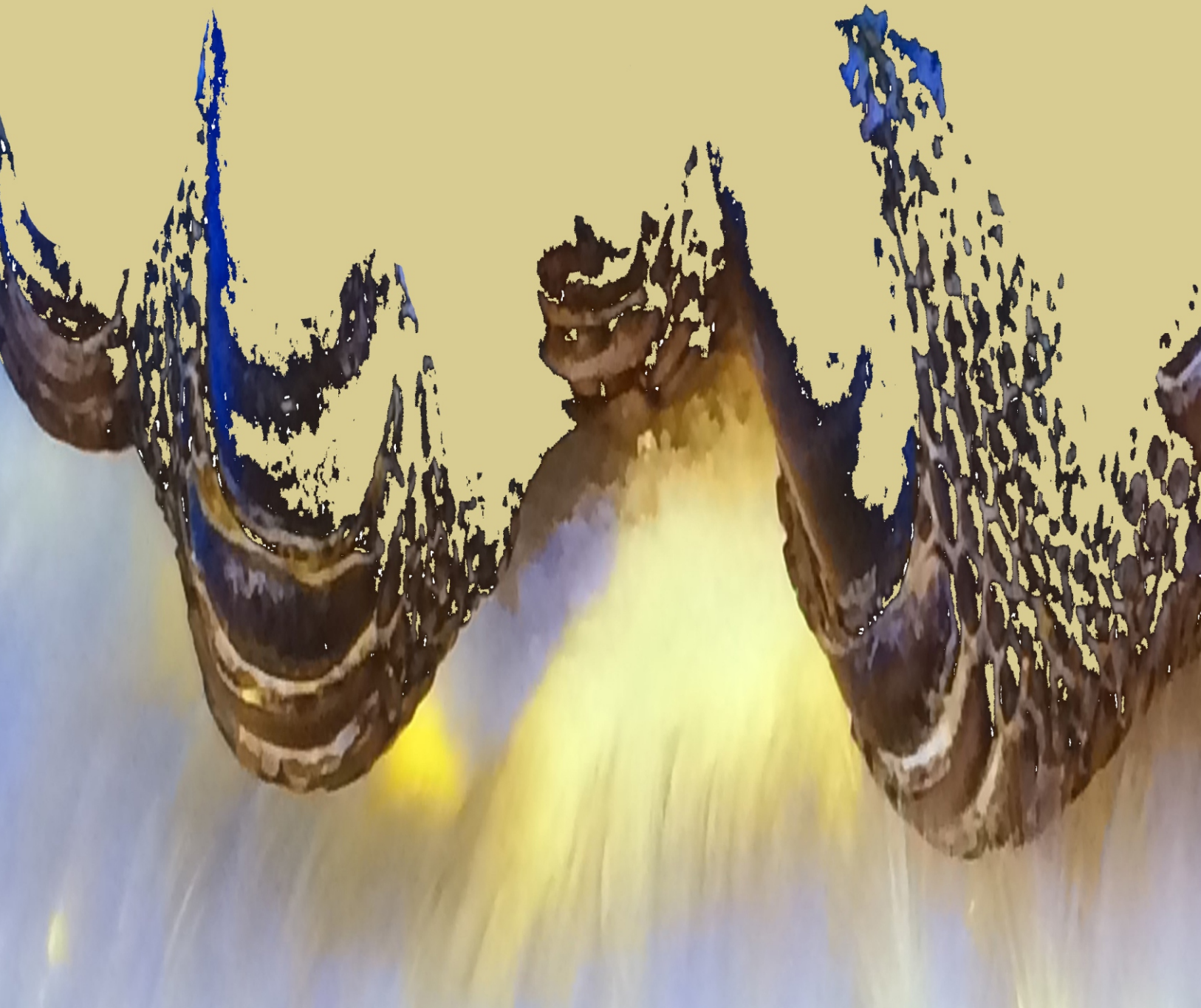

Contents

YOUNG SCIENTIST RESEARCH
Journal in Science Education
ISSN: 2588-5111

Young Scientist Research

Address:

Unit 14, No.32, Malek Ave., Shariati St.
Post Code: 1565843537
Tel:+9821-77507013, 77522395

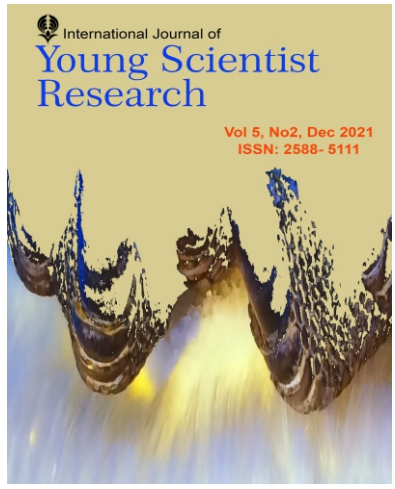

WELCOME TO THE INTERNATIONAL JOURNAL of YOUNG SCIENTIST RESEARCH

Young Scientist Research is a research journal based on scientific projects and we are pleased to present our students' work in scientific activities. This open-access journal includes young students' research in any field of science which publishes full-length and abstract research on any aspects of applied sciences in relation to work presented in both national and international conferences, competitions and tournaments of all types.

Programs that have educational opportunities for high school students to present their distinguished projects from regional, national and international events such as International Conference of Young Scientists (ICYS), International / Persian Young Physicists' Tournament (IYPT/ PYPT), International / Iran Physics' Tournament (IPT/ IRPT), International / Iran Physics' Tournament (IPT/ IRPT), International Music , Science , Engineering Fair (IMSEF).

New manuscripts sent to the Journal will be handled by the Editorial Office who checks compliance with the guidelines to authors. Then a rapid screening process at which stage a decision to reject or to go to full review is made.

By submission of a manuscript to the Journal, all authors warrant that they have the authority to publish the material and that the paper, or one substantially the same, has neither been published previously, nor is being considered for publication elsewhere.

This journal belongs to Ariaian Young Innovative Minds Institute, AYIMI, and one to two issues is published in a year. All details are on the YOUNG SCIENTIST RESEARCH Journal website (http://journal. ayimi.org)

Editor in Chief
Dr. Dina Izadi
Researcher & President of
AYIMI , International Research Institute
ADIB, Cultural and Artistic Institute
http://www.ayimi.org
http://adib.ayimi.org
http://journal.ayimi.org
Email: info@ayimi.org
Unit 14, No. 32, Malek Ave., Shariati St.,
Post Code: 1565843537
Young Scientist Research Journal, ISSN: 2588-5111
Tehran/ Iran

CURRENT ISSUE
Vol 5 NO 2 DEC 2021

Investigation of Looping Pendulum Movements

Rojan Abdollahzade Miralia , Tehran/ Iran, rojan.abzd@gmail.com

ARTICLE INFO

IYPT 2019 Iran Team member in Poland and Winner of Bronze Medal

Accepted in country selection by Ariaian Young Innovative Minds Institute , AYIMI

http://www.ayimi.org ,info@ayimi.org

ABSTRACT

Obviously, a pendulum is a very simple physical object that exhibits periodic movements. We present a physics-based approach to investigate characteristics of looping pendulum movements by several experiments and using tracker for the motion controllers to track in dynamics simulation. To control parameters our motion tracking adopts a method, which computes characters and captures data with real-time response in our experiments. The initial conditions is controlled to get the position of the path of both masses and the most important parameters radius and angle of the light mass and distance of the heavy mass from the origin are investigated.

Key Words *: pendulum , simulation, mass, radius, angle*

1 Introduction

A simple pendulum is composed of a weight, or bob, hanging freely from the end of a string or bar. Gravity pulls the bob in a downward arc, causing it to swing. There are different types of pendulum. Foucault pendulum swings in two dimensions is a type of simple pendulum, which demonstrates the rotation of the earth. Once the Foucault pendulum is set in motion, its swing will tend to rotate clockwise in a circle over the course of about a day and a half. Double pendulum, which is called a chaotic pendulum, consists of two simple pendulums, one suspended from the other. Double pendulums are used primarily in mathematical simulations. Conical pendulum, which was studied by Robert Hooke, is used to analyze the planets' orbital motions.

A looping pendulum consists of two loads, one heavy and one light, with a string over a horizontal rod. By pulling down the light one, the heavy load will lift up and by releasing the light load; it sweeps around the rod and keeps the heavy load from falling to the ground. If observers are able to use it, allow accurate estimation of looping pendulum parameters such as length or period in this study as linear functions or interpreting the results. Together with statements made during experiments we are showing that the rules are affecting the length is a linear function of 'speed', where speed appears to be a function of both period and angular velocity and so on.

2 Experimental Setup

According to the structure of looping pendulum, our experimental setup was installed and then tracked the motion of the masses, to investigate the important parameters affecting on this phenomenon (Fig. 1a,b and c).

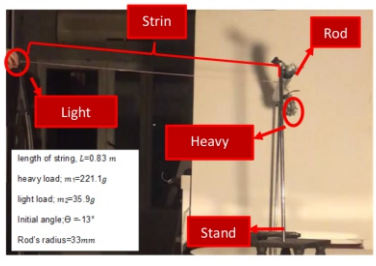

(a)

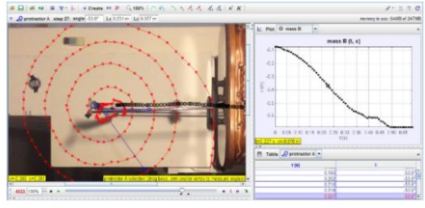

(b)

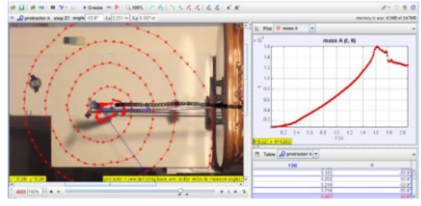

(c)

Fig. 1: a) Experimental setup; b) and c) tracking the motion of two masses A and B

In order to investigate the motion of the light mass we can define the vectors in the cross section of the rod $\hat{e}_r$ which is proportional to the radius of the rod and $\hat{e}_\theta$ which is in the direction of the string connected to the mass (Fig.2). For finding the position of the mass, we can use the $\vec{r}$ where it can be written as a function of the unit vectors (Eq. 1):

$$\vec{r} = R\hat{e}_r + x\hat{e}_\theta \quad (1)$$

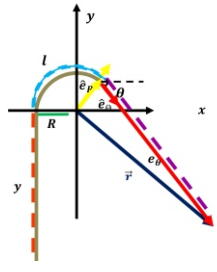

Fig. 2: Vectors in the cross section of the rod

3 Theories and Modeling

The acceleration of the mass is the second derivation of the vector $\vec{r}$ which consist of different terms of acceleration (Eq. 2).

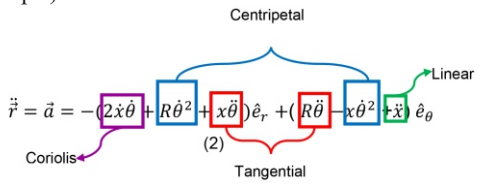

$$\ddot{\vec{r}} = \vec{a} = -(2\dot{x}\dot{\theta} + R\dot{\theta}^2 + x\ddot{\theta})\hat{e}_r + (R\ddot{\theta} - x\dot{\theta}^2 + \ddot{x})\,\hat{e}_\theta \quad (2)$$

We have four terms of acceleration in this system: Coriolis, centripetal, tangential and linear acceleration. By all the forces applying to the mass in the direction of $\hat{e}_\theta$ and $\hat{e}_r$ (Fig. 3); we can write the newton's second law of motion in both directions (Eq. 3 & 4).

$$\frac{-w_2 \cos\theta}{m_2} = -(\dot{x}\dot{\theta} + R\dot{\theta}^2 + x\ddot{\theta}) \quad (3)$$

$$\frac{w_2 \sin\theta - T_2}{m_2} = R\ddot{\theta} - x\dot{\theta}^2 + \ddot{x} \quad (4)$$

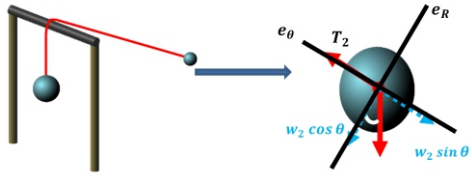

Fig. 3: The components of vectors on light mass

To solve these equations, the motion of the heavy mass in our system should be settled down.

Based on the behavior of the heavy mass we can divide the whole procedure into two phases:

1-The steady phase: both masses are moving and the string is sliding on the surface of riding, which means there is kinetic friction (Fig. 4a).

2-The motion phase: the heavy mass is at rest and we have static friction between the string and the rod (Fig.4b).

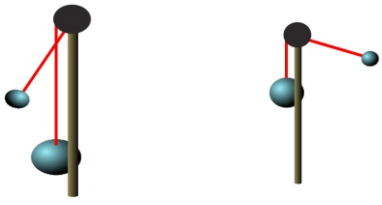

Fig. 4: a) The steady phase b) The sliding phase

The newton's second law is written for the heavy mass (Eq. 5 and 6) (Fig. 5):

$$w_1 - T_1 = m_1 a \quad (5)$$

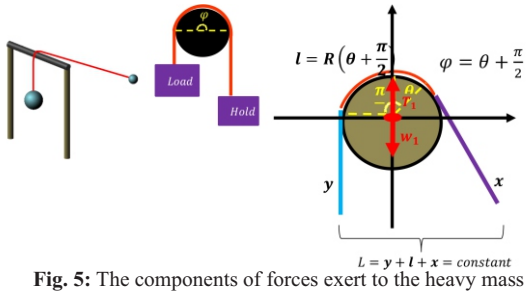

Fig. 5: The components of forces exert to the heavy mass

$$w_1 - T_1 = m_1(-\ddot{l} - \ddot{x}) \quad (6)$$

where the w_1 is the mass and T_1 is the tension force. The acceleration ıs found by assuming the string is always completely stretched without no extension so the length of the string remains constant. In sliding phase, we can write (Eq. 7, 8 and 9):

$$\frac{-w_2 \cos\theta}{m_2} = -(\dot{x}\dot{\theta} + R\dot{\theta}^2 + x\ddot{\theta}) \quad (7)$$

$$\frac{w_2 \sin\theta - T_2}{m_2} = R\ddot{\theta} - x\dot{\theta}^2 + \ddot{x} \quad (8)$$

$$l = R\left(\theta + \frac{\pi}{2}\right) \quad , \varphi = \theta + \frac{\pi}{2} \quad (9)$$

We can also relate the tension forces using the capstan equation (Eq. 10):

$$T_1 = T_2 e^{\mu(\theta + \frac{\pi}{2})} \quad (10)$$

Using numerical model, these equations are solved for the sliding phase (Fig. 6).

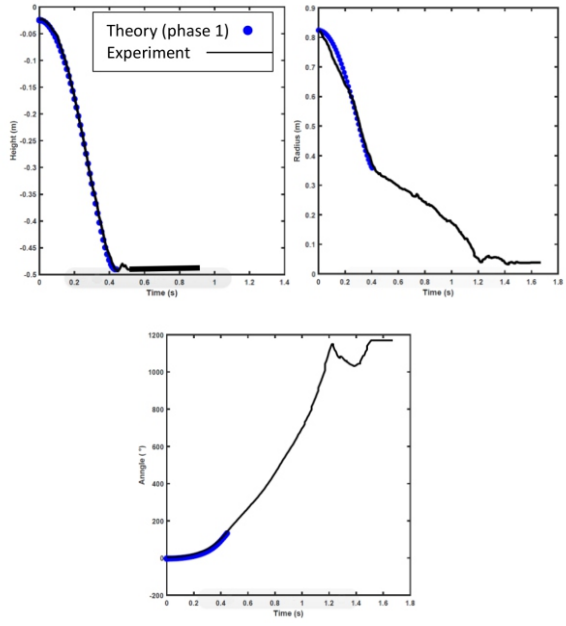

Fig. 6: The changes of height, radius and angle versus time in the sliding phase

L=0.83 m, $m1$=221.1g, $m2$=35.9g
Initial angle=-3°,Rod's radius=33mm
μ = 0.29

In the steady phase, we cannot use the capstan equation because there is no kinetic friction between the surface of the rod and the string. Since the heavy mass is at rest, the height of the heavy mass is constant and we will have the following equation (Eq. 11 and 12):

$$L = x + l + y,\ \dot{x} + \dot{l} = 0,\ \dot{x} = -\dot{l} \quad (11)$$

$$T_1 < T_2 e^{\mu(\theta + \frac{\pi}{2})} \quad (12)$$

Now we can compare our theory and experimental results (Fig. 7).

The coefficient of friction is an important parameter and it can change the behavior of the masses and the whole function of the system. We have calculated the μ using two

different approaches; first by fitting the theoretical predictions and experimental results in different conditions and second by tracking the motion.

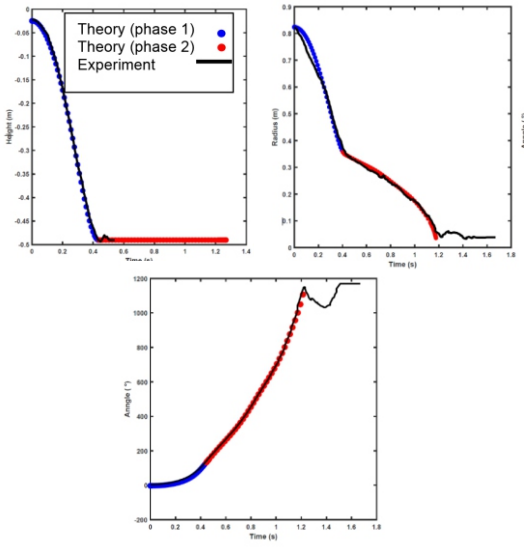

Fig. 7: The changes of height, radius and angle versus time in the steady state

L=0.83 m, $m1$=221.1g, $m2$=35.9g
Initial angle=-3°,Rod's radius=33mm
μ = 0.29

If we track the motion of a mass which is connected to the string and is sliding downward, we can find the coefficient of friction due to the acceleration of mass in different angles (Fig. 8).

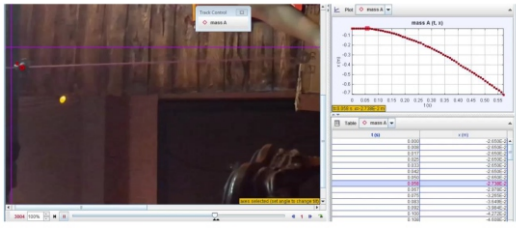

Fig. 8: Tracking the motion of mass to find the coefficient of friction

and by comparing the results we can see a great agreement (Eq. 13):

$$\mu_E = 0.31 \pm 0.03,\ \mu_f = 0.29,\ \mu_E \approx \mu_f \qquad (13)$$

We have also investigated the effect of the μ on the total number of turns on the rod (Fig. 9).

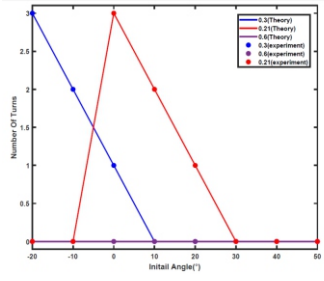

Fig. 9: Comparing the effect of μ in number of turns versus angle, experimental and theoretical

The path of the light mass is shown in figure (10) which is compared with the theoretical predictions.

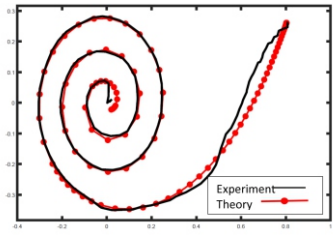

Fig. 10: The path of the light mass , comparing experiment and theory

The path in the second phase is an Archimedes spiral with the following equation:

$$y = bx\ sin(a + x) \qquad (14)$$

where a defines the orientation and is proportional to the initial releasing angle and the b Which is the tightness and it depends on the radius of the rod.
Now we want to investigate the effect of the mass ratio on the motion on the heavy mass (Fig.11).

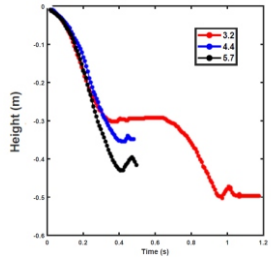

Fig. 11: The effect of the mass ratio on heavy mass

In figure (11), the height of the heavy mass is a function of time for different mass ratios. By decreasing the mass ratio, the minimum height will decrease and after a critical point, the heavy mass will move twice, after it comes at rest for the first time it starts moving downward again and it stops afterwards (Fig. 12).

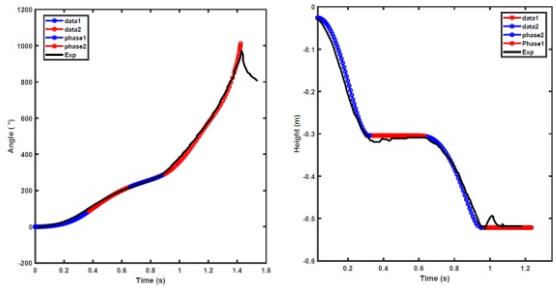

Fig. 12: . Returning Condition

The reason for the special returning condition is that when the light mass moves downward its acceleration will increase and the tension force will increase as a result so it will keep the heavy load. As the light load continues looping it will move upward and while the acceleration is decreasing the tension force will decrease too and the heavy mass will start moving again.

4 Discussion and conclusions

We have four different conditions for the system that under each circumstances we can observe a new behavior from the masses. Using the simulation results based on our

theory we can compare the difference between experimental and theoretical results in different conditions (Fig. 13).

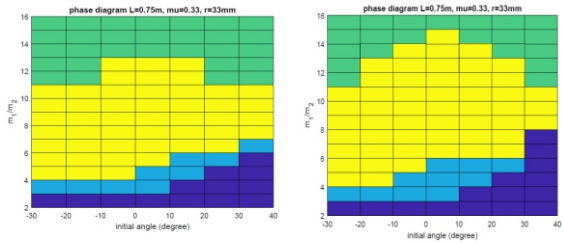

(a) (b)

Fig. 13: Comparing different conditions; a) Simulation, b) Experiment

Explanation of each color in figure (14);
- Dark blue: the initial conditions are not providing the needed energy for the first loop so the mass will fall off.
- Light blue: special returning condition happens and the heavy mass will be kept.
- Yellow: the light mass will loop around the rod and keep the heavy mass.
- Green: the light load will sweep around the rod and then will unloop and fall over the ground.

When the light mass comes at rest at the end, the magnitude of tension force will decrease and the load cannot keep the heavy load from falling anymore and this is the main reason for the special condition in green region in figure (14).

References

[1] D.Halliday , R.Resnick ,J.Walker. Fundamentals of Physics. John Wiley & Sons. (1923)

[2] https://sciencing.com/history-pendulum-4965313.html

[3] https://sciencedemonstrations.fas.harvard.edu/presentations/rope-friction-aroundpole

[4] wikipedia.org/wiki/Capstan_equation

[5] www.stevespanglerscience.com/lab/experiments/magic-pendulum/

[6] looping_pendulum_2_bil.pdf, https://www.istitutotrento5.it/images/test/bre_15_16

Asteroid Classification Using Multilayer Perceptron

Zhina Babania, Farzanegan 1 high School: zhinababania2006@gmail.com

ARTICLE INFO

Gold Medalist in IMSEF 2021 , Izmir, Turkey

Supervisors: Melika Ayoughi, Amirahmad Barekatein

Accepted in country selection by Ariaian Young Innovative Minds Institute , AYIMI

http://www.ayimi.org ,info@ayimi.org

ABSTRACT

Have you ever thought about the destruction of mankind? What causes the destruction of the planet earth? Can we examine one of them? Is there a way to prevent the destruction of the Earth? In this project asteroids are investigated. . A key element of this idea is the new structure of the information processing system. The system consists of a large number of highly interconnected processing elements, called neurons, which work together to solve a problem. We have used python as the programming language to implement the model.

Key Words: *planet earth, asteroids , processing*

1 Introduction

Asteroids play a vital role in the future of humanity, and scientists have shown great attention to them. Asteroids are important for three reasons. The first and most important reason is that they may have been sent by aliens; such as the Oumuamua asteroid, which has been the subject of much debate. The second reason is the possibility that human life continues after the destruction of the planet with the help of asteroids (of course it is not possible to live on asteroids, but it is possible with our knowledge about them, we may be able to reach other planets that are also in the solar system). The third reason is that asteroids can collide with the earth like meteorites and destroy it.

What is our problem? In this project, an attempt has been made to use Python programming language with a computer neural network algorithm to create a program to prevent and threaten the extinction of the Earth's orbit by examining and predicting the most important features of asteroids, and this can answer to some extent. "Are we alone in the world?".

What are our goals now? Building a program to identify and predict the properties of asteroids (large half-diameters), as well as learning more about the space and world we live in, learning about the computer neural network in Python, and encouraging others to Follow up on the possibility of Earth being destroyed by asteroids and becoming interested in knowing one of the types of celestial bodies in space.

In the field of knowledge, we should have some astronomical information about asteroids, which also includes the characteristics of asteroids. Next we need to know enough about the neural network, which is actually our research method as well as programming, because in this project I used the Python programming language, so we need to know Python very well, which includes a number of libraries. Python is important and finally we must know how to make software with Python so that we can create a good relationship between the program and the user.

1-1 Asteroid Criticism

Why asteroid criticism is important to us. Asteroids play a key role in the future of humanity, and scientists have paid close attention to them. Asteroids are important for three main reasons. The first and most important reason is that they may have been sent by aliens, or in fact the same aliens, to spy on Earth (like the much-discussed asteroid Amu Amua). The second reason is the possibility of human life after the destruction of the Earth with the help of asteroids (of course, life on asteroids is not possible, but with proper knowledge of them, other planets can be found for life). The third reason is that asteroids can hit the earth like meteors and destroy it.

Destroying asteroids is not so easy and we must have a lot of information about them to be able to prevent their damage. As you can see, if we try to destroy asteroids with nuclear energy, they will become a large number of little asteroids (Fig.1).

Fig. 1: The importance of Asteroids

1-2 Characteristics of Asteroids

Some important features of asteroids, such as Elliptic orbit by eccentricity, perihelion distance and Longitude of the ascending node are shown in figure (2). By using these features we can be able to predict semi-major axis.

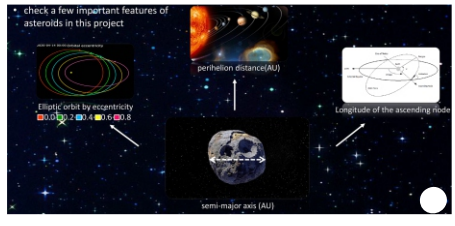

Fig. 2: Some important features of asteroids

1-3 Data in NASA about Asteroid

In 2013, NASA introduced the "Big Asteroid Challenge", to be more prepared for such events. One of the activities offered in this challenge was to collect information about a large number of asteroids in the Solar System and to study the construction of bands for detecting asteroids. Finding out the material composition of the asteroids is also helpful before deciding which strategy is appropriate and what to expect. In this work, we investigate the hypothesis of some scientists about the connection between the destruction of the Earth and asteroids. For this reason, we are using the data collected by NASA about all discovered asteroids (approximately 839737 asteroids).

In this dataset we have features of each asteroid like location, components, and so much more. We adopt a machine learning method to classify asteroids based on these features. Artificial intelligence (AI) is a branch of computer science whose main purpose is to produce intelligent machines capable of performing tasks requiring human intelligence. We have trained neural networks for our asteroid classification task. A neural network is an idea for information processing inspired by the biological nervous system, which processes information like the brain.

I found 2 projects similar to my own project. One is the NASA project. Well, in fact, my project is made easier by the inconvenient project. Since 2013, NASA has categorized all asteroids and predicted all their features; But NASA came to do this, built a robot (I did not write a program) and its activities are still going on. But the good thing about my project is that anyone who is interested in the field of astronomy and asteroids, can easily work with it and does not require any special expertise. It is already available. However, the NASA robot is limited to its own members and the accessibility is a bit tricky. I also found an article that dealt with the same classification of asteroids, but its method and databset were different from mine, and of course its output was different from mine, and this person did not write a program like me at all, as if it were a research on Classification of asteroids done.

2 Methods

Our research method is with neural networks. A neural network is an idea for information processing inspired by a biological nervous system that processes information like the brain. The main element of this idea is the new structure of the information processing system. This system is made up of a large number of interconnected processing elements called neurons that work together to solve problems.

Well now in this project we get a machine learning method for predicting the large half diameter of an asteroid based on input characteristics. Artificial intelligence, or AI, is a branch of computer science that aims to produce intelligent machines capable of performing tasks that require human intelligence. Then we came here to train neural networks for our asteroid task (Fig. 3).

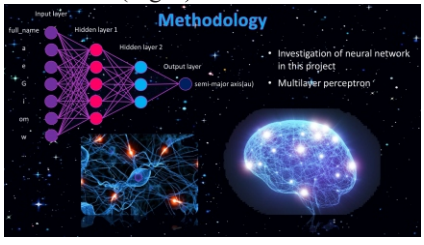

Fig. 3: Methodology

Regarding why we used multilayer perceptron, I must say that: There are different ways to categorize data. Now that we wanted to use artificial intelligence and neural networks, the simplest way we could get good results is multilayer perceptron, When we arrived, we selected two neural layers consisting of several neurons, which are sigmoid and relu.

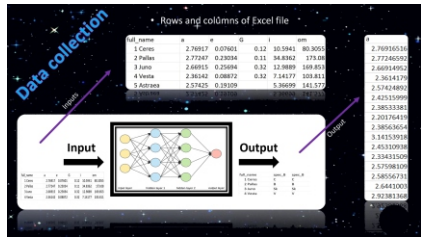

Fig. 4: Data Collection

We have used python as the programming language to implement the model. The libraries which we have primarily used in python are NumPy and pandas for data analyzing, sklearn for pre-processing, implementing the dense layers and model evaluation, matplotlib and seaborn for data visualization and we used Tkinter to build the app. We also used keras , tensorflow and xlrd for the other part of our program.

Now we want to show what it looks like when we run the program: Well! When we run the program, a window called AI opens for us. To use the program, we have to click on the Browse button (browse) exactly as shown in Figure 1, and then we have to select the Excel file we want. Then, this link comes up, we have to click on the Press button. Now the program starts running, but due to the large size of the Excel file, our program takes a while. When the program is completely run, 5 Excel files are saved in a folder called CSV and we can see the program output.

3 Results and Conclusions

In summary: In this work we discussed asteroids and why it is important to learn more about them and predict their properties, and we also used data provided by NASA on about eight hundred thousand asteroids and their characteristics. . In our project, we chose a two-layer neural network that predicts a large half-diameter with relatively high accuracy due to a set of asteroid features that are about twenty. And finally, we will easily complete our program in the form of a few Excel files that are our output.

In this project, like many other projects, there were some limitations, for example, because I did not have all the information about the asteroids, so it made it harder for me to write a program, and it took me a long time to program.

Other than that, many asteroids have not yet been discovered at all, and if they had been discovered, my program could have run much better now. Well, the next limitation was that I could not use all the properties of asteroids like the ones I showed in this photo, because being a string means being a set of letters and not a number, and my program can only categorize and predict based on a set of numbers not strings. The last limitation of my program was that because I coded in Python, the program crashes and runs slower than other programming languages such as C ++. But the slowness of the program is natural. It is a heavy program as well.

Now, if we want to look at the future of the project, for example, we can predict other features of the asteroid

instead of the large half-diameter. We can also work with nebulae, stars or planets instead of asteroids, or we can even use different subjects instead of astronomy.

References

[1] Available: https:// www. sarpoosh. com/ science/ scientific articles/ extinction dinosaurs earth 980623 html.

[2] C.Q. Choi , " Asteroids: Fun Facts and Information About Asteroids," 20 Sep 2017 . Online]. Available: https:// www. space. com/ 51 asteroids formation discovery and exploration. html. [Accessed 19 12 2019.

[3] Deep Asteroid," Open Nasa, [Online]. Available: https:// open. nasa. gov/ innovation space/ deep asteroid/. [Accessed 7 11 1398.

[4] NASA Asteroid Classification," [Online]. Available: https:// towardsdatascience. com/ nasa asteroid classification 6949 bda 3 b 1 da.

SYNCHRONIZED CANDLES

Tahmineh Lohrasbi , Farzanegan 7 high school, Tehran/ Iran, tahminehlohrasbi1383@gmail.com

ARTICLE INFO

Participated in IYPT 2021 , Georgia, Tibilisi and Silver Medalist in IMSEF 2021

Accepted in country selection by Ariaian Young Innovative Minds Institute , AYIMI

http://www.ayimi.org ,info@ayimi.org

ABSTRACT

In this essay, Oscillatory flames which are observed when several candles burn next to each other. are investigated. Depending on the distance between the sets of candles two such oscillators can couple with each other, resulting in in-phase or anti-phase synchronization. We are going to find how the flames work and type of flames and relevant parameters.

Key Words: *Candles, flames, Oscillation, synchronization,*

1 Introduction

In general, heat is transferred through three methods of conduction, radiation and convection. The heat of the flame melts the paraffin of the candle due to its conduction. Melted paraffin rises from the candle wick due to its capillary properties. On the other hand, hot air rises around the flame. The volume of hot air is more than the volume of cold air and its density is less it is from the density of cold air. When hot air loses temperature, it cools down and cold air because of more density is being pulled down by gravity, and this heat transfer current continues, which is called convection. Radiation is another type of heat transfer that takes place through electromagnetic waves. In this study, loss is the most important factor. On the other hand, due to burning paraffin, carbon monoxide, carbon dioxide and water vapor, we produce Exhaust of these light gases causes the tip of the flame to stretch (Fig. 1).

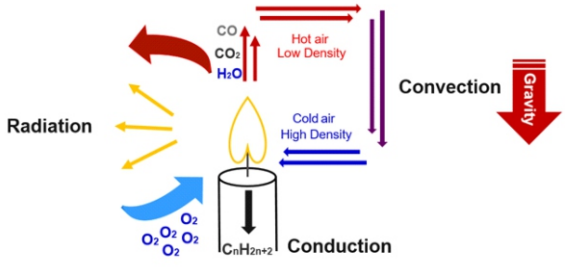

Fig. 1: Heat Transfer

2 Main Concepts

2-1 How do Flames Work and Merge?

The convection between two flames is the reason of coupling (Fig. 2). When we put two flames together, the convection flow around them continues and on the other hand, the air between the two the hotter the flame, the faster the exit and the lower the pressure. The air around the flame, which has a lower temperature and more pressure, causes it to close or so-called coupling . In this condition three types of behavior are observed, non oscillation, coordinated oscillation and uncoordinated oscillation.

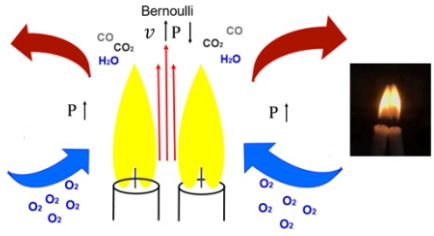

Fig. 2: The convection between two flames is the reason of coupling

2-2 Types of Behavior Observed:

In non oscillation flames there are two modes: Stable and Death modes (Fig. 3 a & b).

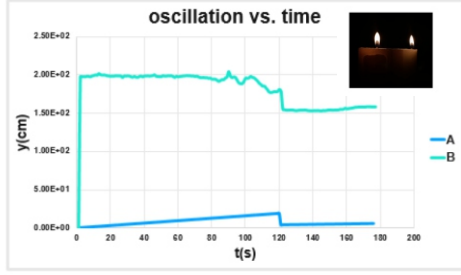

(a)

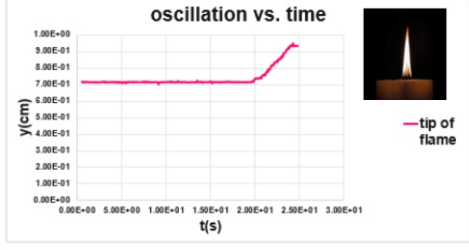

(b)

Fig. 3: Two modes in non oscillation flames, a) Stable mode; b) Death mode

In Coordinated Oscillation there are in-phase and Mexican wave modes (Fig. 4a and b).

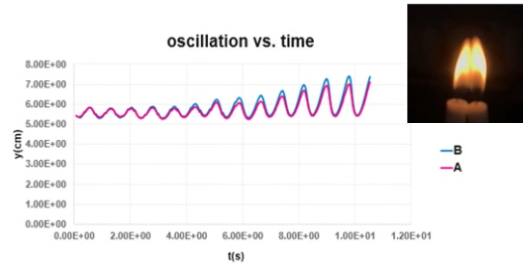

(a)

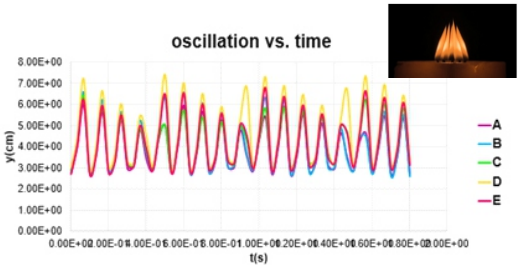

(b)

Fig. 4: Two modes in coordinated oscillation flames, a) in- phase mode; b)Mexican wave mode

In Uncoordinated Oscillation we have anti-phase and desynchronized modes (Fig. 5a and b).

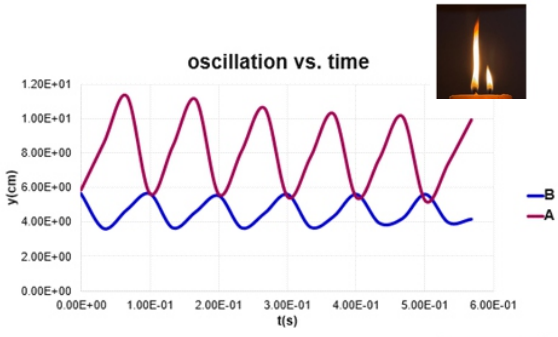

(a)

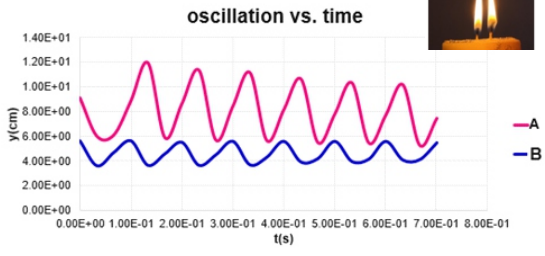

(b)

Fig. 5: Two modes in uncoordinated oscillation flames, a) anti-phase mode; desynchronized mode

3 Materials and Methods

Before starting the experiment, the effective components in the phenomenon such as Number of Flames, Distance between them, Layout and Flame Level are defined. In our experiments wick thickness and Paraffin/Flame sources other than candles are investigated too.

4 Experimental Setup

To prevent the flames from disintegrating, the test space should be kept away from wind and any open air flow. To better see the flames and make the imaging clearer, the experiments were performed in a dark room and also behind the flames were also blacked out to obtain the desired distance at which the phenomenon is observed. First the flames were kept at a distance of 50 mm. They were placed together, but at this distance, the phenomenon was not observed and the distance of the flames was reduced by repeated experiments. The flames flickered at a distance of 9 mm, and at a distance of 8 mm, the desired result (flame synchronization) was obtained and when the flames got closer, they became one and behaved like a single flame (Fig. 6).

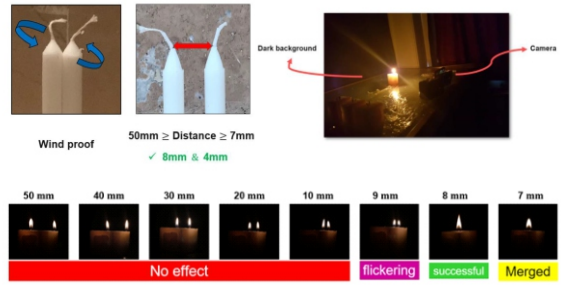

Fig. 6: Experimental Setup with candles in different distances

4-1 Two Candles: in Phase Oscillation

In the first experiment, two candles of the same size were placed at a distance of 8 mm. Due to the symmetry of the flame position, the fresh air which enters and the hot air comes out are the same and there is convection flow around them. The same thing happened and caused flames have in-phase oscillations that with increasing time, their amplitude of oscillation also increased and reached Mexican wave mode. Tracker and Excel software was used to obtain the diagram of all fluctuations (Fig. 7).

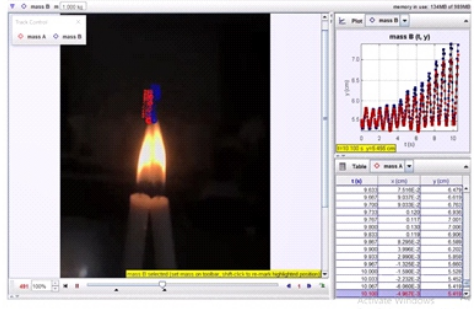

Fig. 7: Two candles in phase oscillation (d= 8mm)

As it is seen the amplitude of the oscillation increases in both phase and Mexican wave modes. These two modes are annualized by the FOURIER Transformation (Fig. 8).

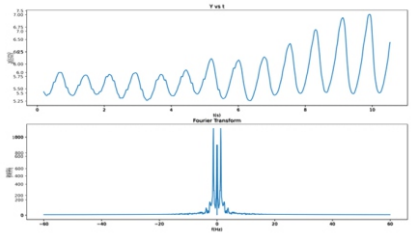

Fig. 8: Fourier Transformation, Peak frequency in two candles: A: 1.25806452; B: 1.25806452

4-2 Two Candles: Desynchronized Mode

In the second experiment, two flames of the same size on the left and another flame of the same size at a distance of 8mm were placed . Due to the fact that the temperature of the two flames on the left was higher than the single flame on the side Right, the flow around them was uneven, fresh air entering the flames and leaving the hot air was not the same between the flames. This caused the flames to oscillate out of phase.

Two flames generate more heat than one flame. Thus there is a stronger and faster convection flow. Since the two flames don't have similar shape, anti-phase oscillation happens . It is analyzed by Fourier Transformation to find the maximum peak (Fig. 9).

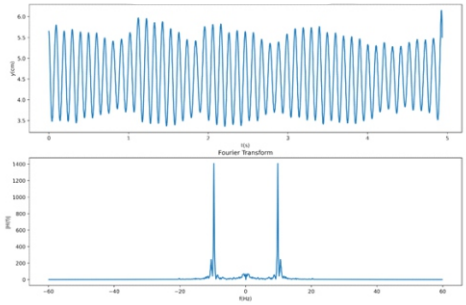

Fig. 9: Peak frequency: A: 9.72000972; B: 9.72000972

4-3 Candles in Anti Phase Mode

In the third experiment, two flames of the same size were placed at a distance of 8 mm. This time the wick sizes were fixed and the length of the right wick was 5 mm longer than the left wick. Due to the difference in the level of the flames, the convection flow around them was uneven and since the two flames did not have the same shape, this caused the flames have asynchronous oscillations (Fig. 10).

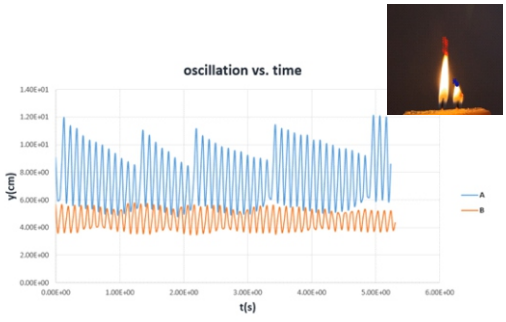

Fig 10: Anti Phase mode

The amplitude of the oscillations are short with different wavelengths (Fig. 11 a and b).

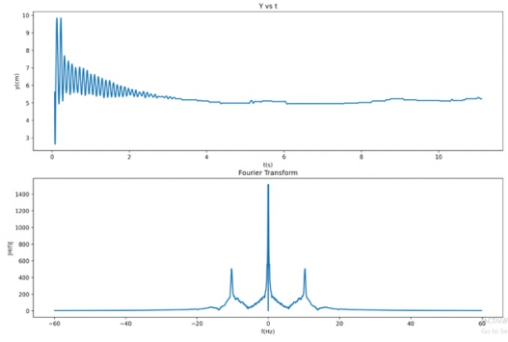

(a)

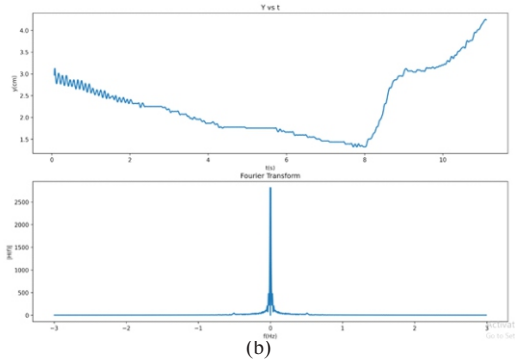

(b)

Fig. 11: Peak frequency; a) A: 0.09053022 and 0.18106044 b) B: 0.00452651 and -0.00452651

5 Comparison of the Setups

By comparing the diagrams, we found that whenever the wicks are in the same condition and at the desired distance, the oscillation is in harmony, but if the flames deviate from the symmetrical state and in different conditions such as temperature, fresh air and light gases between the flames it will be out of symmetry and there is inconsistency. So there are coordinated and uncoordinated oscillations (Fig. 12).

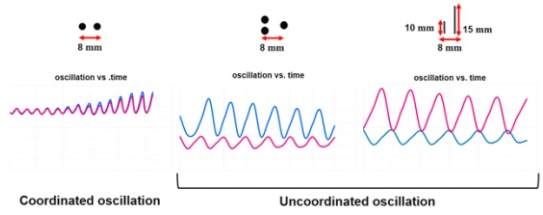

Fig. 12: Comparison of the setups

6 Making the Candles and Layout Design

The candles had to be cut to reach the desired distance for several arrangements. Therefore, special candles for this research and frequent experiments were made (Fig. 13). For proper design, the experiment first started with two wicks and the number of wicks increased and it was observed that the best result is given by five wicks.

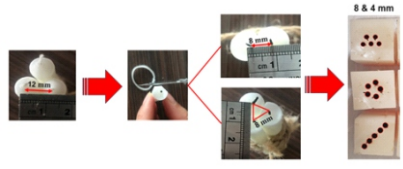

Fig. 13: Making different candles

To design the flame arrangement, the flames were first placed symmetrically pentagonal and round, and then they were arranged in a line next to each other, and at the end, the situation was the same as the previous two arrangements Trapezius. These arrangements were tested at two optimal distances of 8mm and 4 mm (Fig. 14).

Fig. 14: Layout Designs

7 Experiment in Symmetry Situation

In this experiment, the flames of the same size were placed at a distance of 8 mm from each other (Fig. 15). Symmetry of the flames, fresh air entering the flames and hot air leaving from between them, the intensity and speed of convection, the difference in temperature, volume and pressure around the flames and inside them all caused:

- The flames have short-phase oscillations with short wavelengths and amplitude due to the high heat from the very beginning.
- Their oscillation was high and they had a Mexican wave state.

Tracker and Excel software were used to obtain diagrams of all fluctuations and Python program is used to find their frequencies .

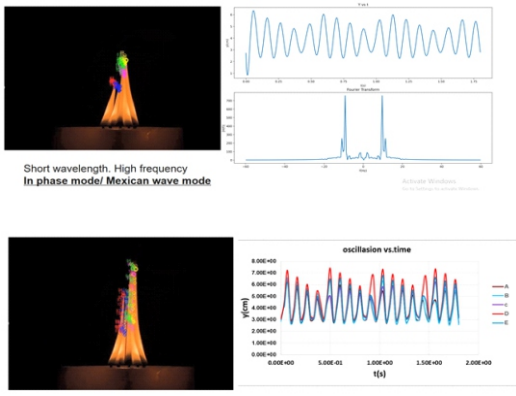

Fig 15: The oscillation in Mexican Wave (Peak: 9.43500944 cm)

In the next experiment, the flames of the same size were placed at a distance of 4mm from each other with short-phase oscillations and wavelengths . In this situation they seems calmer (Fig. 16).

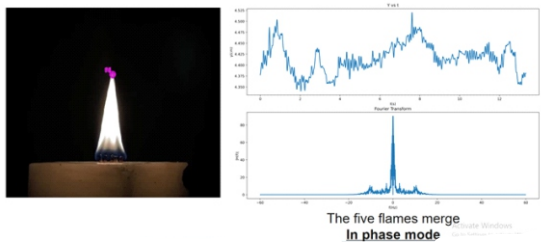

Fig 16: The oscillation in phase mode (Peak: 0.07511286 cm)

Then ;

- The same volume of fresh air entering.
- Hot air exits from the center of the candles.
- Because of the same volume of the air entering, there are same convection for each flames, so they couple equally and we have in-phase.
- In this layout they merged and act like one stable flame so we have stable form.

In other experiment, flames of the same size set side by side at a distance of 8mm and then in trapezoid shape. The condition of the flames is the same, fresh air enters the flames and hot air leaves between the two flames and intensity and the velocity of convection around the flames, which was the same, caused:

in the first shape some flames are almost without oscillation; some of them are in phase oscillations and some in non-simultaneous oscillations. Their wavelength was short and their oscillation amplitude was generally low and high in some parts (Fig. 17) .But in second one The tips of the flames should overlap; some flames had almost no oscillation and some oscillated in phase; their wavelength was short and their oscillation range was generally high (Fig. 18).

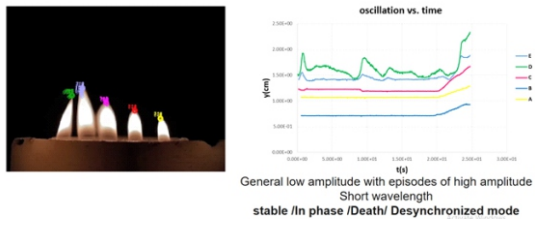

Fig. 17: flames of the same size set side by side at a distance of 8mm

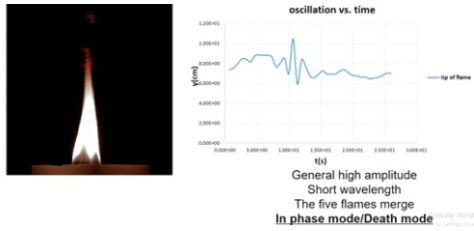

Fig. 18: flames of the same size set in trapezoid shape at a distance of 8mm

When the flames of the same size were placed side by side at a distance of 4 mm in a row fluctuated in both Mexican phase and wave state.Their wavelength is short and their oscillation amplitude was high (Fig. 19) and in trapezoid shape the tips of the flames should overlap; the flames fluctuate in phase; their wavelength are short and their oscillation range is variable (Fig. 20).

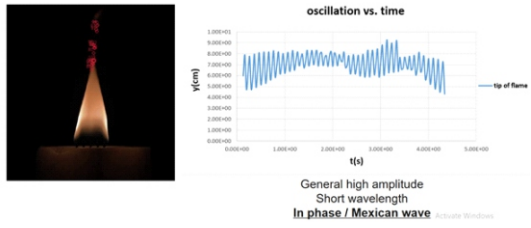

Fig. 19: In phase and Mexican Wave in flames in a distance of 4 mm

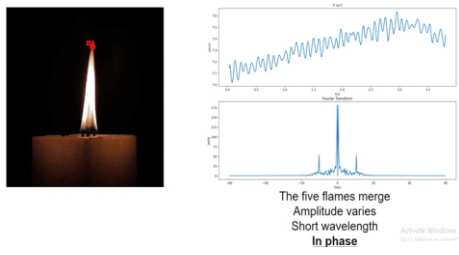

Fig. 20: In phase Wave, flames in a distance of 4 mm but with trapezoid shape

In candles set side by side:

- Hot air exits from the space between each two candles
- More air enters through asides of this layout so they are stable, but in the middle the flow of air enters from 2 sides

so it oscillates faster to suck more volume of air (Fig. 21).

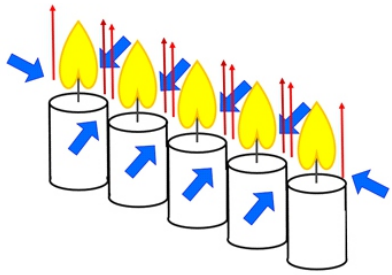

Fig 21: The oscillation in candles side by side

But in candles with trapezoid shape:
-The same volume of fresh air entering from all sides
- Hot air exits from the center of the candles
- Difference in the temperature, volume and air pressure around the flames cause the air to be sucked inside the flame arrangement and it is in phase and stable (Fig. 22).

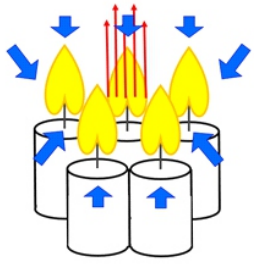

Fig 22: The oscillation in phase mode with candles in trapezoid arrangement

8 Wick Thickness

In order to observe the effect of wick thickness in this phenomenon, all arrangements made with wick with a diameter of 2 mm and 4mm (Fig. 23). Due to the intense heat, the following results was obtained:
- The candle melts faster and more
- It generates more soot and smoke
- The Combination of the states, death and the Mexican wave mode is observed

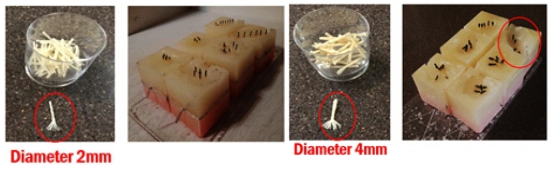

Fig. 23: Candles with different wicks

9 Conclusions

Air flow is symmetric in a single flame arrangement. So we it is a stable flame (Fig 24).

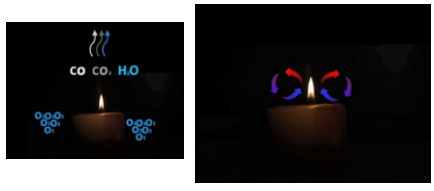

Fig. 24: Stable flame

Mexican wave is same as in phase mode but with short wavelength and High frequency (Fig. 25).

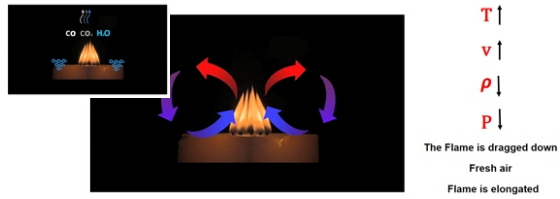

Fig. 25: Mexican Wave

When oscillations stop and show a long and slender shape, we call it Death mode . The flow of the rising hot air causes the flame to elongate (Fig. 26).

Fig. 26: Death Mode Wave

Difference of temperature causes a difference in pressure so we observe asymmetry in the flames, Anti-Phase mode / Desynchronized (Fig. 27).

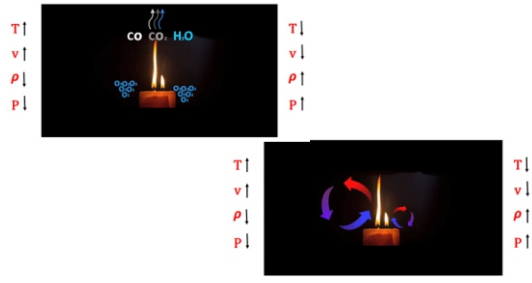

Fig. 27: Anti-Phase mode / Desynchronized

In these experiments the behavior of flames in versus different parameters were observed and analyzed (Fig. 28).

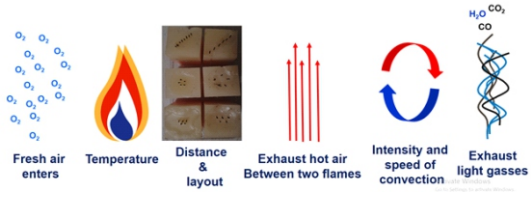

Fig. 28: Different parameters in our experiments were analyzed

Number of Flames which increased hot air and convection speed

Distance:

It was observed in the specific range of 8 mm, with the occurrence of no coupling above and merging below that range.

Layout which causes:
Difference in the volume of fresh air entering
Difference in light gas emission rate
Difference in types of flame and oscillation

Flame Level: Causes the difference in temperature and air pressure around the flame and finally the phase difference.
Wick Thickness: causes more paraffin melts

References

[1] Krishna Manoj, Samadhan A. Pawar & R. I. Sujith , " Experimental Evidence of Amplitude Death and Phase-Fl IP Bifurcation between In-Phase and Anti-Phase Synchronization" ,Nature magazine, Scientific Reports volume8, Articlenumber:11626 (2018).

[2] Keiko Okamoto, Akifumi Kijima, Yoshitaka Umeno & Hiroyuki Shima,"Synchronization in flickering of three-coupled candle flames", Scientific Reports volume 6, Article number: 36145 (2016).

[3] Ting Chen, Xiao Guo, Ji Jia & Jinghua Xiao ," Frequency and Phase Characteristics of Candle Flame Oscillation", Scientific Reports volume 9, Article number: 342 (2019)

[4] Keiko Okamoto, Akifumi Kijima,Yoshitaka Umeno, Hiroyuki Shima ," Synchronization in flickering of three-coupled candle flames", Scientific Reports 6(1):36145

Development of a Communication and Control System Using Eye Tracking for Physically Disabled People

Begüm Atay , Şehit Prof. Dr. İlhan Varank Bilim ve Sanat Merkezi, Turkey
begum.atay0106@gmail.com

ARTICLE INFO

Gold medalist in IMSEF 2021 and Silver medalist in ISAC Olympiad2021
Advisor: Nihal Arı Korkusuz
Accepted by Ariaian Young Innovative Minds Institute,AYIMI

http://www.ayimi.org , info@ayimi.org

ABSTRACT

This study aims to provide opportunities for physically disabled individuals (paralysis, limb deficiencies, Parkinson's, ALS, etc.) to meet specific needs independently in daily life, to communicate, to inform about emergency; and facilitate their care. The system was developed with Python programming language. Commands are on the home page and classified as house control and needs. The system was tested with a house prototype which consisted of servo motors, an LED and a fan controlled by Raspberry Pi.

Key words: *Barrier-free technologies, eye tracking system, image processing, Python, Raspberry Pi*

1 Introduction

Congenital or acquired physical disabilities have negatively affected people's lives for centuries and have caused them to encounter various difficulties. Such physical disabilities affect large number of people when their loved ones who help them are considered as well.

There are many different definitions of disability in the literature due to the difficulty of defining it. However, considering the common points of these definitions, disability can be explained as "the need for additional support due to various disabilities, congenital or acquired as a result of different reasons, that negatively affect one's life" (Yumuşak, 2014).

Disabled people form a large part of the population of society. According to OECD-Eu data, there are 1.559 billion disabled people in the world population of 7.78 billion. This corresponds to approximately 15% of the world's population (Association for Living Without Obstacles, 2018).

Researches on the difficulties faced by disabled people show that the most common problems in their lives are unemployment and financial difficulties, the lack of proper arrangement of the physical environment and lack of communication with the society (Yumuşak, 2014).

The concept of Human Computer Interaction (HCI) has emerged with the need for systems that are easier to use. Human Computer Interaction is an interdisciplinary concept that includes both humans and technology. Human Computer Interaction, which provides easy usability, has many advantages. These advantages can be listed as being pleasing and efficient, easy to learn and remembered even if it is not used for a long time, and minimizing user error (Çağıltay, 2016). Computer use, which has a high prevalence rate as a result of the solutions it offers, is done via computer input devices such as keyboard, mouse and touchpad. However, people with mobility impairments cannot make physical contact with computer input devices, therefore cannot use a computer and benefit the advantages of Human Computer Interaction (Dönmez & Çağıltay, 2016).

In this study, a home control and communication system that uses image processing-based eye tracking system was introduced as a solution for disabled individuals who cannot live independently in their home environment where they spend most of their lives and cannot communicate comfortably in their homes due to their physical limitations. The developed system meets the need for support that will bring disabled people into society and make their lives easier by bringing a solution to the difficulties they experience, which are the physical environment not being properly arranged and lack of communication with the community.

2 Method

In this study, the design-based research method was used. This method was developed to further the interaction of design, theory and practice. In this study, the design-based research steps created by R. C. Reeves, Ron Oliver and Jan Herrington (2004) were followed. The preferred method consists of two main topics and four stages: the predictive and developmental research steps. (Reeves, Oliver, & Herrington, 2004).

Studies concerned about the disabled individuals were analyzed. The founder of the barrier-free informatics platform, also an information technology specialist; a company official that develops technological support products for disabled people, and three people who are experts in the field of information technologies and who work on platforms related to solutions for people with disabilities were interviewed. In the meeting, the needs of disabled people, commercially developed technological products and the feedbacks made about the use of these products, and solution proposals for the development of existing technological systems were discussed. It was decided to develop a home automation system that can be controlled with an eye tracking system that will facilitate the lives of the disabled and increase their independence.

The basis of this study is the concept of "Computer Vision". Computer vision, which is a branch of computer science, makes it possible for computers to produce an appropriate output by performing many operations on the given image (Postacı, 2020). In this study, computer vision was applied via Python programming language. The Opencv (Open Source Computer Vision) library was used for image processing, which forms the basis of this study. In addition to the Opencv library, the Dlib library containing machine learning algorithms to perform operations such as recognition, the Mouse library that can

receive and imitate user inputs to control the mouse cursor on the screen, the Tkinter and Pillow libraries for the design of the interface, the Pygame library for the playback of audio files. Additionally, the Smptlib library for sending e-mails to the relatives of the users and Ctypes library is for detecting whether the user is using the systemand the Rpi GPIO library for controling the prototype using Raspberry Pi was used.

The developed program first detects the faces in the camera with the face detection function of the "Dlib" library, and then determines the eye, mouth, eyebrow and nose elements on the face with the "facial mapping" method (Figure 3). In this study, only the points that give the position of the eyes were focused on, among the items found, since eye tracking will be performed (Fig. 1).

Fig. 1: "Facial mapping" diagram

First, a function was defined to detect whether the eye is blinking or not. This function draws a horizontal line between the rightmost and leftmost points of the eye, and a vertical line passing through the middle of the upper and lower two points, using the points determined by "facial mapping". When the eye is blinked, the horizontal length remains the same, while the vertical length decreases and the obtained ratio increases. The program counts this decrease as the user blinked. Mouse library is used to simulate clicking the mouse cursor when the eye blinks (Fig. 2).

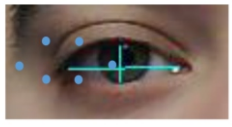

Fig. 2: Identifying points and drawing lines on the eye

Three methods were tried in the eye tracking step, and after the trials, the most suitable one was selected. The first method tried was using the contour finding method in the Opencv library. In this method, the eye image is separated from the camera image by applying a mask. "Gaussian blur", conversion to gray and tones and adaptive thresholding processes are applied on the obtained image. Then, contour finding function of Opencv library is run on the threshold eye image.

Since it was observed that the method used to determine the location of the pupil is affected by the environmental conditions, the use of the trackers in the Opencv library has been tried. In this method, the middle point of the user's eye is given to the tracker in the image when the user looks at the camera. However, after the experiments, it was observed that the determined point changed due to the trackers not being sensitive enough and the point is tracked according to the average color values (Fig. 3).

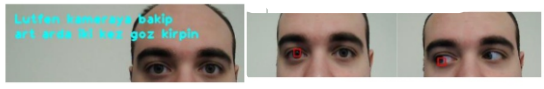

(a) (b)

Fig. 3: a) Configuration screen b) Eye tracking

Then, the third and the final method was tested. Using "facial mapping", the image where the eye is located is extracted and "median blur", "conversion to gray and tones and adaptive thresholding processes are performed respectively. The obtained image is divided into two equal parts, right and left, and the amount of white pixels is taken, the change in this amount is evaluated and the direction the eye looks at is determined. As long as the amount of white in the right half is above a certain amount, it is taken as looking to the left, as long as the amount of white in the left half is above a certain amount, it is considered as looking to the right. Using these directions, the mouse cursor is moved to right if looking to right, and to left if looking to left. This method has also been tried for up and down looking situations, but adequate results could not be obtained. Thereupon, it was decided that the mouse cursor would only move horizontally.

Tkinter and Pillow libraries were used in the interface design. Commands that are included in the program are door, air conditioner, light on/off, bed lowering/raising; medicine, water, requesting food, reporting the need for toilet, thanking, calling out and reporting an emergency. These commands are divided into two categories as "home control" and "needs", and the emergency notification command is placed in all program windows for quick access. A home page was created where the user can choose between two categories (Fig.4). Selected commands notify the user by giving an audible and visual warning.

In the first design of the interface, assuming that the place where the eye looks will be used, it was thought that a circular design would be more comfortable to use, and the commands were placed in the windows of the categories in this way (Fig.5).

Fig. 4: Homepage design

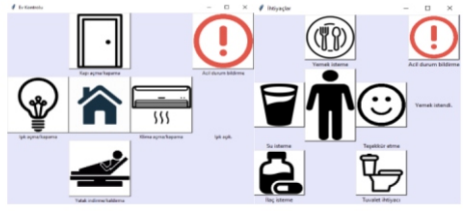

Fig.5: a) Home control window b) Requirement notification window

After it was decided to use only the horizontal direction of the eye, the interface design was rearranged in accordance with the horizontal mouse movement . In the continuation of the development process, the number of commands in the system was increased. A window open/close command was added to the home control category, and a calling command was added to the needs category. Since the increase of the number of buttons may cause difficulties for the users after the increase in the number of commands, the commands were rearranged in two rows and an up/down button has been added to enable the transition between the two rows (Fig. 6).

Fig.6: a) New home control window design b) New needs

The added up/down button works as a "Toggle button", it moves the mouse cursor down if it's up and up if it's down. The movement of the mouse cursor is performed by aligning the mouse cursor with the commands. For this movement, it was tried to use a blink for a certain period of time instead of a button. However, it was observed that the loop added for this purpose reduced the running speed of the program and it was decided to use the button. A return button was added to the home control and needs window, which the users can use when they want to return to the home page from the command window. In addition, it was observed in the experiments that users have difficulties in where they should look. To solve this problem, directional arrows were placed in all windows of the interface to show where they should look to move the mouse cursor, and a circle that shows where they should look to stop the mouse cursor. In addition to these improvements, the interface windows were made full screen (Fig. 7).

(a) (b) (c)

Fig. 7: a) New home page design b) New home control window design c) New needs window design

In the new interface design, it was taken into account that increasing the mouse movement may cause difficulties for the user to switch between the menus. To eliminate possible problems in this regard, the mouse cursor is automatically positioned to coincide with the commands of the user on the main page, and to coincide with the commands in the upper row in the command windows.

After reaching the current design of the interface, the development of the emergency notification system was worked on. Considering the possibility that the person to be notified may not be in the same place as the user at that time, the feature of notifying via e-mail was added to the system. With the addition of this feature, pressing the emergency notification button sends the message "Your relative has reported an emergency." To the relative of the user. In addition, considering that the user's condition may be too serious to use the button from the system, a message asking the user if they are okay is displayed if the system is not used for a certain period of time. The mouse cursor is automatically placed on the confirmation button on the message so that they can more easily press the button if there is not an emergency. If the user does not press the confirmation button on this message within a certain time, an e-mail saying "Your relative is not responding, there may be an emergency." is sent. A letter informing the user that their relative has been notified is shown to the user.

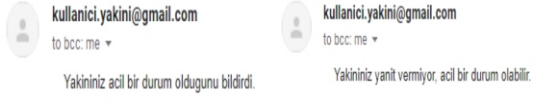

Fig. 8: Emails sent to the user's relatives

Informing the user's relatives via messaging, which is an easier-to-reach communication method is being worked on and will be added to the system in further improvements. In addition, work on customization of the commands is in progress.

The prototype used in this study was first designed in 3D on the Tinkercad program (Fig.9a). After deciding on the design on the 3D model, the diagram of the circuit elements to be used was drawn through the Fritzing program. After the planning phase, the first prototype was developed. The developed prototype contains a fan representing the bed, door, light and air conditioner. Light and fan elements are connected to Raspberry Pi using Relay module relay. SG90 servo motors used in door and bed control are connected to Raspberry Pi by combining their positive ends. After the window control was added to the system, the prototype design was updated and a second prototype was created. The newly built prototype contains a fan representing the bed, door, light, window and air conditioner. The connection of the elements in the previous prototype was left the same, the servo motor used in the window control was also connected to the Raspberry Pi, as was the bed and the door (Fig. 9 a and b) .

Fig.9: a) 3D House Model b) Current prototype

The current version of the developed system has been tested with three users, and users' time to reach the desired commands, ease of use and effect of the distance from the camera on the system performance has been examined. The data of one of the trials are given in Table (1).

Table 1: Trial Data

			Command											Total Time
			Light	Door	Window	Bed	Air Conditioner	Food	Water	Toilet need	Medicine	Thanks	Call Out	
1. Person	Trial 1 – 30 cm	Success	✓	✓	✓	✓	✓	✓	✓	✓	✓	✓	✓	162.4 s
		Time (s)	6.9	19.2	13.5	10.9	13.2	11	20.1	8.7	10.4	33.7	14.8	Avg. : 14.8 s
	Trial 2 – 30 cm	Success	✓	✓	✓	✓	✓	✓	✓	✓	✓	✓	✓	135 s
		Time (s)	8.7	7.8	12.9	9.8	22.5	9.8	10.2	7.2	7	19.2	19.9	Avg. : 12.3 s
	Trial 3 – 40 cm	Success	✓	✓	✓	✓	✓	✓	✓	✓	✓	✓	✓	110.5 s
		Time (s)	8.9	8	15.5	8.2	14	7.5	8	8.5	9.6	11	11.3	Avg. : 10.1 s
	Trial 4 – 50 cm	Success	x	x	x	x	x	x	x	x	x	x	x	-
		Time (s)	-	-	-	-	-	-	-	-	-	-	-	

When the data shown in Table 1 are examined, it is seen that the user's speed of use increases in each trial. As for the distance of use, users have reported that they can move the mouse cursor more easily in a 40-centimeter setup. In other words, it can be said that the system works best at 40 centimeters, but does not give healthy results at longer distances such as 50 centimeters.

3 Discussion

It was seen that the system developed at the end of this study has the quality to increase the quality of lives of individuals with physical disabilities. The eye is one of the organs that loses its function the least in conditions such as paralysis and disability. Therefore, home automation developed with an eye tracking system both appeals to a wide audience around the world and increases the independence of disabled individuals in their daily lives by providing a comfortable use.

Studies based on computer vision-based eye tracking have been found in the literature. For example, the study titled "Design and Development of a Game Based Eye Training Program for Children with Low Vision" by Dönmez (2020) was conducted in the field of eye tracking systems and the target audience was children with low

vision who could not be treated with glasses, lenses and eye surgery. The study aims to create an alternative to rehabilitation centers with low accessibility by offering visually impaired activities to children with low vision. As a result of the study, it shows that eye tracking technology is an effective and accessible way in terms of low vision exercise (Dönmez, 2020).

When these and similar studies are examined, computer vision promises potential both in facilitating the lives of the disabled and in the construction of exercises for rehabilitation purposes.

4 Conclusion

Disabled people, who make up 15% of the world's population, need supports that will make their lives easier. In this study, the physical limitations and miscommunication problems caused by the disability which are the largest problems for the disabled individuals after unemployment and financial were tried to be solved. In order to solve these problems, a home control and communication system has been developed using the eye tracking system.

The factors that were considered in the decision process of the product were that the designed product needed to be suitable for the user group and a reason was needed to be given to the users in order to use the product. Starting from this stage, the importance of suitability for the user group has been reinforced with this study and it has been understood how important it is.

The use of image processing technique in the study increased the program's dependence on environmental conditions. Although the proposed solution aims not to depend on environmental factors, at the end of the study, it has been observed that the image and therefore the image processing processes are affected by the physical factors such as light. A wearable system where the camera is attached on glasses can reduce the influence of environmental factors. In addition, a hybrid system can be developed to solve this problem. Since the perception of eye movements can be easily affected by environmental factors such as light, it is predicted that this system, which the user can control with head movements in addition to eye movements, will give better results. Head movements can be processed using a gyro sensor instead of computer vision to reduce dependence on environmental conditions.

The system and design presented in this study can also be applied to places that are frequently involved in daily life such as workplaces and schools in the future, and can be transformed in order to provide independence to individuals in different areas.

References

[1] Aydın, F. (2020). İnsan ve Bilgisayar Etkileşimi Çerçevesinde EBYS'lerin Kullanılabilirliği ve Teknolojik Hazır Oluşu Üzerine Bir Analiz Çalışması.

[2] Bilgin, N. (2015, Haziran 29). Özel Eğitim ve Engel Türleri. Ocak 17, 2021 tarihinde Özel Bursa Hayat Özel Eğitim ve Rehabilitasyon Merkezi: http://hayatozelegitim.com.tr/V2/ozel-egitim-ve-engel-turleri adresinden alındı

[3] Çağıltay, K. (2016). İnsan Bilgisayar Etkileşimi ve Öğretim Teknolojileri.

[4] Chan, M., & Zoellick, R. B. (2011). Dünya Engellilik Raporu. Dünya Sağlık Örgütü, Dünya Bankası. Ankara: Anıl Group Matbaa. Ocak 17, 2021 tarihinde https://static.ohu.edu.tr/uniweb/media/portallar/engelsizuniversite/duyurular/1345/diwnu3i5.pdf adresinden alındı

[5] Dönmez, M. (2020). Design and Development of a Game Based Eye Training Program for Children with Low Vision.

[6] Dönmez, M., & Çağıltay, K. (2016). Giziksel Engelliler için Göz Hareketlerini İzleme Yöntemi ile Bilgisayar Kullanma Sistemi. Eğitimde Fatih Projesi: Eğitim Teknolojileri Zirvesi. Ankara. https://www.researchgate.net/publication/316087605_Fiziksel_Engelliler_icin_Goz_Hareketlerini_Izleme_Yontemi_ile_Bilgisayar_Kullanma_Sistemi adresinden alındı

[7] Engelsiz Yaşam Derneği. (2018, Mart 5). Sayılarla Dünya'da ve Türkiye'de Engellilik. Ocak 17, 2021 tarihinde Engelsiz Yaşam Derneği (EyDer): https://ey-der.com/ana-sayfa/turkiye-ve-dunyada-engelliler/ adresinden alındı

[8] Kantekin, U., Aytekin, U., Uzunoğlu, C. P., & Cekli, S. (2014). Engelliler için Akıllı Ev Otomasyon Sistemi.

[9] Keskin, S. (2018). Real Time Human Computer Interface Application Based on Eye Gaze Tracking and Head Detection .

[10] Reeves, T. C., Oliver, R., & Herrington, J. (2004). A Development Research Agenda for Online Collaborative Learning. Georgia. Ocak 27, 2021 tarihinde file:///C:/Users/User/Downloads/download%20(2).pdf adresinden alındı

[11] Teke, İ., Kılınç, M., & Kalaç, M. Ö. (2018). Türkiye'de Engellilere Yönelik Bilişim Teknolojileri ve Hizmetleri Üzerine Genel Değerlendirme. BİLTEVT Uluslararası Engelsiz Bilişim 2018 Kongresi.

[12] Yumuşak, M. (2014). Engelli Bireylerin ve Ailelerinin Toplumsal Hayatta Yaşadıkları Zorluklar Araştırma Raporu. Zorluklar,Araştırma,Raporu, Şanlıurfa. . file:///C:/Users/User/Downloads/Engelli%20Bireylerin%20ve%20Ailelerinin%20Toplumsal%20Hayatta%20Yasadiklari%20(3).pdf adresinden alındı

Purification of Water from Herbal Oil, Mineral Oil and Petroleum Products by Being Used Kapok Fiber

Hatice Kübra Eroğlu, İremsu Aşlakçı , Sakarya Science and Art Center
ekubra5454@gmail.com

ARTICLE INFO

Gold medalist in IMSEF 2021and Bronze medalist in ISAC Olympiad 2021
Advisor: Aydın Boğaz
Accepted by Ariaian Young Innovative Minds Institute,AYIMI

http://www.ayimi.org , info@ayimi.org

ABSTRACT

Petroleum is a mineral oil with a very dark color, a specific odor and a density varying between 0.8 and 0.95 g/cm3. Knowing the composition, physical and chemical properties of petroleum and petroleum products and Kapok fibers this investigation has been done about the purification of water by absorbing these substances in water by petroleum products (crude oil-gasoline-diesel-fueloil etc.), mineral oil and vegetable oil mixed with water sources naturally or indirectly by using Kapok (Ceiba pentandra) fiber. Industrially

Key words: *petroleum, Kapok, absorbing, water*

1 Introduction

Kapok is a type of fiber obtained from plant seed such as cotton. This tree (Ceiba pentandra), whose homeland of the Kapok tree is the tropics of America and the West Indies, 2 today, mainly Java, and some Asian countries such as the Philippines, Malaysia and Sri Lanka. It is widely cultivated to obtain fiber in their countries. In general, the regions 15 degrees north and south of the equator are the regions where good kapok products are obtained.

Those grown at an altitude of up to 450 meters above sea level give the most yield and best quality products. Kapok tree exhibits a rather large appearance with its branches located almost perpendicularly to the trunk.

The white or pink kapok flowers turn into large cocoon-shaped fruits after pollination with the help of bats. There are many hairy seeds inside the kapok fruits, which are about 15 cm long. (Picture 1.2.3.) These hairs are removed from the fruit and used as fiber. (Picture 4.) For this, first the fruits are opened by breaking them with sticks, then the seeds are placed in a basket and mixed quickly; With the effect of these blows, the fibers are broken off and collected at the bottom of the basket.

Kapok Fiber; It has an extremely shiny, cream-yellow colour, silky appearance. It is a soft and elastic fiber. It is a single cell, visible under the microscope as thin longitudinal ribbons. Its cross-section is oval or round. The immature ones appear like the immature cotton fibers, that is, in the form of rods. Even in mature fibers, the lumen is wide and the wall is narrow. Its specific gravity is 0.0388 gr/cm³ at 30 degrees and it is very light. Fiber length is 1 - 3.5 cm. It contains 63% cellulose and 13% lignin in its structure. It is one-sixth the weight of cotton. Good air and heat insulation is provided due to the pores in the fiber structure. It does not get wet in water for a long time, dries quickly when wet. (It does not get wet quickly because the surface of the fiber is covered with wax) 1 kg of kapok easily holds a weight of 35 kg on water (1), (2). (Fig. 1).

Petroleum is a mineral oil with a very dark colour, a peculiar smell and a density varying between 0.8 and 0.95 g/cm3. Knowing the composition, physical and chemical properties of petroleum and petroleum products, their behaviour, changes and effects in nature is critical in order to determine the response methods to be applied in case of a spill. The composition of petroleum also differs depending on where it is extracted. For example, an oil extracted from Pennsylvania is fluid and brightly colored because it is paraffinic. Whereas a Venezuelan origin crude oil is black and more viscous due to the presence of highly aromatic hydrocarbons. That's why oil is named after the region where it is extracted. Low-density oils float on water as well as have low viscosity and high volatile components.

1-1 Behaviour of Oil in Marine Environment

After the oil is poured into the marine environment, undergoing some physical and chemical changes is generally called weathering. Knowing the oil leaching process and the factors that play a role is helpful when preparing and implementing response plans for oil spills. Physical properties of oil such as density, viscosity, pour point affect the behaviour of oil in the marine environment. The behaviour of oil in the marine environment is presented in Figure (1).

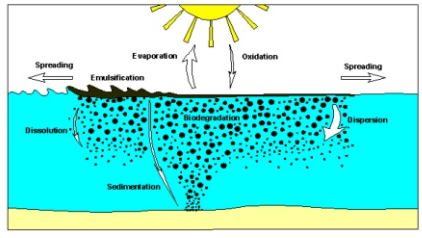

Fig. 1: Behaviour of oil in the marine environment (ITOPF, 2003)

Although the economic effects of oil spills are mostly temporary, such an event could hit some sectors such as

tourism, power generation and fisheries. Petroleum pollution has negative effects on living life due to both physical damage and toxic effects of its chemical components. The methods to be applied to remove oil from the sea are directly related to the length of the aeration phase of the oil. All physical and chemical properties affect the efficiency and therefore the choice of removal methods (Fig. 2).

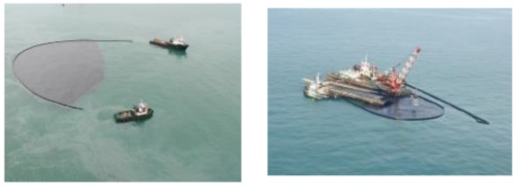

Fig. 2:U-shaped pulling of the barrier and the use of scrapers

Examples of living things affected by oil pollution are shown in Figures (3).

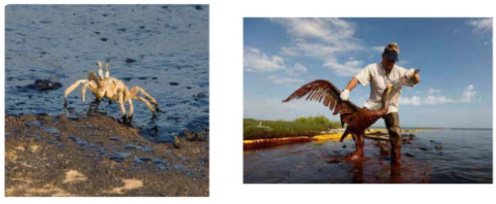

Fig. 3: Oil pollution endangers living organisms

Absorbent materials provide a useful resource in responding to an oil spill, allowing oil to be removed where other techniques are not suitable. However, secondary problems need to be minimized, especially by generating excessive amounts of waste of sorbent, which can contribute greatly to the costs of a response. This booklet considers the types of absorbent materials available and how they can be usefully used in a response. It should be read in conjunction with the ITOPF booklets in this series, particularly on the use of booms, the use of skimmers, shoreline cleaning techniques and oil spill disposal (3) (Fig. 4).

Fig. 4: Surface and coastal pollution caused by oil derivatives in the sea and on the coast (37)

1-2 Oil Absorbent Rolls

Only Oil Absorbent Roller is used to clean up petroleum-based spills and spills to absorb petroleum-based fluids, and is effectively applied in both marine industry and aviation oil spill emergency operations and oil spill in oil tank or car.

1. 100% polypropylene will not rip, tear or fray even when saturated.
2. Highly absorbent, fine fiber structure does not leave behind liquids or fiber residues. Absorbs and retains oils and oil-based fluids (including lubricants and fuels) without absorbing a drop of water.
3. Floats to clean up oil spills in the water
4. Bright white colour makes the absorbed oil easier to see; draws attention to machine leaks and clearly shows saturation level during spill response.
5. After being used to reduce waste or mix fuels, it can be opened and incinerated.
6. Mainly used to absorb crude oil; It is suitable for absorbing light oil, low and medium viscosity oils and volatile chemical liquids with light specific gravity.

Oil Absorbent Roller Applications:

- Transport companies.
- Marine Oil Spill
- Ship and dock
- Chemical and equipment factories
- Oil spill on lake and river (4)

Our Absorbent Pad is designed to absorb Chemical, Petroleum and universal spills. The Absorbent Pad is the fastest way to clean up a spill. The Absorbent Pad is available in a number of different weights and materials. Oil Absorbent Pad, Universal Absorbent Pad and Chemical Absorbent Pad material provide fast capillary action and excellent absorbent capacity and retention.

Oil absorbent pad that absorbs petroleum-based liquids and repellent water. Oil Absorber Pad is recommended for small amount of water oil leakage and indoor use. Perfect for pipelines, shipyards, ship and yacht decks, factories, industrial plants, loading docks, machine and maintenance shops, fire departments, municipal spills or spills of liquid, chemical or oil. The oil absorbent pad is always easily placed and removed (5).

Kapok fibers, which stand out with their hollow fiber structure, lighter-than-water specific gravity, and oil-absorbing character, display a profile quite different from known natural fiber types (7,12,13,36).

The fact that the fibers do not sink in water, provides sound and heat insulation (8,12,16-19,36) and has a high oil absorbing feature in contrast to their hydrophobic feature makes kapok fibers superior to many synthetic fiber types (6,11,20,21,36).

Kapok tree has been grown in large plantations in Southeast Africa for both kapok fiber and wood pulp, but demand for kapok fibers has declined as synthetic materials become more preferable (22,36). Another reason for the decrease in kapok production, whose annual production exceeded 40 million kilograms before the Second World War, was the widespread use of synthetic fibers as well as the destruction of kapok cultivated areas due to the war (23, 36).

Kapok fibers are a type of cellulosic fiber with a soft and silky touch. However, it differs from other cellulosic fibers with its hollow tube-shaped fiber structure (24, 36). Kapok fibers keep mold and harmful insects away, as the fibres contain a large amount of lignin and wax. Kapok fibers, which are yellowish or light brown in colour, have a silky shine (9, 12, 18, 25, 36). Kapok fibers, which are also odorless and soft, are non-toxic or allergenic and resistant to decay. Kapok fibers have similar characteristics with silk grass fibers both in terms of appearance and general characteristics (10, 36). Silk grass fibers, like kapok fibers, are a type of seed fiber that has a hollow fiber structure, low fiber density, and exhibits hydrophobic and oleophilic fiber properties (10, 36).

It has been noted that the rebound (compression

kapok fibers is good (15, 36) (Fig.5).

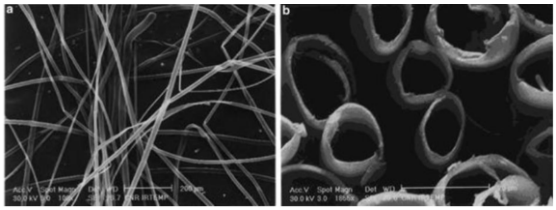

Fig. 5: SEM images of Kapok fiber taken in longitudinal (100x magnification)-(a) and cross-section (1855x magnification)-(b) (26)

The hydrophobic and oleophilic character of Kapok fibers gives very successful results in the separation of fatty substances from aqueous solutions. In particular, kapok fiber filters produced for the separation of oil and similar spills from sea water are both very durable and can be used very effectively in the separation process (10,11,14,21,28,31-33,36). Considering that approximately 10 million tons of petroleum and its products are used in the world every year, it is obvious how high the probability of contamination of water resources such as sea, lake and ocean is during the use or transportation of these products. Cleaning the oil and its derivatives contaminating water resources causes very serious costs. Filters produced with Kapok fibers, on the other hand, can provide a more efficient and more economical alternative to filters produced mostly from synthetic materials.

In the separation of oily substances from water and oil mixtures, separation can be achieved at a process efficiency of up to 100%. In addition, kapok fibers can be used more than once in this separation process and ensure that the separated oil can be reused (11, 36). Polypropylene is used as a raw material in the most widely used products for cleaning oily structures on the water surface (14, 36). In a study comparing the oil absorbing capacities of polypropylene and kapok fibers, it was noted that the kapok fibers absorb almost all the oil on the water surface, but only a very slight oil trace that cannot be seen on the water (6,36). In the evaluation performed using diesel, hydraulic oil (AWS46) and machine oil (HD40), it was observed that the oil absorbing capacity of kapok fibers was much higher than the oil absorption capacity of polypropylene fibers for all three substances. It was reported that after the fourth use of Kapok fibers, only 30% of the initial oil sorption capacity was lost (6, 36). In another study, it was noted that kapok fibers could retain 70% of their oil absorbing capacity even after 15 use [for diesel with a compression (packing) density of 0.04 g/cm3] (11,36). According to the researches, it can be said that kapok fibers have a very successful use in separating substances such as diesel, gasoline, machine oil, hydraulic oil from the water surface (11, 31, 36).

2 Method

All of our work was carried out by our project team in the equipped physics laboratory determined as the research environment. Kapok fiber, cotton, three different microfiber cloth samples were used for impregnation. Other materials used are; glass beaker, fuel-oil, diesel, motor oil, mineral oil and liquid vegetable oil.

The samples were allowed to absorb liquids on the water (impregnation method) and then by measuring how many grams of liquid each sample absorbed (Picture 12-25) Table.2-5 is given.

Each measurement was repeated 5 times, and the completion of our project took 12 weeks (Fig.6).

Fig. 6: Experimental setup and procedure

Fuel-oil, diesel oil, motor oil, mineral oil and liquid vegetable oil, kapok fiber added to the water absorbed much more than other samples, allowing them to separate from the water. Petroleum spillages or accidents can cause irreparable damage to life.

3 Results

Made with Kapok fiber, cotton and three different microfiber cloth samples; Kapok fiber gave very different results compared to other materials in the impregnation of fuel oil, diesel, motor oil, mineral oil and liquid vegetable oil over water, and completely cleaned the water from the liquids used. It also enabled the reuse of liquids purified by absorption from water.

Comparative values of the materials used in the impregnation; Chart.1-4, the values obtained in the multiple use (10 repetitions) of Kapok fiber are given in Figures (7-13).

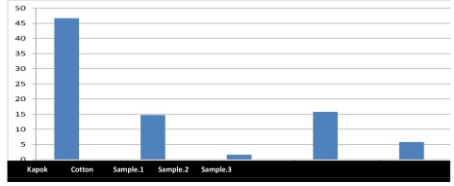

Fig. 7: Liquid-herbal oil absorption - 1 g of material (kapok, cotton and 3 more samples) in gram

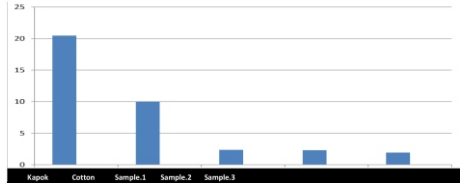

Fig.8: Fuel-oil absorption - 1 g of material (kapok, cotton and 3 more samples) in gram

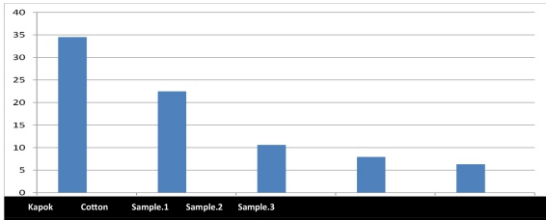

Fig. 9: Motorine absorption - 1 g of material (kapok, cotton and 3 more samples) in gram

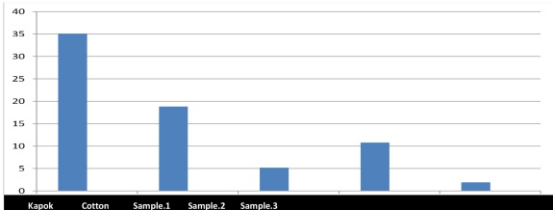

Fig. 10: Diesel fuel absorption - 1 g of material (kapok, cotton and 3 more samples) in gram

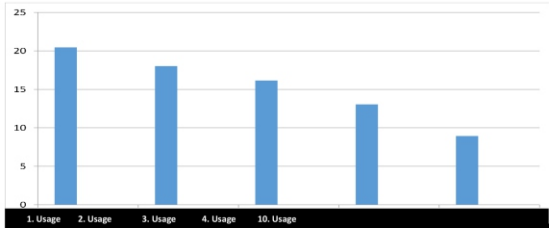

Fig. 11: Fuel oil absorption of 1 g Kapok fiber

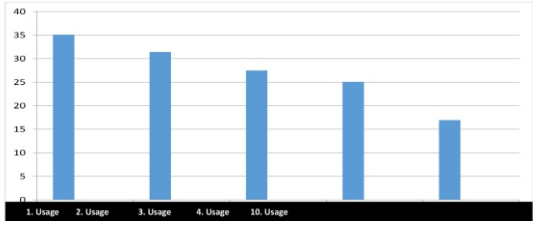

Fig. 12: Diesel fuel absorption of 1 g Kapok fiber

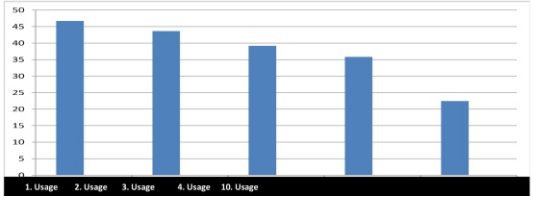

Fig. 13: Herbal Oil absorption of 1 g Kapok fiber

Made with Kapok fiber, cotton and three different microfiber cloth samples; Kapok fiber gave very different results compared to other materials in the impregnation of fuel oil, diesel, motor oil, mineral oil and liquid vegetable oil over water, and completely cleaned the water from the liquids used. It also enabled the reuse of liquids purified by absorption from water.

Comparative values of the materials used in the impregnation;(Figs. 7-10), the values obtained in the multiple use (10 repetitions) of Kapok fiber are given in Figures (11-13).

For example, with 5 kg Kapok fiber (5000 g) For diesel;

5000 x 35.08 = 175.400 g = 175.4 kg at first use,

5000 x 16.94 = 84.700 g = 84.7 kg. It can be separated from water in the 10th use.

For fuel-oil;

5000 x 20.46 = 102.300 g = 102.3 kg at first use,

5000 x 8.94 = 44.700 g = 44.7 kg. It can be separated from water in the 10th use.

For liquid vegetable oil;

5000 x 46.70 = 233.500 g = 233.5 kg at first use,

5000 x 22.45 = 112.250 g = 112.25 kg. It can be separated from water in the 10th use.

5 kg Kapok fiber cost (kg price is between 9-12 TL)

5 x 12 = 60 TL.

The price of petroleum absorbers used for the same purpose is 393 TL.

The price of oil (and chemical) absorbents used for the same purpose starts from 333 TL. Kapok fiber is seen to be very advantageous in terms of usage and price comparison and multi-use.

4 Advices

a) In a study on composite materials that can be used in oil and water filtration/separation processes; Various properties of the composite structure obtained by coating polyvinlidine fluoride (PVDF) on the kapok fiber nonwoven surface using electro-spinning technology were investigated. Polyvinylidene fluoride (PVDF) polymer is a type of material with superior mechanical properties, high chemical resistance, and good pyroelectric and piezoelectric properties. When these unique properties of PVDF fibers are combined with the light, non-sink and water resistant structure of kapok fibers, composite materials with high oil/water separation performance and resistant to a wide variety of environmental conditions can be produced (30,36).

b) Kapok fibers also have the potential to be used in the production of high-performance electrode materials with their hollow structure (34,36).

c) The high absorbency of Kapok fiber is used in large kitchens (hotels, restaurants, food factories, etc.) industrially and in all residential areas (hotel, school, dormitory, etc.) to prevent slipping on the floor, multiple use (in the form of simple mats or mobs or locally covering the floor). It is thought that it will be very useful as it is possible.

d) With the use of Kapok fiber in car wipers; Incidents such as oil on the windshield, fuel spilled on the roads, etc., which will cause complete loss of vision during the operation of the wiper, can be prevented and accidents can be prevented. (We are still working on this subject)

e) It is thought that kitchen drains, waste water drains, blockages caused by oil or petroleum-derived products that may occur in all types of sinks, and the filter system, where water can be separated, can significantly prevent water pollution.

f) Since it is possible to turn it into a product that can also allow cleaning of large areas (sea, lake, river, tanker leaks and accidents, factory wastes, etc.), it is also suitable for this purpose.

g) In addition, we continue to work on the use of the Archimedean Screw filtering system (Fig.14) for waste water installations and drains.

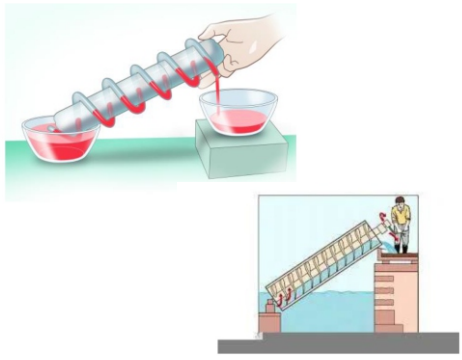

Fig. 14: Filtering System

References

[1] https://tekstilsayfasi.blogspot.com /2013/01/kapok-lifleri.html

[2] https://tekstilbilgii.blogspot.com /2016/10/kapok-elyafi.html

[3] ITOPF Teknik Bilgi Kitapçıkları - Petrol Döküntüsüne Müdahalede Emici Maddelerin Kullanımı. (ITOPF : Uluslararası tanker sahipleri kirlilik federasyonu limited olup; petrol, kimyasallar ve diğer tehlikeli maddelerin denize kazara dökülmesine etkili bir şekilde müdahale edilmesinidesteklemek için dünyadaki gemi sahipleri ve sigortacıları adına kurulan kar amacı gütmeyen bir kuruluştur.)

[4] http://turkish.marine-safetyequipment.com/sale-10863370-100-polypropylene-industrialoil-absorbent-rolls-for-cleaning-up-petroleum-spills.html

[5] https://mavideniz.com.tr/tr/uretimlerimiz /emiciler/emici-ped-yag-kimyasal-evrensel/

[6] T. T. Lim and X. Huang "Evaluation of Kapok (Ceiba Pentandra (L.) Gaertn.) as a Natural Hollow Hydrophobic–Oleophilic Fibrous Sorbent for Oil Spill Cleanup," Chemosphere, vol. 66, no. 5, pp. 955-963, 2007.

[7] Y. Zheng, J. Wang, Y. Zhu and A. Wang "Research and Application of Kapok Fiber as an Absorbing Material: A Mini Review," Journal of Environmental Sciences, vol. 27, no.1, pp. 21-32, 2015.

[8] G. Yazıcıoğlu, Pamuk ve Diğer Bitkisel Lifler, İzmir, Türkiye, Tekstil Mühendisliği Bölümü Mühendislik Fakültesi Basım Ünitesi, 1999.

[9] B.H. Gürcüm, Tekstil Malzeme Bilgisi, İzmir, Türkiye, Güncel Yayıncılık, 2010.

[10] R. Sinclair, Textiles and Fashion: Materials, Design and Technology, Cambridge, UK: Woodhead Publishing Limited, 2014.

[11] M. Abdullah, A.U. Rahmah and Z. Man "Physicochemical and Sorption Characteristics of Malaysian Ceiba Pentandra (L.) Gaertn. As a Natural Oil Sorbent," Journal of Hazardous Materials, vol. 177, no. 1, pp. 683-691, 2010.

[12] J. Yan, C. Fang, F.-M. Wang ve B. Xu "Compressibility of the Kapok Fibrous Assembly," Textile Research Journal, vol. 83, no. 10, pp. 1020-1029, 2013.

[13] Y. Zheng and A. Wang, "Kapok Fiber: Structure and Properties," Biomass and Bioenergy,Springer, 2014.

[14] Y. Zheng and A. Wang, "Kapok Fiber: Applications," Biomass and Bioenergy: Applications, Cham, Switzerland: Springer, 2014.

[15] A. Briggs-Goode and K. Townsend, Textile Design: Principles, Advances and Applications, Cambridge, Woodhead Publishing Limited, 2011.

[16] H.-f. Xiang, D. Wang, H.-c. Liua, N. Zhao ve J. Xu "Investigation on Sound Absorption Properties of Kapok Fibers," Chinese Journal of Polymer Science, vol. 31, no. 3, pp. 521-529, 2013.

[17] E. Kalayci, F.F. Yildirim, O.O. Avinc and A. Yavas, "Textile Fibers Used in Products Floating on the Water", Textile Science and Economy VII, Zrenjanin, Serbia, 2015, ss. 85-90.

[18] K. Hori, M.E. Flavier, S. Kuga, T.B.T. Lam and K. Iiyama "Excellent Oil Absorbent Kapok [Ceiba Pentandra (L.) Gaertn.] Fiber: Fiber Structure, Chemical Characteristics, and Application," Journal of Wood Science, vol. 46, no. 5, pp. 401, 2000.

[19] M.S. Smole, S. Hribernik, K.S. Kleinschek and T. Kreže, "Plant Fibres for Textile and Technical Applications," Advances in Agrophysical Research, Intechopen, 2013.

[20] R. Rengasamy, D. Das and C.P. Karan "Study of Oil Sorption Behavior of Filled and Structured Fiber Assemblies Made from Polypropylene, Kapok and Milkweed Fibers," Journal of Hazardous Materials, vol. 186, no. 1, pp. 526-532, 2011.

[21] J. Wang, Y. Zheng and A. Wang "Superhydrophobic Kapok Fiber Oil-Absorbent: Preparation and High Oil Absorbency," Chemical Engineering Journal, vol. 213, no.1, pp. 17, 2012.

[22] M. Mert, Lif Bitkileri, Ankara, Türkiye: Nobel Yayın Dağıtım, 2009.

[23] J. R. Robertson, C. Roux and K. Wiggins, Forensic Examination of Fibres, Philadelphia, USA: Taylor & Francis, 2002.

[24] R. Kozlowski, Handbook of Natural Fibres: Types, Properties and Factors Affecting Breeding and Cultivation, Cambridge, UK: Woodhead Publishing Limited, 2012.

[25] R.R. Mather, and R. H. Wardman, The Chemistry of Textile Fibres, Cambridge, UK: The Royal Society of Chemistry, 2011.

[26] L.Y. Mwaikambo and E.T. Bisanda "The Performance of Cotton–Kapok Fabric– Polyester Composites," Polymer Testing, vol. 18, no. 3, pp. 181-198, 1999.

[27] Y. Bozkurt ve N. Erdin "Odunsu Lifler Ve Tanımı," Journal of the Faculty of Forestry Istanbul University, c. 39, s. 4, ss. 1-16, 1989.

[28] J. Wang, A. Wang and W. Wang "Robustly Superhydrophobic/Superoleophilic Kapok Fiber with Zno Nanoneedles Coating: Highly Efficient Separation of Oil Layer in Water and Capture of Oil Droplets in Oil-in-Water Emulsions," Industrial Crops and Products, vol. 108, no.1, pp. 303-311, 2017.

[29] T. Nilsson and C. Björdal "The Use of Kapok Fibres for Enrichment Cultures of Lignocellulose-Degrading Bacteria," International Biodeterioration & Biodegradation, vol. 61, no. 1, pp. 11-16, 2008.

[30] D. Das and B. Pourdeyhimi, Composite Nonwoven Materials: Structure, Properties and Applications, Cambridge, UK: Elsevier, 2014.

[31] X. Huang and T.-T. Lim "Performance and Mechanism of a Hydrophobic–Oleophilic Kapok Filter for Oil/Water Separation," Desalination, vol. 190, no. 1, pp. 295-307, 2006.

[32] A.U. Rahmah and M. Abdullah "Evaluation of Malaysian Ceiba Pentandra (L.) Gaertn. For Oily Water Filtration Using Factorial Design," Desalination, vol. 266, no. 1, pp. 51-55, 2011.

[33] K.R. Hakeem, M. Jawaid and U. Rashid, Biomass and Bioenergy: Applications, Springer, 2014.

[34] W. Xu, B. Mu and A. Wang "Three-Dimensional Hollow Microtubular Carbonized Kapok Fiber/Cobalt-Nickel Binary Oxide Composites for High-Performance Electrode Materials of Supercapacitors," Electrochimica Acta, vol. 224, no. 1, pp. 113-124, 2017.

[35] H. Wang, (Eylül 2018), Carbon Nanomaterials for Supercapacitors, [Online]. Erişim: http://large.stanford.edu/courses/2012/ph240/wang-hu2/

[36] Türkoğlu K. B., Kalaycı E., Avınç O., Yavaş A. 'Oleofilik Buoyans Özellikli Kapok

Lifleri ve Yenilikçi Yaklaşımlar' Düzce Üniversitesi Bilim ve Teknoloji Dergisi, 7 (2019) 61- 69 .

[37] Mavi Gezegen Dergisi, Sayı: 20, 2015

Alternative to Environmental Pollution Plastics: Production of Hydrogel Film Using Clove Plant Extract and Controlling it with a Robotic System

Ceylin Afacan, Enes Kahraman , Balıkesir Şehit Prof. Dr. İlhan Varank Bilim ve Sanat Merkezi
ceylinafacan2006@gmail.com

ARTICLE INFO

Gold medalist in IMSEF 2021
Advisor: Dr. Leyla Ayverdi
Accepted by Ariaian Young Innovative Minds Institute,AYIMI

http://www.ayimi.org , info@ayimi.org

ABSTRACT

Although petroleum derived synthetic plastics have important advantages, they cause ecological pollution because they are produced more than 250 million tons per. Biodegradable packaging has emerged as an alternative to petroleum-derived plastics. In this project, a robotic system was combined with hydrogels produced to extend the shelf life of food. In the study, after hydrogels were produced with 5 extracts as 0%(control), 12.5%, 25%, 50%, 100%, the water holding capacity, water solubility, water vapor permeability of the hydrogels were examined. aromaticum extract increased.

Key words: *hydrogels, petroleum, ecological pollution, robotic system*

1 Introduction

The macromolecules formed by many small molecules bound together are called polymers. Polymers are formed by the chemical bond that monomers form as a result of the reaction under suitable conditions. Polymers are studied as natural and artificial. In the natural polymers section, proteins, cellulose, chitin, starch, RNA and DNA; In the artificial polymers section, there are synthetic rubber, PVC, silicone, nylon and plastics (Saçak, 1998). Some artificial polymers are widely used in packaging (Sarıgül, 2018).

Packaging, in the most general sense, can be defined as wraps and containers that protect the products included in the distribution process from environmental factors in the distribution process, keep the product as a whole, and facilitate transportation, distribution, storage and promotion. Having an important place in the food industry, packages ensure that foodstuffs are delivered to consumers in a healthy way. However, the main reason that makes the packaging important for the food sector is its importance for public health. If the foods prepared in healthy conditions are not packaged correctly, the foods become spoiled and threaten the health. Therefore, the right packaging and packaging selection is important (Öztürk, 2020). Thus, it is possible to keep food for a long time without spoiling.

One of the most used products as packaging is plastics. Plastics have become lighter, more sophisticated and versatile with innovative applications in recent years, and have replaced traditional packaging products such as paper and glass. In the past, materials such as cellophane transparent cellulose film and cellulose acetate were used in addition to traditional packaging such as wood, glass and paper, while plastic packaging began to be used extensively with the production and introduction of polyethylene in the 1950s. With the production of PVC, polystyrene, polyester, polypropylene and polyethylene copolymers, plastics have become increasingly common in the packaging industry (PAGEV, 2019). The important advantages of plastics that are used so heavily are that they are lightweight, they are durable, they are safe when used as containers, they are easy to shape, they are flexible, they have good insulation, they can be used for moist foods and they are suitable for use in microwave ovens (Güler and Çobanoğlu, 1997). Despite its advantages, approximately one-third of the petroleum-derived synthetic plastics, which are produced more than 250 million tons per year and are widely used, are used as packaging, then left to nature in the form of waste, and the processes of fragmentation and mixing into the soil negatively affect the living things. These wastes, especially plastic bags, are blown away from the area where they are left by the wind and drifted to different regions or they are transported by rivers and cause visual pollution and pollution of living spaces. For this reason, petroleum-based synthetic plastics have become an important environmental problem today. Since oil is not a renewable resource and synthetic plastics increase dependence on oil, it is a serious problem (Bölükbaşı, 2012).

With the understanding of the harmful effects of petroleum-derived synthetic plastics to the nature, biodegradable polymers of biological origin have started to be used more in plastic production in recent years (Şahin, Demir, İlsay, & Doğdubay, 2017). Biodegradable plastics; These are plastics produced from renewable sources such as plant starches and cellulose (Mehmet KILINÇ, Oktay TOMAR, Abdullah ÇAĞLAR, 2017). Biodegradable plastics obtained from different sources have some advantages over synthetic plastics. These; It can be listed as reducing dependence on oil, providing energy efficiency, causing less greenhouse gas emissions during production, and being more environmentally friendly since they do not contain toxic substances. Despite these advantages, it also has some disadvantages. These are; The cost is higher than synthetic plastics, recycling problems and the use of polymers such as starch-protein in the production process are seen as a disadvantage as these polymers meet the nutritional needs of the world population (Köksal, Aydın Er, Adalı, & Sağlam, 2019). When these disadvantages are overcome, it can be predicted that biodegradable plastics will take an important place in the plastics industry. However, biodegradable plastics used in different sectors account for 1.5% of total plastic production (PAGEV, 2020). However, the global market for biodegradable plastics is expected to grow further in the coming years. According to the latest market data compiled in collaboration with Nova-Institute and European Bioplastics, global production capacities of biodegradable plastics are estimated to increase from approximately 2.11

million tons in 2019 to approximately 2.42 million tons by 2024.

Some of the hydrogels are in the biodegradable polymers class (Çelik & Tümer, 2016). Hydrogels are used in the production of artificial retina and muscle in the health sector (Güngör & Erkan, 2004). In the literature, it has been observed that hydrogels are generally used in the health sector, and there are also studies on their use as packaging (Şahiner, Sağbaş, Turan, Erduğan, & Şahiner, 2018).

The food industry is a sector with a lot of plastic packaging waste, which creates a huge ecological problem. The food sector is also intertwined with the electronics sector, because people are now more sensitive about the packaging conditions of food, the place of production and date, and at the same time, many different advertising strategies are applied in the food sector (Aydın, 2012). In this project, we decided to use arduino to measure some parameters we have determined in order to unite the food and electronics sectors.

Many different projects can be carried out due to the fact that the open source equipped and software Ardunio controllers, which have been widely used in recent years, can detect some chemical parameters with additional sensors. The Ardunio platform enables work to be carried out more cheaply and quickly (Dipova, 2017). Ardunio has types that appeal to many different functions. Some of these are UNO for small-scale projects, MEGA for larger projects, and LILYPAD for use on clothing. (10) NodeMCU creates a platform that enables the Internet of Things (iot) to be remotely detected, connected and controlled by devices via a network server. It is known that many physical objects cannot be connected to the network. Thanks to the Internet of Things, inter-machine communication technologies and ecosystem, it is aimed to control and monitor these objects on the network.

In this project, we aim to observe the effect of hydrogels on the shelf life of foods using Arduino.

1- 1 Aim

The aim of this study is to synthesize hydrogel films using clove (Syzygium aromaticum) extract, to examine the properties of these films, to determine their usability as nutrition storage material, and to create a system that provides information about the state and shelf life of nutrition by obtaining some information on the environment through a system created with Arduino and sensors. The investigated features are; microscopic images of films, their thickness, water solubility, water vapor permeability, water holding capacity and antibacterial properties, and their effects on extending nutrition shelf life. If the synthesized films have the properties required for preserving nutrition, these materials will be important in terms of protecting the nature as they will be an alternative to petroleum-based plastics that dissolve in nature in a very long time. If these materials have antibacterial properties and effects to extend the shelf life of nutrition, they will be suitable materials to preserve nutritions in a healthy way. In addition, taking certain features of the environment in an environment created with the Arduino system will contribute to gaining a healthy idea about the characteristics of the indoor environment without opening the nutrition.

2 Method

2- 1 Devices Used in Experimental Procedures

The devices used in the study; analytical balance, magnetic stirrer, ultrasonic water bath, Soxhlet extraction device, oven, caliper and McFarland densitometer.

2- 2 Production of Hydrogel Films

The devices used in the study; analytical balance, magnetic stirrer, ultrasonic water bath, Soxhlet extraction device, oven, caliper and McFarland densitometer.

50 g clove plants were extracted in 500 ml purified water using Soxhlet extractor for 2 hours. The extract obtained at the end of 2 hours was made ready to be used in the production of hydrogel films. Hydrogel films were produced by the method of dissolving-drying, taking into account the proportions used by Topdağ (2015) in his study. In the production of each film, sodium alginate measured by analytical balance at 0.2 g was taken into a beaker. By adding 10 ml of distilled water on it, it was heated in a magnetic stirrer at 600C at 600 rpm for 1 hour and then dissolved completely. The solution obtained was cooled down to 25 ° C and 39 µl of glycerol was added on it and kept in an ultrasonic water bath for 15 minutes. The prepared mixtures were kept in ultrasonic water bath for 15 minutes, then poured into petri dishes and dried for 24 hours. 0.2 M CaCl2 solution was poured on the dried films and kept for 5 minutes. At the end of this period, the films were washed with distilled water for 5 minutes and dried at room conditions to obtain hydrogel films. The control group (0% extract) hydrogel film was synthesized in this way. In other examples, clove (Syzygium aromaticum) extract concentrations were added instead of water in the part where the alginate was dissolved in water, at concentrations of 0%, 12.5%, 25%, 50% and 100%.

2-3 Examination of Hydrogel Film Properties

2- 3- 1 Examining the Thickness of Hydrogel Films

Calipers were used to measure the thickness of the hydrogel films. Measurements were made by taking three samples for each film, and the results were presented on average values.

2-3-2 Examination of Hydrogel Films' Water Vapor Permeability

Water vapor permeability of hydrogel films was determined using ASTM E96 / E96M standards. After adding 5 grams (W1) of pure water to each Falcon tubes, the films were glued to the mouth of the tubes and the edges were wrapped with Teflon tape. The samples were stored in the oven at 25°C for 24 hours and the remaining water (W2) was weighed. (A= surface area of falcon tubes). The water vapor permeability of hydrogel films was calculated (Eq. 1).

$$Water\ vapor\ permeability = \frac{W1-W2}{A} \quad (1)$$

The experiments were repeated with three films for each concentration.

2-3-3 Examination of Hydrogel Films' Water Solubility

In order to examine the water solubility of hydrogel films, the (W0) films weighed before the experiment were left in a beaker containing 20 ml of distilled water and kept in a magnetic stirrer at 120 rpm at 25°C for 24 hours. The films were then removed from the water, dried with filter paper and reweighed (W1). Then, the water solubility of the films was calculated(Eq. 2).

$$Water\ solubility = \frac{W0-W1}{W1} x100 \quad (2)$$

The experiments were repeated with three films for each

2-3-4 Examination of Hydrogel Films' Water Storing Capacity

In order to determine the water retention properties of hydrogel films, first the dry films were weighed (W0), then they were thrown into pure water and kept in the oven at 25ºC for 24 hours. The films were then removed from the container and dried on filter paper for 5 minutes and the films were weighed (W1). The water holding capacity of the films was calculated (Eq. 3).

$$\text{Water storing capacity} = \frac{W1-W0}{W0} x100 \quad (3)$$

2-3-5 Investigation of Antibacterial Properties of Clove (Syzygium Aromaticum) Extract used in Hydrogel Films

To examine the antibacterial properties of the clove (Syzygium aromaticum) extract used in hydrogel films, gram-positive bacteria Staphylococcus aureus and a gram-negative bacterium Escherichia coli were used and the zone diameters of the extract were determined by agar diffusion method. After the bacteria were obtained from the university in our city, they were incubated at 37ºC for 24 hours in the medium before the study and the study was carried out with fresh bacteria. Bacteria were diluted to 0.5 McFarland using a McFarland Densitometer. After the prepared bacterial suspension was added to the media, wells with a diameter of 6 mm were opened in the middle of the media and 50 µL of extracts of different concentrations were added. After the bacteria in the media were incubated in the oven at 37ºC for 24 hours, the zone diameters formed in the medium were measured.

2-4 Monitoring and Investigation of the Decay Amount of the Food Wrapped in Hydrogel Film with Arduino System

MQ-2 (Gas Sensor) and DHT11 (temperature and humidity sensor) sensors were used to examine the spoilage amount of food wrapped in hydrogel film. The values read from the sensors used were transferred to the Blynk application over the internet via the Blynk library and the ESP-8266 Wifi module. The transferred data was checked and analyzed with the time-value graph on the application. As long as the ESP-8266 Wifi module is connected to the internet, a system has been created that can examine the data transferred from the Blynk application from any point in the world. The condition of the food wrapped in Hydrogel film was monitored with the system created.

2-5 Control of Films with Robotic System

2-5-1 Examination of Gas Amount in Closed Environment with MQ-2 Gas Sensor

In order to determine the shelf life of the food placed in the closed environment, the gas amount in the system was measured with the MQ-2 Gas sensor. When the obtained values are examined, the increase in gas in the system can be used to understand that there is an increase in bacteria. Because as the number of bacteria in the environment increases, the amount of gas produced as a result of the vital activities of the bacteria is expected to increase.

2-5-2 Inspection of Indoor Temperature with DHT-11 Temperature-Humidity Sensor

In order to estimate the shelf life of the food placed in the closed environment, the temperature of the environment was measured with the DHT-11 Temperature-Humidity sensor. When the obtained values are examined, the temperature increase can be used to understand that there is an increase in bacteria. It is expected that the vital activities performed by the bacteria will cause an increase in the ambient temperature. Bacteria and the increase in temperature in the environment are also one of the important causes of food spoilage.

Monitoring and Examining the Data Collected in the System over the Internet. The data obtained from the temperature-humidity and gas sensor were monitored over the internet using the Blynk application and library via the Arduino NodeMCU Wifi card. The collected data were analyzed in graphics and with SPSS (Fig.1).

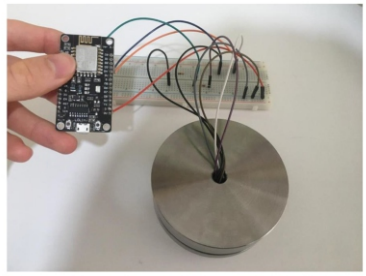

Fig. 1 : The Robotic System

3 Results and Findings

3-1 Results for Examining the Thickness of Hydrogel Films

Calipers were used to measure the thickness of the hydrogel films and average film thicknesses were calculated by taking three samples from each film. The measured film thicknesses are presented in Table (1).

Table (1) : Results regarding the thickness of hydrogel films

Extract Concentration Used in Film	Film Thickness (µm)
%100	208
%50	202
%25	212
%12,5	215
%0 (Control)	209

When Table 1 is examined, it is seen that the thicknesses of the films (for 100% -50% -25% -12.5% -0% (control) extract concentrations) are 208 µm, 202 µm, 212 µm, 215 µm and 209 µm, respectively.

3-2 Results for Investigation of Water Vapor Permeability of Films:

The measured values obtained to examine the water vapor permeability of hydrogel films and the calculated water vapor permeability of the films are presented in Table (2).

Table (2): Results regarding the water vapor permeability of hydrogel films

Extract Concentration Used in Film	W1 (g)	W2 (g)	A (m^2)	Water vapor permeability
%100	5.0554	4.6169	0.000314	1396.4968
%50	5.0193	4.5891	0.000314	1370.0637
%25	5.0315	4.6357	0.000314	1260.5095
%12,5	5.0358	4.6992	0.000314	1071.9745
%0 (Control)	5.0112	4.7713	0.000314	764.0127

When Table (2) is examined, the sample with the highest water vapor permeability is the sample with a concentration of 100%. Him respectively; 50% 25%; It is followed by films containing 12.5% and 0% (Control) Syzygium aromaticum (Clove) extract concentrations. The findings show that the addition of Syzygium aromaticum (Clove) extract to the films increases the water vapor permeability.

3-3 Results for Investigation of Water Solubility of Hydrogel Films

The measured values obtained to examine the water solubility of hydrogel films and the calculated water solubility of the films are presented in Table (3).

Table (3): Results regarding the solubility in water of hydrogel films

Extract Concentration Used in Film	W0 (g)	W1 (g)	Solubility in Water (%)
%100	0.0697	0.0628	9.90
%50	0.1366	0.1231	9.88
%25	0.1256	0.1133	9.79
%12,5	0.0946	0.0856	9.51
%0 (Control)	0.1458	0.1442	1.10

When Table (3) is examined, the findings obtained in the water solubility analysis of hydrogel films prepared with Syzygium aromaticum extract at different concentrations show that the water solubility of the films increases as the extract concentration increases. While the least soluble in water is the hydrogel film with a concentration of 0%, it is the most soluble film with a concentration of 100%.

3- 4 Results for the Investigation of the Water Holding Capacity of Hydrogel Films

The measured values obtained to examine the water holding capacity of hydrogel films and the calculated water holding capacity of the films are presented in Table (4).

Table (4): Results regarding the water holding capacity of hydrogel films

Extract Concentration Used in Film	W0 (g)	W1 (g)	Water Holding Capacity (%)
%100	0.0229	0.0697	204.37
%50	0.0133	0.0374	181.20
%25	0.0171	0.0439	156.72
%12.5	0.0157	0.0335	113.38
%0 (Control)	0.0190	0.0390	105.26

When Table (4) is examined, it shows that the hydrogel films prepared with Syzygium aromaticum (Clove) extract in different concentrations have the best water holding capacity, the one with 100% concentration. It was followed by 50%, 25%, 12.5% and 0%, respectively. As the concentration increases, the water holding capacity increases.

3-5 Results of the Antibacterial Properties of Syzygium aromaticum (Clove) Extract Used in Hydrogel Films

In order to examine the antibacterial properties of the extract obtained from Syzygium aromaticum (Clove) plant, bacteria were cultivated, 60 µl of extract was placed in 6 mm diameter wells and the zone diameters formed in the media after 24 hours of incubation were measured. The findings obtained are presented in Table (5).

Table (5). Results regarding the zone diameter for E. coli

Extract Concentration Used in Film	Zone Diameter for E. coli(mm)
%100	28
%50	24
%25	22
%12,5	19
%0 (Control)	6

When Table (5) is examined, the zone diameters of different concentrations of Syzygium aromaticum (Clove) extract (0%, 12.5%, 25%, 50% and 100%) in S. aureus and the zone diameters formed in the media in which E. coli are cultivated are 6 mm, 19 mm, 22 mm, 24 mm and 28 mm, respectively. It is seen that the zone diameter formed in the medium increases as the extract concentration increases.

3-6 Results of Investigation of Values from MQ-2 Gas Sensor and DHT-11 Temperature Sensors

When the water holding capacity, water vapor permeability, water solubility and antibacterial properties are examined, it has been seen that the hydrogel film containing 100% extract is a more suitable material for food storage than the others. Therefore, by using gas and temperature sensors, a closed environment in which 100% extract-containing hydrogel film is used was created, and measurements related to the food placed in this environment were taken, and as a control group, measurements of the food in an environment that did not use hydrogel film were compared. For the experimental group, the foods wrapped in hydrogel were kept in a closed container for 1 week. For the control group, the foods that were not wrapped in hydrogel were kept in a closed container for 1 week. The values taken from the temperature and gas sensors have been converted into tables (The values given by the sensors are numerical values that indicate the gas density or temperature change in the environment and are not expressed according to any unit. Therefore, the unit is avoided in the tables created. This is due to the presence of a single analog input on the NodeMCU. One of the circuit methods used when solving the problem of getting values from 2 sensors is to get values in Celcius format from the temperature sensor with the DHT-11 library) (Table 6).

Table (6): Values from MQ-2 and DHT-11 sensors for the experimental group

MQ-2	DHT-11	Day	Hour
163	191	Day 1 Morning	9.00
168	190	Day 1 Noon	12.00
175	192	Day 1 Evening	21.00
182	190	Day 2 Morning	9.00
186	191	Day 2 Noon	12.00
195	193	Day 2 Evening	21.00
203	193	Day 3 Morning	9.00
215	194	Day 3 Noon	12.00
232	193	Day 3 Evening	21.00
245	192	Day 4 Morning	9.00
261	196	Day 4 Noon	12.00
294	203	Day 4 Evening	21.00
314	211	Day 5 Morning	09.00
327	215	Day 5 Noon	12.00
331	219	Day 5 Evening	21.00
333	221	Day 6 Morning	09.00
337	222	Day 6 Noon	12.00
341	223	Day 6 Evening	21.00
339	221	Day 7 Morning	09.00
340	224	Day 7 Noon	12.00
342	223	Day 7 Evening	21.00

Table (7): Values from MQ-2 and DHT-11 sensors for the control group

MQ-2	DHT-11	Day	Hour
148	194	Day 1 Morning	9.00
153	195	Day 1 Noon	12.00
184	195	Day 1 Evening	21.00
202	198	Day 2 Morning	9.00
217	203	Day 2 Noon	12.00
235	209	Day 2 Evening	21.00
243	234	Day 3 Morning	9.00
231	246	Day 3 Noon	12.00
242	259	Day 3 Evening	21.00
321	267	Day 4 Morning	9.00
348	257	Day 4 Noon	12.00
336	256	Day 4 Evening	21.00
337	248	Day 5 Morning	09.00
335	251	Day 5 Noon	12.00
338	242	Day 5 Evening	21.00
335	231	Day 6 Morning	09.00
337	241	Day 6 Noon	12.00
336	224	Day 6 Evening	21.00
330	211	Day 7 Morning	09.00
324	225	Day 7 Noon	12.00
341	220	Day 7 Evening	21.00

When the tables were examined, when the results obtained from the experimental group were compared with the control group, it was observed that the temperature and gas increase in the experimental group was slower in the environment where the food was present. The data obtained from the experimental and control groups were compared with the t-test using the SPSS 22 program. The values obtained from the analysis of the obtained data with the t-test are presented in Table (8).

Table (8): T-test results of data obtained from MQ-2 and DHT-11 sensors in experimental and control groups

Sensor	Group	N	Ort.	SS	Sd	t	p
MQ-2	Example	21	263.000	69.9157	40	-.775	.443
	Control	21	279.667	69.5358			
DHT-11	Example	21	204.619	14.0658	40	-4.015	.000
	Control	21	228.857	23.8250			

When Table (8) is examined, it is seen that the mean temperature and gas density for both temperature and gas sensors are higher in the control group than in the experimental group. This situation shows that the temperature of the environment and the gas density in the environment increase when the food is placed in the environment without being wrapped in hydrogel film, in terms of the values obtained from both sensors. The increase in temperature and gas density in the environment is an important reason for food to spoil more easily. When the t-test was performed to examine whether the increase in temperature and gas density in the experimental and control groups was statistically significant, it was seen that the difference between the experimental and control groups was not significant for the gas sensor, but was significant for the temperature sensor. Although the difference between the groups in the gas sensor is not statistically significant, it should not be ignored that the mean of the control group is higher. When the values taken from both sensors and the statistical analysis are evaluated together, it can be said that the environment in which the hydrogel film produced can be a longer-term storage environment for foods.

When the studies in the literature are examined, food industry wastes (Yu, Chua, Huang, Lo and Chen, 1998), tequila pulp (Alva Munoz and Riley, 2008), corn cob (Bölükbaşı, 2012), algae (Özdemir and Erkmen, 2013; Civelek Yörüklü). , 2020), tea factory waste (Ersoy and Sutay Kocabaş, 2014), pomace (Demir and Sutay Kocabaş, 2014), fatty acid waste (Reddy, Amulya, Rohit, Sarma and Mohan, 2014), beverage waste (Elçiçek and Tanyıldızı, 2015), wastewater (Amulya, Reddy, Rohit, and Mohan, 2016; Yadav, Pandey, Kumar, and Tyagi, 2020), juice industry wastewater (Bezirhan Arıkan, et al., 2016), sage (Salvia tomentosa miller), black pepper thyme (Zahter, Thymbra Spicata) and lemon-scented thyme (Thymus zygioides) extracts (Afacan and Kundakcı, 2017), sea lettuce (Ulva lactuca) (Kılıç, 2017), banana peel, pepper stalk and red pine (Özdemir and Ramazanoğlu, 2019) , food waste (Karakuş and Ayhan, 2019), agricultural waste (Samer, et al., 2019), pumpkin (Berkol, 2020), corn husk (Gündüz, 2020) and Posidonia oceanica (Fidan, 2020) was used to produce storage material. In a significant part of these studies, the polymer production process was explained and various properties of the produced polymers were examined. The number of studies (Afacan and Kundakcı, 2017; Gündüz, 2020) in which trials were conducted directly on food is quite limited. In our study, various properties of the produced materials were examined, a direct controlled experiment was carried out on the food, and the results obtained from the gas and temperature sensors were analyzed statistically. Thus, it is thought that our study will contribute to the literature.

References

[1] Afacan, C. & Kundakcı, S. M. (2017). Ballıbabagiller familyasından bitki özütleri kullanılarak sentezlenen biyoplastiklerin besinlerin raf ömrünü uzatmaya etkisi. TÜBİTAK 11. Ortaokul Öğrencileri Araştırma Projeleri Final Yarışması Kitapçığı.

[2] Alva Munoz, L. E., & Riley, M. R. (2008). Utilization of cellulosic waste from tequila bagasse and production of polyhydroxyalkanoate (PHA) bioplastics by Saccharophagus degradans. Biotechnology and bioengineering, 100(5), 882-888.

[3] Amulya, K., Reddy, M. V., Rohit, M. V., & Mohan, S. V. (2016). Wastewater as renewable feedstock for bioplastics production: understanding the role of reactor microenvironment and system pH. Journal of Cleaner Production, 112, 4618-4627.

[4] Aydın, M. Ç. (2012). Fast food, television spectatorship, advertisements as a global mass culture and obesity. The Journal of Akdeniz University's Faculty of Communication, (16), 101-119.

[5] Bahçegül, E. (2011). Tarımsal atıkların çevre dostu plastiklere dönüşümü, Bilim ve Teknik, 251, 68-74.

[6] Berkol, B. (2020). Kendisinden adsorban, ligninden biyopolimer: balkabağı kabuklarından daha neler neler? TÜBİTAK 14. Ortaokul Öğrencileri Araştırma Projeleri Final Yarışması Kitapcığı.

[7] Bezirhan Arıkn, E. & Özsoy, H. D. (2014). Bitkilerden Biyoplastik Üretimi. Bursa Tarım Kongresinde sunulan bildiri.

[8] Bezirhan Arıkan, E., Özsoy, H. D., Abdullah, E. R. O. L., İslamoğlu, A., Kaya, D. N., & Çakmak, S. (2016). Investigation of Microbial Biopolymer Production from Fruit Juice Industry. Çukurova University Journal of the Faculty of Engineering and Architecture, 31(ÖS2), 205-210.

[9] Bölükbaşı, U. B., (2012) Mısır koçanından eş zamanlı olarak glikoz ve biyoplastik üretimi sürecinde ön işlem parametrelerinin incelenmesi chrome-extension://oemmndcbldboiebfnladdacbdfmadadm/https://open.metu.edu.tr/bitstream/handle/11511/50385/TVRJek5EYzM.pdf

[10] Civelek Yörüklü, H. (2020). Conversion of waste macroalgae collected from coastal area into useful products: The case of İstanbul, PhD Thesis, Yıldız Teknik University, İstanbul.

[11] Çelik, İ., & Tümer, G. (2016). New Developments in Food Packaging. Akademik Gıda, 14(2), 180-188.

[12] Demir, Ayşe Nur,Sutay Kocabaş, Didem"Zeytinyağı Endüstrisi Atığı Prinadan Biyobozunur Film Üretimi" Gıda Mühendisliği 5. Öğrenci Kongresi,2014.

[13] Dipova, N. (2017). Use of Open Source Development Platforms in Geotechnical Laboratory Solutions. Mehmet Akif Ersoy Üniversitesi Fen Bilimleri Enstitüsü Dergisi, 8(2), 153-160.

[14] Elçiçek, S., & Tanyıldızı, M. (2015). Production of hydroxymethylfurfural (hmf) for synthesis bioplastic and biofuel from beverages waste. Adıyaman Üniversitesi Mühendislik Bilimleri Dergisi, 2(3), 16-20.

[15] Ersoy, M., Sutay Kocabaş, D. (2014). "Çay Fabrikası Atıklarının Biyobozunur Film Üretimi İçin Değerlendirilmesi"Gıda Mühendisliği 5. Öğrenci Kongresi.

[16] Fidan, Z. (2020). Posidonia oceanica atıklarından üretilen biyoplastiğin ambalaj malzemesi olarak kullanımı. TÜBİTAK 14. Ortaokul Öğrencileri Araştırma Projeleri Final Yarışması Kitapcığı.

[17] Güler, Ç., & Çobanoğlu, Z. (1997). Plastikler. Sağlık Projesi Genel Koordinatörlüğü.

[18] Gündüz, M. T. (2020). Polivinil alkol esaslı mısır kabuğu/nanografen katkılı biyobozunur kompozitlerin karakterizasyonu ve ambalaj maddesi olarak kullanılabilirliğinin incelenmesi. TÜBİTAK 14. Ortaokul Öğrencileri Araştırma Projeleri Final Yarışması Kitapcığı.

[19] Güngör, İ. U., & Erkan, D. (2004). Contact Lenses: Physical Features of Materials and Types: Compilation. Deneysel ve Klinik Tıp Dergisi, 21(4).

[20] Hazer, B. (2011). Biyobozunur Plastik Ambalaj Malzemeleri "Çerçeve Çalışması". https://docplayer.biz.tr/HYPERLINK "https://docplayer.biz.tr/4198509-Biyobozunur-plastik-ambalaj-malzemeleri-cerceve-calismasi.html"4198509 HYPERLINK "https://docplayer.biz.tr/4198509-Biyobozunur-plastik-ambalaj-malzemeleri-cerceve-calismasi.html"-Biyobozunur-plastik-ambalaj-malzemeleri-cerceve-calismasi.html, 20.10.2020 tarihinde erişildi.

[21] Karakuş, E., Ayhan, Z. (2019). Productıon of envıronmentally frıendly bıodegradable packagıng materıals from food waste. The Journal of Food, 44 (6), 1008-1019 doi:

10.15237/gida.GD19102

[22] Kılıç, Z. (2017). Deniz marulu (Ulva lactuca)'dan organik ürünler elde ediyoruz. TÜBİTAK 11. Ortaokul Öğrencileri Araştırma Projeleri Final Yarışması Kitapcığı.

[23] Köksal, Ö., Er, B. A., Ardalı, Y., & Sağlam, M. (2019). Biodegradation of Bioplastics. Sinop Uni J Nat Sci, 4(2), 151-167.

[24] Özdemir, N., & Erkmen, J. (2013). Yenilenebilir biyoplastik üretiminde alglerin kullanımı. Karadeniz Fen Bilimleri Dergisi, 3(8), 89-104.

[25] ÖZDEMİR, F., & RAMAZANOĞLU, D. (2019). Atık muz kabuğu, biber sapı ve kızılçam odun unu kullanılarak biyoplastik kompozit üretimi. Türkiye Ormancılık Dergisi, 20(3), 267-273.

[26] Öztürk, S. (2020). Gıda Ambalajlama ve Depolama. Online: https://www.foodelphi.com/gida-ambalajlama-ve-depolama-yrd-doc-dr-serpil-ozturk/, 20.10.2020 tarihinde erişildi.

[27] PAGEV (Türk Plastik Sanayicileri Araştırma, Geliştirme ve Eğitim Vakfı). (2020). Dünya biyoplastik üretimi 2020 yılında 15 milyon tona çıkacak. 20.12.2020 tarihinde https://pagev.org/dunya-biyoplastik-uretimi- HYPERLINK "https://pagev.org/dunya-biyoplastik-uretimi-2020-yilinda-15-milyon-tona-cikacak"2020 HYPERLINK "https://pagev.org/dunya-biyoplastik-uretimi-2020-yilinda-15-milyon-tona-cikacak"-yilinda- HYPERLINK "https://pagev.org/dunya-biyoplastik-uretimi-2020-yilinda-15-milyon-tona-cikacak"15 HYPERLINK "https://pagev.org/dunya-biyoplastik-uretimi-2020-yilinda-15-milyon-tona-cikacak" -milyon-tona-cikacak adresinden alınmıştır.

[28] PAGEV (Türk Plastik Sanayicileri Araştırma, Geliştirme ve Eğitim Vakfı). (2019). Türkiye Plastik Ambalaj Sektör İzleme Raporu. İstanbul.

[29] Reddy, M. V., Amulya, K., Rohit, M. V., Sarma, P. N., & Mohan, S. V. (2014). Valorization of fatty acid waste for bioplastics production using Bacillus tequilensis: Integration with dark-fermentative hydrogen production process. international journal of hydrogen energy, 39(14), 7616-7626.

[30] Saçak, M. (1998). Polimer Kimyasına Giriş. http://dspace.ankara.edu.tr/xmlui/bitstream/handle/20.500.12575/9148/Polimer%20Kimyas%C4%B1na%20Giri%C5%9F.pdf?sequence=1&isAllowed=y,

[31] Samer, M. (2019). Bioplastics production from agricultural crop residues. Agricultural Engineering International: CIGR Journal, 21(3), 190-194.

[32] Sarıgül T. (2018) https://bilimgenc.tubitak.gov.tr/makale/plastikler-dunyayi-nasil-degistiriyor

[33] Şahin, N. N., Demir, Ö., İlsay, S., & Doğdubay, M. Biyoplastiklerin Yiyecek ve İçecek İşletmelerinde Kullanılabilirliği. The First International Congress on Future of Tourism: Innovation, Entrepreneurship and Sustainability.

[34] Sahiner, M., Sagbas, S., Turan, A., Erdugan, H., & Sahiner, N. (2018). Yara Collagen based Hydrogel Films as Wound Dressing Materials . Çanakkale Onsekiz Mart Üniversitesi Fen Bilimleri Enstitüsü Dergisi, 4(2), 103-116.

[35] Yadav, B., Pandey, A., Kumar, L. R., & Tyagi, R. D. (2020). Bioconversion of waste (water)/residues to bioplastics-A circular bioeconomy approach. Bioresource technology, 298, 122584.

[36] Yu, PH, Chua, H., Huang, AL vd. Gıda sanayi atıklarının biyoplastiklere dönüştürülmesi. Appl Biochem Biotechnol 70, 603–614 (1998). https://doi.org/ HYPERLINK "https://doi.org/10.1007/BF02920172"10.1007 HYPERLINK "https://doi.org/10.1007/BF02920172"/BF HYPERLINK "https://doi.org/10.1007/BF02920172"02920172

High Precision and Accuracy Temperature Sensor Design Using 1 Dimensional Defect Layered Photonics Crystals Composed of Air, TiO_2, InP, and Ta_2O_5 Layers

Hüseyin Ya˘gız Devre , Uskudar American Academy, Istanbul, Turkey, hdevre22@my.uaa.k12.tr

ARTICLE INFO

Gold medalist in IMSEF 2021 and Bronze medalist in ISAC Olympiad 2021
Accepted by Ariaian Young Innovative Minds Institute, AYIMI

http://www.ayimi.org , info@ayimi.org

ABSTRACT

First observed by Lord Rayleigh in 1887, the work of Eli Yablonovitch and Sajeev John in 1987 on photonics crystals is truly a revolution in physics. These crystals have many applications in many fields such as nanotechnology, solar cells and color displays in the era of modern civilization. Because these crystals only transmit waves within certain band gaps, they are widely used in electromagnetic applications. With these manipulations over the band gaps and transmittance, full control over electromagnetic waves can be achieved. Similar to other materials, these periodic structures are affected to temperature changes.

Key words: *Photonics Crystals Defect Modules High Sensitivity Temperature Sensor*

1 Introduction

In order to fully understand the characteristics of the periodic structure of photonics crystals formed by dielectric and superconductors, it is beneficial and crucial to examine the foundations of photonics crystals. Based on these foundations, the analysis of band gaps can also be carried out and examined more deeply.

1-1 Photonics Crystals

The dielectric periods, first observed by Lord Rayleigh in 1887, led to a complete revolution in photonics crystals in physics as a result of the work of Eli Yablonovitch and Sajeev John in 1987. In fact, photonics crystals are medians with dielectric properties that are periodically arranged [1].

This means that they are actually made up of dielectric and superconducting layers in an arranged sequence. Made using not only dielectrics, but also superconductors, semiconductors and metals, these periodic systems have crucial features that make them different. Because of these periodic structures, photonics crystals pass only certain frequencies and wavelengths in the electromagnetic spectrum such as light, preventing the spread of other wavelengths. The ranges in which these electromagnetic waves cannot pass are called band gaps.[2] Therefore, with this feature of photonic band gaps, a complete control can be established over electromagnetic spectrum (Fig. 1).

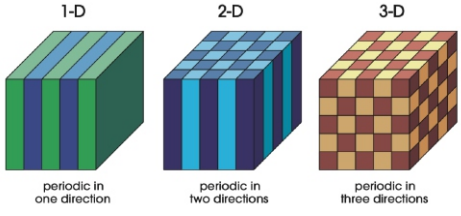

Fig. 1: 1D, 2D and 3D Periodic Photonic Crystal Topologies without Defect Modules [5]

As shown in Figure (1), photonic crystal structures can be created in 1 1D, 2D and 3D. And since only 3D periodic structures of these different topologies contains a versatile and all directional periodic structure, only 3D photonic crystal structures feature band gaps in all 3 directions[2].

1-2 Defect Modules

From the fundamental perspective, not all photonic crystals have to consist of only 2 materials. Essentially, it is possible to transform a perfect photonic crystal into an irregular photonic crystal byinserting or removing a different material called defect layer in certain layers of these dielectric materials that continue periodically.

As illustrated in Figure (2), in fact, there are 2 perfectly periodic dielectric materials in photonic crystals with single defects. On the contrary, a layer of defect is present, which is like a buffer between them. Furthermore, a defective structure can also be obtained by changing the thickness or location of a layer [3] .

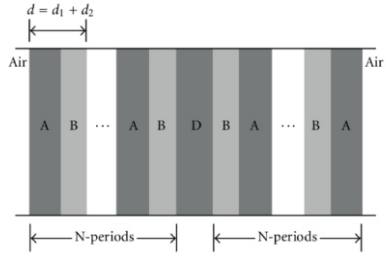

Fig. 2: Single Defect Layered 1D Photonic Crystal Structure [3]

Defect layers also significantly change the bandwidth of a periodic structure and form peak transmission values at certain band gaps where no transmission occurs in normal periodic structures [4]. Moreover, any temperature change in periodic systems can significantly change the band gap ranges in the structure, so that even the smallest temperature changes can be measured.

1-3 Band Gaps

Fundamentally, photonic band gaps occurs on ranges of values were given Maxwell Equations (1), (2), and (3) have no real solution of ~k wave vectors.

$$\vec{\nabla} \times \frac{1}{\varepsilon}\vec{\nabla} \times \vec{H}(\vec{r}) = \left(\frac{\omega}{c}\right)^2 \vec{H}(\vec{r}) \quad (1)$$

$$\hat{\Theta} = \vec{\nabla} \times \frac{1}{\varepsilon}\vec{\nabla} \quad (2)$$

$$\hat{\Theta}\vec{H}(\vec{r}) = \left(\frac{\omega}{c}\right)^2 \vec{H}(\vec{r}) \quad (3)$$

Furthermore, using the Bloch-Floquet Theorem described in (4), the equation (5) can be derived.

$$\vec{H}(\vec{r}) = e^{i\cdot\vec{k}\cdot\vec{r}}\vec{H}_{n,\vec{k}}(\vec{r}) \tag{4}$$

$$\left(\vec{\nabla}+i\vec{k}\right)\times\frac{1}{\varepsilon}\left(\vec{\nabla}+i\vec{k}\right)\times\vec{H}_{n,\vec{k}} = \left(\frac{\omega_n\left(\vec{k}\right)}{c}\right)^2\vec{H}_{n,\vec{k}} \tag{5}$$

The value n in (5) is essentially a positive integer, therefore this indicates discrete eigenvalues of n. In such a case, even though n is a continuous function, when it is plotted with varying n values, the specific separations can be observed where no such eigenvalue for n is obtained. These separations, as stated earlier, are essentially the band gaps of the given ~k wave vectors. These band gaps can be represented as in Figure (3).

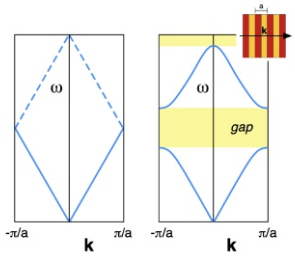

Fig. 3: Band Gap for a 1D Photonic Crystal[2]

2 Purpose and Rationale

This band gap can be manipulated much more effectively with the use of aperiodic and irregular structures obtained by inserting or removing a different superconducting or dielectric material inside the periodic structure, which is fundamentally a defect layer. Because of the thermo optic and thermal expansion effects on defect layers, the structural properties of the defective layers used is highly affected by the environmental temperature differences. The change in temperature changes the refractive index and thickness of the defective layer, resulting in a detectable change in the band gap. By observing this change in the band gap region, temperature change can be measured very precisely with defected photonic crystals. This research project examines the 1D triple defect layered photonic crystal structures of different dielectric and superconducting mixtures and finds the most effective and precise sensor design according to permeability and transmittance in mathematical and simulation-based methods.

3 Literature Review

3.1 Historical Background

In fact, the periodic placement of dielectric materials began to be examined on by Lord Rayleigh in 1887. In Lord Rayleigh's 1917 article "On the Reflection of Light from a Regularly Stratified Medium"[7], he made some determinations on the bandwidth and permeability(transmittance) of 1D dielectric material structures.

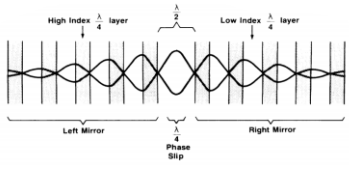

Fig. 4: Fabry-Pérot Interferometer Created with 1D Dialectic Defective Photonic Structure[8]

However, research on photonic crystals did not progress much until Eli Yablonovitch's "Inhibited Spontaneous Emission in Solid-State Physics and Electronics"[8] in 1987 and Sajeev John's "Strong Localization of Photons in Certain Disordered Dielectric Superlattices"[9] in 1987. In these two articles, unlike before, various studies were made in multidimensional geometric topologies. These studies can be illustrated as in Figure 4 and Figure (5).

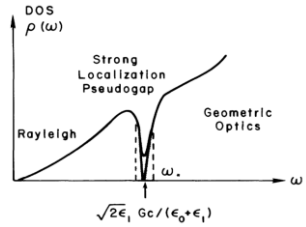

Fig. 5: Photon Density Graph at Low and High Frequencies for An Irregular Super Lattice Structure[9]

3.2 Current State of the Art

The use of photonic crystals in temperature sensor design is actually a subject that has been researched for decades. In 2010, in an article titled "Multicore Photonic Crystal Fiber Thermal Sensors" [10] prepared by a group of researchers at Villanova University in the USA, presented a 1, 2 and 3 core sensor design that can measure the temperature changes with a margin of error of 3.6% for temperatures of <0.2 °C with 0.0036nm K .

In 2015, researchers at Shandong University of Technology published a paper titled "Low-Temperature Sensor Based on One-Dimensional Photonic Crystals with a Dielectric- Superconducting Pair Defect"[11] presenting a temperature sensor design that can measure 0.0096nm K in precision using both dielectric and superconducting defect layers. Similarly, in another article published in 2012, 0.001nm K value of sensitivity was obtained using aperiodic irregular (defective) 1D photonic crystal obtained by removing only one layer from aperiodic system[12].

In a 2018 study titled "Designing a Temperature Sensing Device Using an Defect Based Photonic Crystal"[6] in Turkey, the sensor design obtained using indium antimonite as a defective layer achieved a sensitivity of 0.077nm K .

4 Method

First of all, it is necessary to examine the structure of a perfect 1D photonic crystal before examining the structure of a 1D photonic crystal containing irregularities. Therefore, it is crucial and beneficial to make calculations of the periodic part initially, which is essentially the main element of the whole system. In this process it is necessary to represent each layer in the periodic system through an individual matrix. Therefore, calculations can be made using this Transfer Matrix Method(TMM)[12][16].

By using the different combinations of these matrices with each other, it is possible to obtain different photonic crystal structures. To accomplish these combinations, high and low refractive index layers of the regular periodic structure made of 2 materials can be represented as H (High) and L (Low) respectively. Based on this, a perfect periodic structure with only two layers, it can be shown as a periodic order of H L. If this system contains a total of 2N layers, the expression for this 1D photonic crystal is obtained as in equation (6).

$$(H\cdot L)(H\cdot L)(H\cdot L)\ldots(H\cdot L)(H\cdot L) = (H\cdot L)^N \tag{6}$$

Similarly, for a 1D photonic crystal with only one defect layer D and 2N + 1 layers the periodic order can be represented as equation (7).

$$(H \cdot L) \dots (H \cdot L)\ (Defect)\ (H \cdot L) \dots (H \cdot L) = (H \cdot L)^{\frac{N}{2}}\ (Defect)^{1}\ (H \cdot L)^{\frac{N}{2}} \quad (7)$$

The matrices can be defined for the transfer matrix of layers containing high refractive index as MHigh, low refractive index as MLow, and defect layers as MDefect. From here, transfer matrices can be expressed as multiplication of "D" dynamic and "P" propagation matrices. These expressions
are written as equation (8).

$$\begin{aligned} M_{High} &= D_{High} \cdot P_{High} \cdot D_{High}^{-1} \\ M_{Low} &= D_{Low} \cdot P_{Low} \cdot D_{Low}^{-1} \\ M_{Defect} &= D_{Defect} \cdot P_{Defect} \cdot D_{Defect}^{-1} \end{aligned} \quad (8)$$

Each D dynamic matrices represented as equation (8) can be written as equations described in (9). Furthermore, each P propagation matrix can be represented as equation (10). In equation (10), ~ k refers to the wave vector described in equation (5), n refers to the refractive index of the material selected for the layer, and d refers to the thickness of the layer. Similarly, shows the phase in the selected layer.

$$D_\alpha = \begin{pmatrix} 1 & 1 \\ n_\alpha \cos\Theta_\alpha & -n_\alpha \cos\Theta_\alpha \end{pmatrix} \Rightarrow \text{If } \vec{E} \text{ electric field vector is perpendicular to the propagation}$$

$$D_\alpha = \begin{pmatrix} \cos\Theta_\alpha & \cos\Theta_\alpha \\ n_\alpha & -n_\alpha \end{pmatrix} \Rightarrow \text{If } \vec{H} \text{ magnetic field vector is perpendicular to the propagation}$$

$$\alpha \equiv High,\ Low,\ Defect$$

$$P_\alpha = \begin{pmatrix} e^{i\phi_\alpha} & 0 \\ 0 & e^{-i\phi_\alpha} \end{pmatrix} \quad (9)$$

$$\phi_\alpha = k_\alpha d_\alpha$$

$$\begin{aligned} k_\alpha &= \frac{2\pi n_\alpha}{\lambda} \\ \phi_\alpha &= \frac{2\pi n_\alpha}{\lambda} d_\alpha \end{aligned} \quad (10)$$

As a result, the transfer matrix defined for a single layer is written as equation (11).

$$M_\alpha = \begin{pmatrix} \cos\phi_\alpha & \frac{-i}{n_\alpha}\sin\phi_\alpha \\ -in_\alpha \sin\phi_\alpha & \cos\phi_\alpha \end{pmatrix} \quad (11)$$

Since this research project examines 1D photonic crystals made using 3 defective materials, the transfer matrix MT defined for the definition of the whole crystal can be done with equation (12).The coefficient of transmittance can be calculated as equation (13).

$$M_{Total} = (M_{High} \cdot M_{Low})^{\frac{N}{2}}\ (M_{Defect_1} \cdot M_{High} \cdot M_{Defect_2} \cdot M_{Low} \cdot M_{Defect_1})$$

$$(M_{High} \cdot M_{Low})^{\frac{N}{2}} \quad (12)$$

$$T = \frac{4}{(M_{T_{11}} + M_{T_{22}})^2 + (M_{T_{12}} + M_{T_{21}})^2} \quad (13)$$

As shown in equation (12) 4 materials will be used in this research project to calculate the matrix operations. As shown in equation (9) and (10) the thickness d and refractive indices n of these selected materials must be determined in order to calculate the matrices. Finally, the Python programming language, NumPy library, and the Matplotlib library were used to calculate and visualize the expressed matrix operations in this project.

5 Results

As stated in the method section, the sensor design on which this research project is concentrated fundamentally consists of 4 different materials in nanoscale. While 2 of these materials continue periodically, the other 2 are selected only for layers of irregularity, defect layers. Since the selected periodic materials will form a basis over the photonic crystal structure, they are crucial for this project. Therefore, in this perspective, the thickness and refractive index of the selected materials should be taken into account.

Table (1): Determination of Periodic High and Low Index of Refraction Dielectric Layers

Material Name	Chemical Formula	Index of Refraction n_α	Thickness d_α *nm*	$n_\alpha \cdot d_\alpha$ *nm*
Air	*N/A*	*1.0*	*1110.7*	*1110.7*
Titanium Dioxide	TiO_2	*3.83*	*290*	*1110.7*

In order for the experiment to function properly and consistently, the two selected materials must have the same result when their thickness and their refractive indices are multiplied. At the same time, the sensor should take up as little space as possible, but in doing so should be able to give the greatest differentiation in the refractive index. Air is preferred for the low refractive index "L" because the air has a low in refractive index, and it is easy to use. Similarly, Titanium Dioxide was preferred for the high refractive index "H" layer because it demonstrates a high refractive index in a thin layer. The total transfer matrix for a 12-layer periodic system consisting only of Air and Titanium Dioxide can be shown with equation (14).

$$M_{Total} = (M_{TiO_2} M_{Air})^6 \quad (14)$$

The refractive indices of the titanium dioxide layer and air layers ($nTiO_2$ and nAir respectively) and the thickness of these layers (nHava and nHava) are given in Table 1. Based on this data, the transmittance versus wavelength graph in for this perfect periodic system can be drawn as in Figure (6).

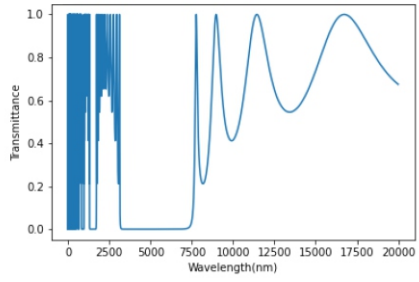

Fig. 6: The Graph of Transmittance VS Wavelength for a Perfect Photonic Crystal with TiO2 and Air Layers

As can be seen from Figure (6), there is a band gap range between approximately 3000 nm and 7500 nm for the perfect 1D photonic crystal with TiO2 and Air layers. No incident electromagnetic wave with the wavelength within the boundaries of this band gap passes through the photonic crystal.

Therefore, there is no transmittance in this region. To more effectively analyze values between 1 nm and 2000 nm, Figure (7) can be used. As can be seen from Figure 7, this 12-layer crystal structure can form repeated band gaps where no transmittance occurs.

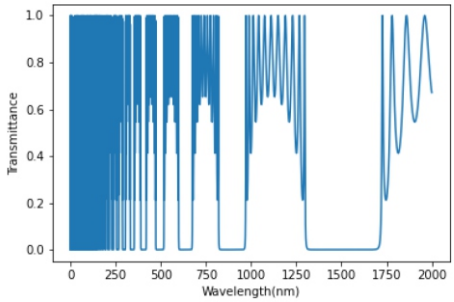

Fig.7: The Zoomed Graph of Transmittance VS Wavelength for a Perfect Photonic Crystal with TiO2 and Air Layers

As mentioned earlier, Figures (6) and (7) are designed for a non-defected periodic crystal. To achieve the structure in equation (12) two defect layers must be selected. This selection will be made from the materials specified in Tables (2)and (3).

Table (2): Determination of Two Defect Layers for the Photonic Crystal

Material Name	Chemical Formula	Index of Refraction n_α	Thickness d_α *nm*
Silicon Dioxide	SiO_2	*1.46*	*500*
Tantalum Pentoxide	Ta_2O_5	*2.16*	*500*
Indium Phosphide	InP	*3.80*	*500*

Table (3): Thermal Expansion and Thermo-optic Effect Coefficients of Materials on Table (2)

Material Name	Chemical Formula	Thermal Expansion Coefficient $\alpha\,(\frac{1}{K})$	Thermo-optic Coefficient $\beta\,(\frac{1}{K})$
Silicon Dioxide	SiO_2	*1.46*	*500*
Tantalum Pentoxide	Ta_2O_5	*2.16*	*500*
Indium Phosphide	InP	*3.80*	*500*

The materials contained in Tables (2) and (3) which has a high thermal expansion coefficient show a much greater expansion when exposed to the same temperature change as others. Therefore, since the refractive index of Tantalum Pentoxide, Ta2O5, at 500 nm thickness is higher and the thermal expansion coefficient is much higher than other materials, it has been selected for the defect layer Defect2. Similarly, due to its high refractive index and thermo-optical coefficient, Indium Phosphide InP, it was selected for the Defect1 defect layer. As a result, the transfer matrix shown in equation (15) was obtained.

$$M_T = (M_{TiO_2} \cdot M_{Air})^3 \, (M_{InP} \cdot M_{TiO_2} \cdot M_{Ta_2O_5} \cdot M_{Air} \cdot M_{InP}) \, (M_{TiO_2} \cdot M_{Air})^{\infty} \quad (15)$$

Based on the matrix shown in the equation (15), the graph in Figure (8) can be calculated. Compared to Figure (6), it can be understood that there is transmittance between 3000-7500 nm, which was the band gap for Figure 6. Moreover, Figure 9 is obtained for the range of 3000-7500 nm to further analyze the transmittance values.

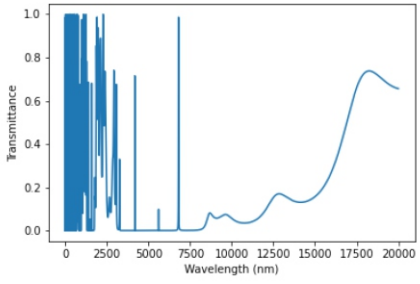

Fig. 8: The Graph of Transmittance VS Wavelength for a Defected Photonic Crystal With TiO2 and Air Periodic and InP and Ta2O5 Defective Layers

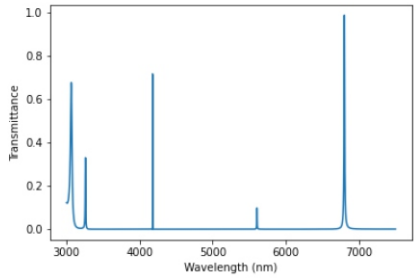

Fig. 9: The Zoomed Graph of Transmittance VS Wavelength for a Defected Photonic Crystal with TiO2 and Air Periodic and InP and Ta2O5 Defective Layers

Based on Figure (9), it is possible to design a temperature sensor that can operate within wavelengths of 5600-7500 nm. For this temperature sensor, the defect layers of InP and Ta2O5 are used. Furthermore, it would be possible to calculate the precision value from the Figure (9). To calculate this, it is needed to model how thickness and refractive index of the material changes under a temperature change. Finally, because the refractive index and thickness is changing, the transmittance changes. To calculate the precision, the shift in transmittance due to the temperature change should be modeled. In order to model this change, it is first necessary to use the Thermal Expansion Coefficient() and Thermo-Optical Coefficient() in Table 3. To model the change, the equations (16) and (17) are used for this.

$$d = d_0 \, (1 + \alpha \Delta T) \quad (16)$$

$$n = n_0 + \beta \Delta T \quad (17)$$

The new graphic representing the temperature change using the equations in (16) and (17) is shown in Figure (10).

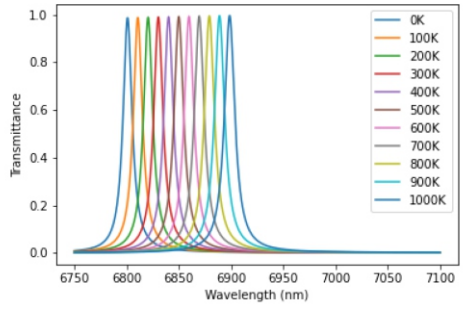

Fig. 10: The Graph of Transmittance VS Wavelength for a Defected Photonic Crystal with TiO2 and Air Periodic and InP and Ta2O5 Defective Layers With Varying Temperature

The sensitivity of the sensor proposed in this article can be found by calculating the temperature dependent change of peak wavelengths in the graph in Figure (10). The temperature-related change of peak wavelengths is shown in Figure (11). By calculating the slope of the graph in Figure (11), a precision value of the sensor is obtained as 0.0978 nm K , which is a more precise value than the sensors presented in all research mentioned at the current level. This proposed state-of-the-art sensor design presented with this research project is given in Figure 12. Considering the melting temperatures of solids used(TiO2, InP, and Ta2O5 respectively), this proposed sensor has can work up to 1335.15 K which is the melting point of InP.

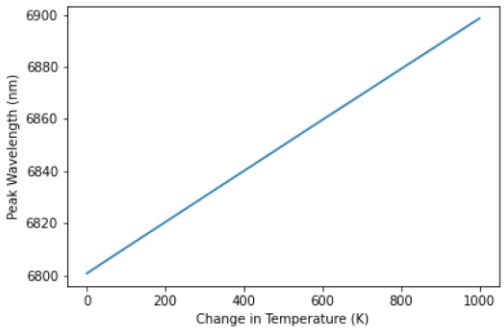

Fig.11: The Graph of the Proposed Sensor's Peak Wavelength VS TemperatureChange

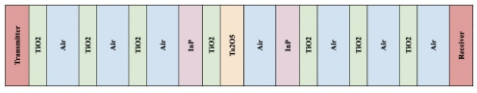

Fig. 12: Proposed Sensor Structure with 0.0978 nm/K Precision

6 Conclusion

The new state-of-the-art crystal proposed by this research article consists of Air, TiO2, InP, and Ta2O5 layers. It has a sensitivity value of 0.0978 nm/K , which is the most precise and wide measurement ranges ever calculated. This value is a sensitivity far beyond the other values specified at the current level. Moreover, it has a much wider working range with a maximum operating temperature of 1335.15 K. This proposed sensor has a width of 11.3 m which can be used for temperature monitoring on patients for intelligent diagnostics.

In this research project, a 1D photonic crystal temperature sensor with 3 defect layers was designed using mathematical calculations. However, due to the Covid-19 pandemic, calculations were made using only computer simulations. Therefore, this project was developed with mathematical simulations. Its performance in the real laboratory environment is an important topic of discussion. The production and testing of this sensor proposed in this research project will prove firsthand evidence on the accuracy of the project's thesis. For this reason, it is very important to test this sensor in a laboratory environment. Similarly, calculations were made on a 1D photonic crystal in this project. However, the precision of photonic crystals of 2D and 3D shapes can be calculated, produced, and tested for further investigation.

References

[1] L., O., S., V., Ya., R., E., Y. (2011). Electromagnetic wave propagation in two-dimensional photonic crystals. Wave Propagation. doi:10.5772/14165

[2] Johnson, S. (2003). Introduction to Photonic Crystals : Bloch ' s Theorem , Band Diagrams , and Gaps (But No Defects).

[3] Kumar, A., Kumar, V., Suthar, B., Bhargava, A., Singh, K.S., Ojha, S. (2012). Wide Range Temperature Sensors Based on One-Dimensional Photonic Crystal with a Single Defect. International Journal of Microwave Science and Technology, 2012, 1-5.

[4] Guida, G., De Lustrac, A., Priou, A. C. (2003). An introduction to photonic band gap (pbg) materials. Progress In Electromagnetics Research, 41, 1-20. doi:10.2528/pier02010801

[5] Joannopoulos, J. D., Johnson, S. G., Winn, J. N.,, Meade, R. D. (2008). Photonic Crystals: Molding the Flow of Light (Second Edition). Princeton University Press. ISBN: 0691124566

[6] Unsal, M. (2018). Designing a Temperature Sensing Device Using a Defect Based Photonic Crystal. https://www.academia.edu/37524884/Designing a Temperature Sensing Device Using a Defect Based Photonic Crystal

[7] On the reflection of light from a regularly stratified medium. (1917). Proceedings of the Royal Society of London. Series A, Containing Papers of a Mathematical and Physical Character, 93(655), 565-577. doi:10.1098/rspa.1917.0040

[8] Yablonovitch, E. (1987). Inhibited spontaneous emission in solid-state physics and electronics. Physical Review Letters, 58(20), 2059-2062. doi:10.1103/physrevlett.58.2059

[9] John, S. (1987). Strong localization of photons in certain disordered dielectric superlattices. Physical Review Letters, 58(23), 2486-2489. doi:10.1103/physrevlett.58.2486

[10] Coompson, J., Colalillo, A., Twigg, S., amp; Wynne, R. (2010). Multicore photonic crystal fiber thermal sensors. 2010 IEEE Sensors. doi:10.1109/icsens.2010.5691019

[11] Wu, J., Gao, J. (2015). Low temperature sensor based on one-dimensional photonic crystals with a dielectric-superconducting pair defect. Optik, 126(24), 5368-5371. doi:10.1016/j.ijleo.2015.09.148

[12] Chang, Y., Jhu, Y., amp; Wu, C. (2012). Temperature dependence of defect mode in a defective photonic crystal. Optics Communications, 285(6), 1501-1504 doi:10.1016/j.optcom.2011.10.053

[13] Ramanujam, N., Wilson, K. J., Revathy, V., Lenin, M. M., Jothy, V. B. (2015). Properties of one Dimensional photonic crystals with Defects thickness and temperature dependence. Materials Today: Proceedings, 2(3), 959-964. doi:10.1016/j.matpr.2015.06.016

[14] Thompson, R. (1990). Optical waves in layered media. Journal of Modern Optics, 37(1), 147-148. doi:10.1080/09500349014550171

[15] Born, M., Wolf, E., Bhatia, A. B., Clemmow, P. C., Gabor, D., Stokes, A. R., . . . Wilcock, W. L. (1999). Principles of optics. doi:10.1017/cbo9781139644181

[16] Missoni, L. L., Ortiz, G. P., Martínez Ricci, M. L., Toranzos, V. J., Mochán, W. L. (2020). Rough 1d photonic crystals: A transfer matrix approach. Optical Materials, 109, 110012. doi:10.1016/j.optmat.2020.110012

[17] Li, Z. (2005). Principles of the plane-wave transfer-matrix method for photonic crystals. Science and Technology of Advanced Materials, 6(7), 837-841. doi:10.1016/j.stam.2005.06.013

[18] Filmetrics, I. (n.d.). Refractive index database. Retrieved February 23, 2021, from https://www.filmetrics.com/refractive-index-database

[19] RefractiveIndex.INFO. (n.d.). Retrieved February 23, 2021, from https://refractiveindex.info/

[20] Wu, C., Hung, Y., Fan, R., Ou, D., Huang, J., Yen, T., . . . Lee, C. (2019). Tantalum pentoxide (ta2o5) based athermal micro-ring resonator. OSA Continuum, 2(4), 1198. doi:10.1364/osac.2.001198

[21] Coefficients of linear thermal expansion - SILVER CTE: Mse Supplies L. (n.d.). Retrieved February 23, 2021, from https://www.msesupplies.com/pages/list-of-thermal-expansion-coefficientscte- for-natural-and-engineered-materials

[22] Elshaari, A. W., Zadeh, I. E., Jons, K. D., Zwiller, V. (2016). Thermo-Optic characterization of silicon Nitride resonators for CRYOGENIC Photonic circuits. IEEE Photonics Journal, 8(3), 1-9. doi:10.1109/jphot.2016.2561622

[23] Della Corte, F. G., Cocorullo, G., Iodice, M., Rendina, I. (2000). Temperature dependence of the thermo-optic coefficient OF Inp, GaAs, and sic from room temperature to 600 K at the wavelength of 1.5 M. Applied Physics Letters, 77(11), 1614-1616.

End-to-end Encrypted Native Software Using the Sieve of Eratosthenes and Binet Formula MA_T CHAT / MA_T SOHBET

Mehmet Akif Karakaş and Taylan Yalçın, İzmir Fen Lisesi, yalcin.taylan02@gmail.com

ARTICLE INFO

Gold Medalists in IMSEF 2021 , Izmir Turkey and Silver Medalists in ISAC Olympiad 2021Tehran, Iran
Accepted by Ariaian Young Innovative Minds Institute,AYIMI

http://www.ayimi.org , info@ayimi.org

ABSTRACT

If the need-to-know principle is seen as the basic principle of opposing intelligence, the question "Is it possible for scientists to correspond in a secure and location-independent manner on subjects with a high degree of confidentiality?" may arise. Our MA_T Chat software, which was created with the Python Programming Language, is proof that it is possible to securely communicate between two points without data loss, with a system consisting of two separate encryption, two separate hashing algorithms and shelling over the TCP/IP Reference Model.

Key words: *Encryption, Hash, Eratosthenes, Binet, Algorithm*

1 Introduction

The principle of need-to-know, defined in the three paragraphs of Article 4 of the Defense Industry Security Regulation, published in the Official Gazette No. 27601 and dated 04.06.2010, states that we must encrypt our highly confidential information while moving it from one point to another.

In the conversation between a scientist at T point and a scientist at MA point, if information with a high confidentiality level is shared, end-to-end encryption may be preferred here.

Although Ermoshina, Musiani and Halpin created an overview of end-to-end encryption protocols in 2016, in 2017 Musiani and Ermoshina asked "What is a good secure messaging tool?" In their article on the question "If your keys are stolen, will past communications be safe?" With the question of the theft of keys used in encryption, it has opened up discussion. AIM reviewed BlackBerry Messenger, BlackBerry Protected, Ebuddy XMS, Facebook Chat, and ChatSecure+Orbot. Only in ChatSecure+Orbot did the theft of the key not compromise the security of past communications. In other words, we can say that only end-to-end encryption is not enough.

In 2016, Yılmaz and Ballı compared the confidentiality, integrity, authentication, non-repudiation, performance and security features of Symmetric and Asymmetric Encryption Algorithms in their work on Developing an Intelligent Selection System for the Use of Data Encryption Algorithms. They determined that the security feature depends on the key length. They also revealed that symmetric algorithms have faster performance than asymmetric algorithms.

In 2018, Chakraborty, Jana, Mandal, and Kule showed that neural network-based RSA provides better results than Standard RSA scheme in performance analysis. A Comparative Study of Different Techniques for Basic Testing in RSA Implementation by Banerjee, Mandal, and Das, published in 2020, and Comparative Studies of Rathod, Sreenivas, Chandavarkar, from Beginning to Present, Between RSA Algorithm and Variants in RSA Application, published in 2020, still continue to face the dilemma of security and performance in asymmetric encryption algorithms. reveals that.

To solve this current situation, it is necessary to work on encryption algorithms that can simultaneously provide the performance speed of symmetric encryption and the strong security of asymmetric encryption. It is also necessary to research for a correspondence software that uses these algorithms.

While doing this research, it should be taken into account that while some scientists are dealing with cryptography or steganography, some scientists are dealing with cryptanalysis or steganalysis. In their article Cryptography and Cryptanalysis: A Review published in 2013, Tiwari, Nandi and Mishra used encryption (cryptography) and encryption analysis (cryptanalysis) methods, and in their article published in 2014 named Review of various steganalysis techniques, Kaur and Kaur used text hiding (steganography) and hidden text. They talked about finding (steganalysis) techniques.

Safitri, Ali and Ibrahim used the graph regarding the pre-cryptanalysis in their article entitled Cryptology Techniques and Methodologies (Fig. 1).

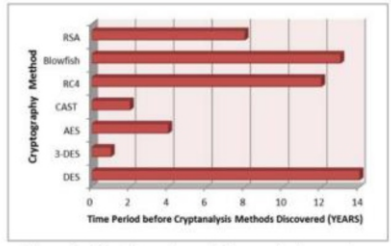

Fig.1: Visual Overview of Cryptanalysis over time

Carroll and Martin (1986) The automated cryptanalysis of substitution ciphers. With their work called Cryptologia, they emphasized that the password can be cracked according to the usage frequencies of the characters.

There are three types of cryptanalysis that tries to decrypt only ciphertext, known ciphertext and raw text pairs, and selected raw text or selected ciphertext.

Considering all these, it may be worth examining the question of what would be the result of developing a system that can be resistant to cryptanalysis, instead of creating and using an encryption algorithm, and using encryption and hashing algorithms together.

Starting from this point, we started our research on T

encryption and T hashing algorithm and shelling of MA encryption and MA hashing algorithms.

2 Main Aim

With the current version of our MA_T Chat software created with Python Programming Language, it is aimed to prove that it is possible to securely communicate between two points without data loss, with a system consisting of two separate encryption, two separate hashing algorithms and shelling that we created over TCP/IP Reference Model. Our second aim is to produce prime numbers by using the Sieve of Eratosthenes and to examine the effect of using these numbers in character-level encryption and shifting algorithms on the complexity of the operation.

Our final goal is to analyze a chat software created with the Caesar encryption algorithm in terms of frequency analysis with the MA_T Chat software we created.

3 Method

3-1 T Encryption Method

The T encryption algorithm encrypts the raw data as shown in the screenshot (Fig. 2).

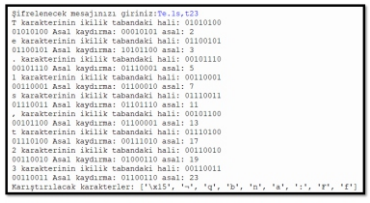

Fig.2: Screenshot 01 – Application of T Encryption Method

A prime number equal to the number of characters of the data to be encrypted is generated. This prime number sequence starts from 2 and grows without skipping prime numbers, forming a set with as many elements as the number of characters in the data. Each character in the data is matched with the prime number sequence on the condition that their indices (orders) remain the same. For each character, first the character is converted to binary. It is shifted bitwise to the right by the prime number to which it is mapped. The resulting new binary number is converted to a character in the ASCII table. These characters are stored in a list. Thus, our data is encrypted.

While the standard algorithm used when creating prime numbers has O(n2) complexity, this complexity is reduced to O(nloglogn) by using the Sieve of Eratosthenes in the T encryption algorithm. This increases the performance speed. Since each character will match a different prime number according to its location, its image will be a different character. Thus, it will not be possible to easily match in frequency analysis during cryptanalysis. In addition, the space characters that separate the words from each other may remain as spaces in the encrypted data after the data is processed, while some of them may turn into a different character. Thus, word detection will not be possible by looking at the spaces (Fig.3).

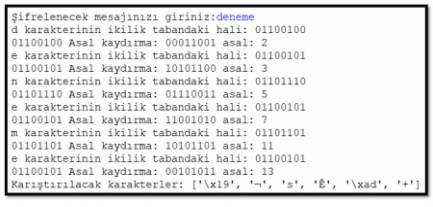

Fig. 3: Screenshot 02 – The letters "e" in the word "deneme" are paired with different characters according to their place in the word. ['¬','Ê','+']

3-2 T Hashing Method

How the raw data encrypted with the T encryption algorithm is mixed with the T hashing algorithm is shown in Figure (4).

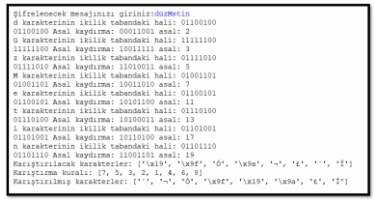

Fig. 4: Screenshot 03 – T Encryption and then T Hash algorithm is applied to the word "düzMetin".

The T Hash Algorithm first creates a set of counting numbers from 1 to the number of characters of the encrypted data. In this set, if any, prime numbers are found first and they are ordered from largest to smallest. The remaining elements of the set are ordered from smallest to largest, and these two lists are combined. The character order of the encrypted text is rearranged according to the resulting list. Thus, our data is encrypted.

Since the presence of prime numbers in the hashing algorithm uses the already created prime number list for the T Encryption Algorithm, the complexity of the T Hash Algorithm is O(n).

Changing the number of prime numbers to be used in hashing according to the character length of the ciphertext and changing the spaces in the ciphertext will make the decryption more difficult compared to the unscrambled cipher during cryptanalysis.

3-3 MA Encryption Method

It is similar to the T Encryption algorithm. The only difference is that the Fibonacci sequence is used instead of the prime number sequence for shifting. If the calculation of the Fibonacci sequence is done iteratively, it is O(n) and if it is done recursively, it is O(2n) complexity. When we use the matrix form, the Fibonacci sequence is calculated with O(logn) complexity. We can find O(1) complexity by memorizing with dynamic programming. n. For the Fibonacci number, Binet (18th century French mathematician Jacques Binet) produces a number of O(1) complexity (Eq. 1).

$$\text{Fib}(n) = \frac{\text{Phi}^n - (-\text{Phi})^{-n}}{\sqrt{5}} = \frac{\text{Phi}^n - (-\text{phi})^n}{\sqrt{5}} \quad (1)$$

The Fibonacci number calculation algorithm used in the MA Encryption Method is a dynamic programming and memorization algorithm.

3-4 MA Hashing Method

To shuffle it is necessary to create a new sequence. The integer number closest to the total number of characters is taken and the characters are grouped according to their square root. Afterwards, each group is mixed in itself so that the right and left sides are swapped. The data is mixed according to the new order created (Fig. 5).

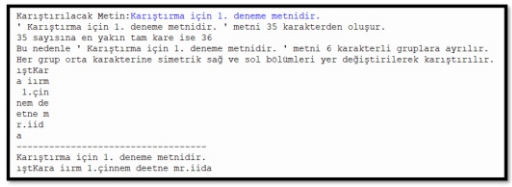

Fig. 5: Screenshot 04 – Example Application of MA Hashing Algorithm

3-5 Shelling of Encryption and Hashing Methods

For correspondence between point T and point MA, the original message is created at point T. The original message is encrypted with the T encryption algorithm using the sequence of prime numbers and mixed with the T hashing algorithm, taking its first form and sent to the MA point. The T hashing algorithm is applied in reverse, the message is encrypted with the MA encryption using the Fibonacci number sequence, mixed with the MA hashing algorithm, and sent back to the T point, taking its second form. At T point, first the MA hashing algorithm and then the T encryption application is applied in reverse, and the message is sent to the MA point with T scrambling in its third form. At the MA point, first the T hashing algorithm and then the reverse MA encryption algorithm are applied and the original message is reached without data loss.

Table 1: MA_T Shelling Algorithm 01

Order of process	T Point	State of Data	MA Point
1	The user writes the message to be sent.	Raw Data	-
2	T Password is done.	T Encrypted Data	-
3	T Hashing is done.	T Encrypted and T Scrambled Data (FIRST STATE)	-
4	Data is sent from T Point.	FIRST STATE	Data is taken from T Point.
5	-	FIRST STATE	T Hashing is applied in reverse.
6	-	T Encrypted and MA Encrypted Data	MA Encryption is done.
7	-	T Encrypted, MA Encrypted and MA Hashed Data (SECOND STATE)	MA Hashing is done.
8	The data is taken from the MA Point.	SECOND STATE	Data is sent to T Point.
10	MA Hashing is applied in reverse.	T Encrypted and MA Encrypted Data	-
11	T Encryption is applied in reverse	MA Encrypted Data	-
12	T Hashing is done.	MA Encrypted and T Hashed Data (THIRD STATE)	-
13	Data is sent from T Point.	THIRD STATE	Data is taken from T Point.
14	-	THIRD STATE	T Hashing is applied in reverse.
15	-	MA Encrypted Data	MA Encryption is decrypted.
16	-	Raw Data	The user sees the message which is sent

The table shows that assuming the first author has input T, the raw message has been sent and will display the MA news; but this is not required. The first message can also be sent from the MA. Such a preference is assumed to be MA and T is shelled.

4 MA_T Chat Softwareı

The program prepared using the Python programming language establishes the connection between the T point and the MA point with the TCP/IP Reference Model on the Internet using Microsoft Windows Socket (WinSock). After the connection is established, a secure correspondence is made with the MA_T shelling system. When the correspondence is completed, the program is closed without any recording (Fig.6).

```
MA_T Güvenli Sohbet Yazılımı
----------------------------
1- Sunucu (T Noktası)
2- İstemci (MA Noktası)
3- Çıkış
Seçiminiz: 2
IP Adresini Giriniz: 144.122.145.154
Yanlış IP Adresi
IP Adresini Giriniz: 144.122.145.153
Port Numarasını Giriniz: 80
Port Numarası başka bir servis tarafından kullanılıyor.
Port Numarasını Giriniz: 8080
Sunucu bekleniyor. Bağlantı kuruluyor.
Bağlantı Sağlandı.
T Noktası: Merhaba
Merhaba
T Noktası: Bu bir test mesajıdır.
O halde test mesajı bana başarılı bir şekilde ulaştı :)
T Noktası: Tamamdır. Kapatalım.
Tamamdır.
<!exit!>
MA_T Güvenli Sohbet Yazılımı
----------------------------
1- Sunucu (T Noktası)
2- İstemci (MA Noktası)
3- Çıkış
Seçiminiz: 3
Güvenli bağlantı sonlandırılmıştır.
```

Fig. 6: Screenshot 05 – Example of running MA_T Chat Software as a client

```
MA_T Güvenli Sohbet Yazılımı
----------------------------
1- Sunucu (T Noktası)
2- İstemci (MA Noktası)
3- Çıkış
Seçiminiz: 1
IP Adresiniz: 144.122.145.153
Port Numarasını Giriniz: 80
Port Numarası başka bir servis tarafından kullanılıyor.
Port Numarasını Giriniz: 8080
8080 portu dinleniyor. İstemci bekleniyor.
Bağlantı Sağlandı.
Merhaba
MA Noktası: Merhaba
Bu bir test mesajıdır.
MA Noktası: O halde test mesajı bana başarılı bir şekilde ulaştı :)
Tamamdır. Kapatalım.
MA Noktası: Tamamdır.
MA Noktası bağlantıyı sonlandırdı!
MA_T Güvenli Sohbet Yazılımı
----------------------------
1- Sunucu (T Noktası)
2- İstemci (MA Noktası)
3- Çıkış
Seçiminiz: 3
Güvenli bağlantı sonlandırılmıştır.
```

Fig. 7: Screenshot 06 – Example of running MA_T Chat Software as a server

MA_T Chat Software can communicate between T point and MA point with known IP and Port number. With this type of connection, the software neither records the connection nor the entries. If there is no active listening on the network (sniffing) or the keyboard listening system (keylogger) software is not running on the computer, the encrypted messages of the MA_T Chat software cannot be accessed.

Table 2: MA_T Chat Software Client Tests

Tests to be made	Variable	Explanation
Connection Test	IP Adress	Entering Wrong IP Address (For example, merhaba.122.153.tr)
Connection Test	IP Adress	Entering an unused IP Address
Connection Test	IP Adress	Entering the IP Address of the server that does not accept external connections
Connection Test	IP Adress	Entering the IP Address of the server accepting external connection
Connection Test	Port	Entering a port that is not open on the server
Connection Test	Port	Entering a port where a different service/service is running on the server (conflict)
Connection Test	Port	Entering an open and unused port on the server
Connection Test	Port	Entering the port opened for the MA_T Chat software on the server
Connection Test	Network Card	Entering the IP Address of the server that accepts external connection when the network card is disabled
Connection Test	Network Card	Entering the IP Address of the server that accepts external connections when the network card is active

Connection Test	MODEM	Entering the IP Address of the server that accepts external connection when the MODEM is turned off and the network card is active
Connection Test	MODEM	Entering the IP Address of the server that accepts external connection when the MODEM is on and the network card is active
Connection Test	Phone Line	Entering the IP Address of the server that accepts external connection when the telephone line is disconnected but the MODEM and Network card are active
Connection Test	Phone Line	Entering the IP Address of the server that accepts external connection when the telephone line is open but MODEM and Network card are active
Connection Test	Disconnection	Disabling the client computer's network card during correspondence
Connection Test	Disconnection	Disabling the network card of the server computer during correspondence
Message Test	Message	Entering only uppercase letters as a message
Message Test	Message	Entering only lowercase text as a message
Message Test Message Test	Message Message	Entering a text consisting of numbers only as a message Entering only special characters (such as space, period, comma, root sign) as a message
Message Test	Message	Entering mixed-character text (24-4) as a message
Message Test	System Message	Entering a message containing the <!exit!> phrase (at the beginning, middle, or end of the phrase)
Message Test	System Message	Entering the <!exit!> block

Table 3: MA_T Chat Software Server Tests

Tests to be made	Variable	Explanation
Connection Test	IP Adress	Can't get IP Address
Connection Test	Port	Entering a port that is not open on the server
Connection Test	Port	Entering a port where a different service/service is running on the server (conflict)
Connection Test	Port	Entering an open and unused port on the server
Connection Test	Handshake	Client not sending request from long listening port
Connection Test	Network Card	Server's IP Address request with network card disabled
Connection Test	MODEM	Server's IP Address request when MODEM is off and Network card is active
Connection Test	MODEM	Server's IP Address request when MODEM is on and Network card is active
Connection Test	Phone Line	Server's IP Address request with phone line down but MODEM and Network card active
Connection Test	Phone Line	Server's IP Address request when phone line is on but MODEM and Network card are active
Connection Test	Disconnection	Disabling the client computer's network card during correspondence
Connection Test	Discconection	Disabling the network card of the server computer during correspondence
Message Test	Message	Entering only uppercase letters as a message
Message Test	Message	Entering only lowercase text as a message
Message Test	Message	Entering a text consisting of numbers only as a message
Message Test	Message	Entering only special characters (such as space, period, comma, root sign) as a message
Message Test	Message	Entering mixed-character text (2^4-4) as a message
	Message	beginning, middle, or end of the phrase)
Message Test	System Message	Entering the <!exit!> block

Table 4: MA_T Chat Software Algorithm Tests

Yapılacak Testler	Değişken	Açıklama
Encryption Test	T Encryption	Checking whether messages containing characters that can be entered with the keyboard in the ASCII Table can be encrypted
Encryption Test	T Encryption	Checking the reversal of generated ciphertexts without data loss
Encryption Test	MA Encryption	Checking whether messages containing characters that can be entered with the keyboard in the ASCII Table can be encrypted
Encryption Test	MA Encryption	Checking the reversal of generated ciphertexts without data loss
Encryption Test	T ve MA Encryption	Checking the reversal of generated ciphertexts without data loss
Hashing Test	T Hashing	Checking whether messages containing keyboard-enterable characters in the ASCII Table can be shuffled
Hashing Test	T Hashing	Checking the rendering of generated hashed texts without data loss
Hashing Test	MA Hashing	Checking whether messages containing keyboard-enterable characters in the ASCII Table can be shuffled
Hashing Test	MA Hashing	Checking the rendering of generated hashed texts without data loss
Shelling Test	Whole Shelling System	Checking that messages containing characters that can be entered with the keyboard in the ASCII Table are shelled and decoded without data loss
Complexity Test	Big Data	Testing algorithm performance
Complexity Test	Prime Numbers	Comparison of the standard method and the Sieve of Eratosthenes method
Complexity Test	Fibonacci	Comparison of the standard method and the Binet method
Strenght Test	Cryptanalysis	Testing the strength of the algorithm

Table 5: Project Deed-Date Schedule

MONTHS											
Deed	March	April	May	June	July	August	Septemb	October	Novemb	Decemb	January
Programming Tutorials	X	X	X	X							
Literature Review			X	X	X	X					
Programming of the Software						X	X	X	X		
Performing Software Tests, Recording of Data and Analysis									X	X	
Writing the Project Report											X

5 Results

Table 6: MA_T Chatting Software Client Tests Results (Part 1)

Test Performed	Variable	Result
Connection Test	IP Adress	When IP Addresses that are not between 0.0.0.0 – 255.255.255.255 IP Address block are entered, the software asks to enter the IP Address again. When the entered address is in this block range but an unused IP Address, the software first asked for the port, then tried to establish a connection 3 times, and when it could not establish the connection (pinged), it asked to enter the IP Address again. The same situation occurred in the case of entering a server IP Address that does not accept external connections. In case the IP Address of the server that accepts external connection is entered, port tests are started. If the IP address of any server that accepts external connection is entered, not the server to be connected, it has been determined that the software does not work properly. A different handshake protocol should be developed between the client and the server, other than TCP/IP Protocol.
Connection Test	Port	In case a port that is not open on the server is entered, the client software tried to establish a connection 3 times and when it could not establish the connection (pinged), it asked to enter the IP Address again. It has been determined that the software does result was seen when an open and unused port was entered on the server. A different handshake protocol should be developed between the client and the server, other than TCP/IP Protocol. If the port opened for MA_T Chat software is entered on the server, it has been determined that the software works properly. Network Card tests have been passed.
Connection Test	Web Card	While the network card was disabled, the client software tried to establish a connection 3 times, and when it could not establish the connection (pinged), it asked to enter the IP Address again. Pinging the 127.0.0.1 ip address of the software and getting a response should be checked and the error that there is a problem with the network card should be given to the user. The software has been found to work properly with the network card enabled. MODEM tests were started.

Table 7: MA_T Chatting Software Client Tests Results (Part 2)

Test Performed	Variable	Result
Connection Test	MODEM	While MODEM was turned off, the client software tried to establish a connection 3 times and when it could not establish the connection (pinged), it asked to enter the IP Address again. It has been determined that the software is working properly when MODEM is on. Telephone line tests have been started.
Connection Test	Phone Line	While the phone line was down, the client software tried to establish a connection 3 times, and when it could not establish the connection (pinged), it asked to enter the IP Address again. The software has been found to work properly when the phone line is open. The rupture tests have been passed.
Connection Test	Breaking	When the Internet connection of the client computer or the server computer is lost during correspondence (network card, modem, telephone line or Internet Service Provider), the function that performs a connection test by pinging 3 times a minute in the background detected the disconnection and gave an error message to the user. Message tests have been passed.
Message Test	Message	Text combinations (24) consisting of uppercase letters, lowercase letters, numbers and special characters (such as space, period, comma, root sign) were all transmitted to or received from the server without error and data loss. The system message test has been passed.
Message Test	System Message	The connection is closed when the <!exit!> block is entered. It has been observed that all other messages are transmitted from client to server or from server to client without loss of message data.

Table 8: MA_T Chatting Software Server Test Results (Part 1)

Test Performed	Variables	Result
Connection Test	IP Adress	Server software can obtain IP Address; but when it receives with IP addresses such as 192.168.XXX.XXX, 127.0.0.1 or 10.0.XXX.XXX, it may not be healthy to connect with the client. Since it passed the IP Address acquisition test, these healthy connection failures were examined in other tests. Port tested.
Connection Test	Port	If a port that is not open on the server is entered, the server software activated that port and listened. The same result was seen when an open and unused port was entered on the server. It has been determined that the software does not work properly in case of entering a port (conflict) where a different service/service is running on the server. Handshake tests have been passed.
Connection Test	Hand Shaking	As a result of the client not sending a request from the listening port (while there is a connection) for a long time (3 minutes), the connection was interrupted and an error message was given to the user. It's on to the next test.
Connection Test	Web Card, MODEM, Phone Line	The server software received an ip address when the network card was disabled. It is necessary to write a function that checks whether the received IP Address can be accessed by the client over the Internet. The same situation was found in the MODEM and Telephone Line tests.

Table 9:MA_T Chatting Software Server Test Results (Part 2)

Test Performed	Variable	Result
Connection Test	Breaking	When the client or server computer is disconnected from the Internet during correspondence (network card, modem, telephone line or Internet Service Provider), the function that performs a connection test by pinging 3 times detected the disconnection and gave an error message to the user. Message tests have been passed.
Message Test	Message	Text combinations (24) consisting of uppercase letters, lowercase letters, numbers and special characters (such as space, period, comma, root sign) were all transmitted to or received from the server without error and data loss. The system message test has been passed.
Message Test	System Message	The connection is closed when the <!exit!> block is entered. It has been observed that all other messages are transmitted from client to server or from server to client without loss of message data.

Table 10: MA_T Chatting Software Algorşitm Test Results (Part 2)

Test Performed	Variable	Result
Encyrption Tests	T Encryption	It was able to encrypt messages containing characters that can be entered with the keyboard in the ASCII Table and rejected the encrypted message without data loss.
Encryption Tests	MA Encryption	It was able to encrypt messages containing characters that can be entered with the keyboard in the ASCII Table and rejected the encrypted message without data loss.
Encryption Tests	T and MA Encryptions	It was able to encrypt the messages containing the characters that can be entered with the keyboard in the ASCII Table with T encryption, re-encrypt the encrypted message with MA encryption, decrypt the encrypted message with T encryption, decrypt the decrypted message with MA encryption without data loss and reach the message.
Hashing Tests	T Hashing	It was able to scramble messages containing characters that can be entered with the keyboard in the ASCII Table and rejected the scrambled message without data loss.
Hashing Tests	MA Hashing	It was able to scramble messages containing characters that can be entered with the keyboard in the ASCII Table and rejected the scrambled message without data loss.

Table 11: MA_T Chatting Software Algoritm Test Results (Part 2)

Test Performed	Variable	Result
Shelling Test	All Shelling System	It was able to decode the messages containing the characters that can be entered with the keyboard in the ASCII Table, by starting to shell from the T point without losing data at the MA point.
Complexity Test	Big Data	
Complexity Test	Prime Numbera	It was able to decode the messages containing the characters that can be entered with the keyboard in the ASCII Table, by starting the shelling from the MA point, without losing data at the T point.
Complexity	Fibonacci	While the encryption and hashing algorithms calculate the prime numbers with O(nloglogn) in the first processing while processing big data, they calculate the Fibonacci series with O(1). Since it uses numbers calculated in the second time, it performs operations with O(1) complexity.
Strenght Test	Cryptanalysis	While the O(n2) complexity problem was solved with the standard method, the O(nloglogn) complexity prime numbers were calculated with the Eratosthenes Sieve method.

6 Discussions

It has been determined that our MA_T Chat software does not work properly. It is foreseen that these problems can be solved by developing a different handshake protocol between client and server computers other than TCP/IP Protocol.

It has been determined that our MA_T Chat software does not work properly in cases where the server computer receives an IP address that cannot be reached over the Internet in the connection to be made from the server to the client, or a service/service is selected for the connection (conflict). It is envisaged that these problems can be eliminated by adding a function that checks port conflict and a function that checks whether the IP address can be accessed over the Internet or not.

In that case, it has been proved in the current tests that our MA_T Chat software prepared with Python Programming Language, apart from the connection problems between the server and the client, can safely communicate between two points with the encryption and hashing algorithms and the shelling system over the TCP/IP Reference Model without any data loss. We can say it does.

In addition, the production of prime numbers by utilizing the Sieve of Eratosthenes used during encryption O(nloglogn) and the production of the terms of the Fibonacci series with the Binet formula is O(1), and the stored and reused numbers of the produced numbers are O(1) complexity.

It has been observed that encryption and scrolling at the character level affects the complexity of the operation as much as the number of characters. In that case, it can be said that the encrusted system is O(n) complexity.

If MA_T Chat software used only Caesar encryption, the key would be detected and the communication could be decrypted due to the matching of domain and image set in frequency analysis tests. As a result of using T and MA mixing and encryption algorithms with shelling in the current version of MA_T Chat software, it has been observed that the mapping of Domain and Image Set could not be detected in frequency analysis. The software then allowed secure correspondence.

7 Suggestions

Research on generating a handshake protocol such as password (Moon) – sign (star) between client and server can improve the server – client connection of MA_T Chat software. Doing research on checking port conflicts and checking whether the IP address is reachable over the Internet can improve the server-client connection of MA_T Chat software.

Apart from frequency analysis, the degree of security of MA_T Chat software can be examined with different password cracking (cryptanalysis) studies.

Apart from correspondence, research can be made on how to increase the functions of the MA_T Chat software by researching on the sharing of picture, video and audio files between T and MA points.

A new interface can be designed for the MA_T Chat software and compared with the existing interface, and the usability of these interfaces by various target groups can be investigated.

References

[1] Savunma Sanayii Güvenliği Yönetmeliği (2010). T.C. Resmi Gazete (27601, 4 Haziran 2010).

[2] Dooley, J. F. (2018). History of cryptography and cryptanalysis: Codes, Ciphers, and their algorithms. Springer.

[3] Musiani, F., & Ermoshina, K. (2017). What is a good secure messaging tool? The EFF secure messaging scorecard and the shaping of digital (usable) security. Westminster Papers in Communication and Culture, 12(3).

[4] Carroll, J. M., & Martin, S. (1986). The automated cryptanalysis of substitution ciphers. Cryptologia, 10(4), 193-209.

[5] Tiwari, G., Nandi, D., & Mishra, M. (2013). Cryptography and Cryptanalysis: A Review. International Journal of Engineering Research & Technology, 2(10), 1898-1902.

[6] Kaur, M., & Kaur, G. (2014). Review of various steganalysis techniques. International journal of computer science and information technologies, 5(2), 1744-1747.
Safitri, C., Ali, H. S., & Ibrahim, J. B. A Study: Cryptology Techniques and Methodologies.

[7] Agrawal, M., & Mishra, P. (2012). A comparative survey on symmetric key encryption techniques. International Journal on Computer Science and Engineering, 4(5), 877.

[8] Ermoshina, K., Musiani, F., & Halpin, H. (2016, September). End-to-end encrypted messaging protocols: An overview. In International Conference on Internet Science (pp. 244-254). Springer, Cham.

[9] Yılmaz, M., Ballı, S. (2016). VERİ ŞİFRELEME ALGORİTMALARININ KULLANIMI İÇİN AKILLI BİR SEÇİM

SİSTEMİ GELİŞTİRİLMESİ. Uluslararası Bilgi Güvenliği Mühendisliği Dergisi, 2 (2) , 18-28.

[10] Chakraborty, M., Jana, B., Mandal, T., & Kule, M. (2018, July). An Performance Analysis of RSA Scheme Using Artificial Neural Network. In 2018 9th International Conference on Computing, Communication and Networking Technologies (ICCCNT) (pp. 1-5). IEEE.

[11] Rathod, U., Sreenivas, S., & Chandavarkar, B. R. (2021). Comparative Study Between RSA Algorithm and Its Variants: Inception to Date. In ICCCE 2020 (pp. 139-149). Springer, Singapore.

[12] Banerjee, K., Mandal, S. N., & Das, S. K. (2020). A Comparative Study of Different Techniques for Prime Testing in Implementation of RSA. American Journal of Advanced Computing, 1(1), 1-7.

Investigation of the Effects of Wall Paint and Films Produced Using Aloe Vera Gel in Radiation Protection

Yusuf Alper Dirak, Sena Ozcan, ADEN COLLEGE , Tekirdag/Turkey , yusufalperdirak@gmail.com , senacanayer@hotmail.com

ARTICLE INFO

Gold Medalist in IMSEF 2021 Izmir, Turkey, and participants in ISAC Olympiad 2021, Tehran, Iran
Advisor: Dr. Gülsemin Savaş Tuna
Accepted by Ariaian Young Innovative Minds Institute,AYIMI

http://www.ayimi.org , info@ayimi.org

ABSTRACT

Emission or transmission of energy in the form of electromagnetic waves or particles is called radiation. Besides natural radiation, people are also intertwined with electromagnetic waves due to the development of technology. In this study; It is aimed to investigate the effect of Aloe vera in the protection of ionizing and non-ionizing radiation by producing wall paints and films containing aloe vera gel. The plants, in the form of seedlings, were multiplied and the gel was obtained when the leaves got matured. Gel was used to produce wall paint and film.

Key words: *Aloe vera, Wall Paint, Film, Ionizing and Non-Ionizing Radiation*

1 Introduction

The emission of energy in space in the form of waves or particles is called "radiation". Radiation is classified as ionizing and non-ionizing radiation (Bor, 2015). The ionizing radiation is the radiation that forms ion pairs by removing electrons from the orbits of the atom it encounters. The ionizing radiation is divided into two; Particle-type radiation: They are very fast-moving particles with specific mass and energy. Alpha (α) and beta (β+, β-) radiations can be given as examples. Wave-type radiation: It is a type of radiation that has a certain energy but is massless. This group contains X and gamma (γ) rays. Non-ionizing radiation is radiation that does not form ions in the substance it interacts with. Radio waves, microwaves, red and ultraviolet light, and visible light are examples of this type of radiation (Ince, 2002; Togay, 2002). All living beings are exposed to ionizing radiation from natural sources and this is an indispensable feature of the natural life. There are two main so-urces of the natural radiation exposure. These are high-energy cosmic ray particles entering the atmosphere and radioactive nuclei found in the earth's crust. In addition, there is also artificial radiation exposure that is often caused by medical applications. The annual radiation doses, which humans are exposed to, are 0.39 mSv from high-energy cosmic ray partic-les, 0.46 mSv from earth and 0.23 mSv from in-body irradiation. On the other hand, the most common cause of radiation in the world is Radon gas with its annual effective dose of 1.3 mSv (Çimen et al., 2017). Since un-derstanding the presence of radiation is not possible with the sense or-gans, its detection and measurements are made with radiation-sensitive devices (e.g., radiation detector) (Dönmez, 2017). When these radiations exceed certain doses, they cause various ailments instantly or after a pe-riod of time. For example, it has been identified that there are radiation-in-duced increases in breast, thyroid, colon, stomach, ovary, esophagus, bladder, liver, and lymph cancers. Moreover, it is known that radiation ca-uses hereditary disorders, nervous and immune system disorders, cata-ract, hyperparathyroidism, microcephaly, and growth-development and mental retardation (Sugarman et al., 2009). Although radiation sources have negative effects on living beings, they are used for diagnostic and therapeutic purposes in medicine and for beneficial purposes in industry, nuclear reactors, and various research activities. For radiation protection, those, working in this area, often use folding screens, gonadal protectors, lead glasses, lead aprons, gloves, glasses, and neck protectors (Çimen et al., 2017). Studies are also carried out for protection from natural radiation, and dyes, glasses, screen protectors, and films are produced using vario-us metals and chemical materials. The most important problem today is the use of too many chemicals, their recycling, and the pollution and dis-turbances that they cause. For struggling with this problem, by using plants such as aloe vera, natural solutions should be sought and tried.

Aloe vera, which is a member of the liliacea family and also called Aloe barbadensis Miller, has over 275 species in the world (Rahman et al., 2017). Four species of these are used for commercial purposes. It is att-racted to attention that numerous studies related to the plant have been done in many different areas in the world. Studies such as polyamide nanocapsule production (Esmaeili and Ebrahimzadeh, 2015), investigation of its usability as a natural plasticizer (Pandey et al., 2016), creating tissue scaffold by using nanofibers, and producing gel and film by using biomole-cules such as polycaprolactone (PCL), chitosan, and polyvinyl alcohol (PVA) (Rahman et al., 2017) have been carried out. Furthermore, the ef-fect of aloe vera extract on the radiation-induced oxidative stress (Nada et al., 2013) and the effect of it on wounds occurred on skin due to radiation in the radiotherapy process have been investigated (Olsen et al. 2001; Haddad et al., 2013; Ahmadloo et al.,2017; Rao et al., 2017). In our co-untry, the antimicrobial effect of the plant has been studied (Çete et al., 2005) and by adding it into the structure of fishmeal, the effect of it on the growth of fish has been investigated (Yılmaz et al., 2019). By using poly (vinyl alcohol) (PVA), poly (ethylene glycol) (PEG) and PVA + PEG toget-her with Aloe vera, Uslu et al. (2010) produced a nanofiber dressing mate-rial. In this study, it was aimed to investigate the effect of Aloe vera on protecti-on from ionizing and non-ionizing radiation by producing wall paint and film containing Aloe vera gel.

2 Material and Method

2-1 Obtaining Gel from the Aloe Vera Plant

The mature leaves of the plants bought and grown as seedlings were selected and cut; then, the green parts of the leaves were peeled with a knife and the gel part was taken. The samples collected in the plas-tic container were turned into gel by thoroughly broken down with the help of blender and Mixer Producing Dye Containing Aloe Vera Gel While the dye was produced, after 275 ml of water was put into the container where the materials would be mixed, 75 g of rejuvenating liquid, 10 g foam blocker, 90 g natrosol preventing dye collapse, 35 g antibacteri-al protective material preventing dye odor, 50 g antifreeze preventing dye freezing, and 135 g powder filler (omyacarb calcite) were added as auxili-ary materials. Then, they were mixed and cooked at the appropriate tem-perature until it reaches the desired consistency. After the dye cooled, 30 g acrylic glue, 90 g foam blocker, 10 g thinner, and 200 ml water were ad-ded, and it was made ready by mixing for 1 hour. In the second phase of the study, after the dye cooled, instead of 200 ml water, 100 ml water+100 ml Aloe vera gel was added and mixed. The resulting dyes were used to paint the clay-made building bricks, which were the main elements of constructions (Fig. 1).

Fig.1: Preparation of the painted samples

Investigation of Ionizing Radiation Shielding Properties of the Produced Dye In the study, which was conducted at a university's Energy Institute, two methods (gamma and neutron analysis) were used. In the analyses, bricks painted with the produced dyes were used. After the painted bricks were placed in the device, the analysis began and the necessary measu-rements were taken. In the analysis, the neutron count was performed with the Polimaster (PM1401K) device (Fig. 2).

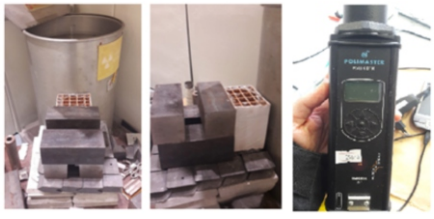

Fig. 2: Neutron analysis with the Polimaster device

Another analysis related to the ionizing radiation, on the other hand, was conducted by using the HpGe detector and performing gamma counting (Fig.3).

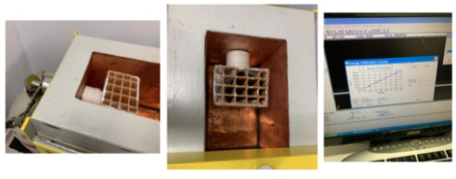

Fig. 3: Gamma counting with the HpGe detector

3 Film Production for Non-Ionizing Radiation Analysis

At this stage, 3 different films that did not contain Aloe vera gel, contained 10% gel and contained 10% gel + nano-silver were produced. First, nano-sil-ver particles were obtained. 20 ml aloe vera gel and 2ml AgNO3 were added to the glass beaker and they were mixed in a magnetic mixer; the examination was per-formed at the spec t rophotometer (380-500nm) every 30 minutes. After being washed with pure water 7 times (5000 rpm, 3 min) by using a centrifuge, it was dried, and measurement was carried out by taking photos with SEM (Fig. 4).

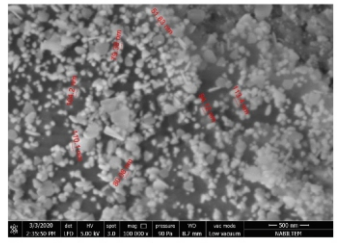

Fig. 4: Silver nanoparticles

To obtain a film that does not contain Aloe vera gel, the glass be-aker containing 190 ml distilled water, 10 ml glycerol and 2 g HEC was placed in a magnetic mixer (500-600 rpm, 2 unit temperature) and mixed for 1.5 hours until the gel consistency was obtained. In the production of the film containing 10% gel, 170 ml distilled water, 20 ml gel, 10 ml glyce-rol, and 2 g HEC were used. In the production of the third film, by setting the quantities, the same method was also followed. The prepared gels were poured into glass containers and placed in a vacuum sterile cabinet for drying After two days, it was determined that the films were dried in the desired level. Then, the films were taken out of the containers and packa-ged (Fig. 5).

Fig. 5: Sample films; A: Gel-free, B: 10% gel, C: 10% gel + silver nano-particle

4 Investigation of Non-Ionizing Radiation Protection/Shielding Proper-ties of the Produced Films

The produced films' protection or shielding effect against the non-ionizing radiation emitted from computers, mobile phones, or internet modems, which we continuously keep in touch, were examined by using the RF-An lyzer (HF 58B-R). To evaluate the result of the films, X (made of Polyester + silver) and Y (made of cotton, polyester, and stainless steel) samples produced by a company working in this field were used for comparison purposes (Fig. 6).

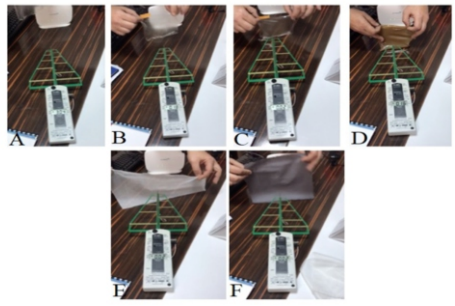

Fig. 6: A: Amount of electromagnetic radiation emitted from the modem, B: Film without Aloe vera gel, C: Film containing 10% Aloe vera gel, D: Film containing 10% Aloe vera gel+silver nanoparticle, E: sample X, F: sample Y

5 Results

The neutron count, in which the protection or shielding effect of the dye samples containing and not containing the produced Aloe vera gel is analyzed, is given in Table (1).

Table 1: Neutron count results

Measure-ment Num-ber	Dye containing Aloe vera gel (Cps)*	Dye without Aloe vera gel (Cps)*
1	250.6	275.3
2	250.3	278
3	250	275.5
4	250.7	275.2
Mean	250.4	276

*Cps: Number of neutrons per second

The results of the gamma count, which is the second analysis of the produced dyes' protection or shielding effect against the ionizing radiation, are given in Table (2). At this stage, in order to get a healthy result, the HpGe detector was first operated as empty 3 times for 10 minutes and the average was taken. Then, when it is empty, when the brick painted by the dye containing Aloe vera gel was placed in it, and when the brick painted by the dye that did not contain Aloe vera gel was placed in it, the detector was operated for 3 hours for each condition and measurements were done (3 hours is accepted as standard). The measurements were repeated 2 times.

Table 2: Gamma count results

	Detec-tor	Sample with dye that do not contain A.v. gel	Sample with dye containing A.v. gel
1st Measure-ment	14100	39667	39754
2nd Measure-ment	13600	37936	38560
Mean	13850	38801.5	39157

In Table (3), the results of the analysis in which 3 different films' non-ionizing radiation protection or radiation shielding effects were examined by using the internet modem found in almost all houses and workplaces are given through comparing them with the standard X and Y samples.

Table 3: Radio frequency analysis results of the produced film and the standard samples

Samples	RF Analyzer (mW/m²)	Shielded amount (mW/m²) and its percentage
Modem	3.04	-
Film that do not contain A.v. gel	0.18	2.86 (%94.07)
Film containing 10% A.v. gel	0.02	3.02 (%99.34)
Film containing 10% A.v. Gel + silver nanoparticle	0.16	2.88 (%94.73)
X	0.02	3.02 (%99.34)
Y	0.02	3.02 (%99.34)

* The shielded amount was calculated according to the difference between the modem and the samples.
* mW/m²: Milliwatt/square meter

6 Discussion and Conclusions

There is a view that is known and practiced in most places in our country: "If plants such as cactus and aloe vera are placed next to the computer, the person will not be affected by the radiation emitted". Is it true or not? Although we do not know a clear answer, these views arouse curiosity in people and lead to many scientific studies. In this study, it was aimed to produce wall paint and film by using Aloe vera gel and to investi-gate the effect of aloe vera in protection/shielding from ionizing and non-ionizing radiation by doing various analyses with these materials. In the investigation of the plant's usability in the protection from ion-izing radiation, two different analyses were performed. Based on the re-sults of the neutron count analysis conducted with the Polimaster device (Table 1), it was determined that while the neutron count of the brick paint-ed with dye containing Aloe vera gel was 250.4 Cps, the neutron count of the brick painted with gel-free dye was 276 Cps on average. There are natural sources of radiation in the structure of the brick too. However, it is clearly seen that there is no significant difference between the dye with aloe vera gel and the dye without gel in terms of neutron permeability; the neutron absorption property of the gel is quite low. Therefore, aloe vera gel can be used as material in studies requiring neutron permeability. When Table 2 in which gamma count results are presented was examined, it was determined that the gamma value was 13850 for HPG detector where the analysis is conducted, 38803.5 on average for the brick painted with the dye that did not contain the plant gel, and 39157 on average for the brick painted with the dye containing gel. If the analyzed samples had a protec-tive effect against the ionizing radiation, the value of the brick painted with the dye containing the gel should have been less than the sample painted with the dye that did not contain the gel. When the experts in the field were consulted, they stated that the fact that this value was found in the 35000s may be sufficient to explain that it showed a positive effect. In the results of the two analyses conducted, it should not be overlooked that the brick is rich in radiation factors such as thorium and uranium which it obtained from nature. If the dye produced by adding gel is tried only on cement or different materials used in building construction, different results can be obtained. When studies related to Aloe vera and radiation are examined, it is seen that studies are mostly done on the ailments caused by radiother-apy. While in some sources, it is stated that the plant is effective in wounds caused by ionizing radiation during the radiotherapy process (Olsen et al. 2001; Haddad et al., 2013; Rao et al., 2017), in some other sources, on the other hand, it is explained that it is not effective in prevention and heal-ing of these wounds (Ünlü et al., 2016; Ahmadloo et al., 2017). In their ex-periments conducted on rats, Nada et al (2013) reported that aloe vera ex-tract created a protective effect against the radiation-induced oxidative stress. Apart from method and techniques, the differences in the results may be due to the fact that the quality of the aloe vera gel varies depend-ing on its species type, growth conditions (e.g., climate, water, fertilization), harvest, extraction method, and ambient conditions (tempera-ture, sterilization) (Rahman et al., 2017). It is known that the techniques of protecting and shielding people from the electromagnetic radiation (non-ionizing radiation) emitted by the technological products that we use very often in our daily lives are b coming a need everywhere. In this context, curtains, fabrics, dyes, and glass films are produced and studies are keeping on. In this study, film production by using HEC natural polymer was attempted and non-ionizing radiation-related studies were analyzed using these produced films. In the previous studies, films containing aloe vera gel had been produced. How-ever, in those films, substances such as PCL, PVA, PEG, chitosan, algi-nate, and pectin gelatin were used as polymers (Pereira et al, 2013, 2014; Silva et al., 2013; Anjum et al., 2016; Rahman etal., 2016; Tummalapalli et

al, 2016) and films were tested in health or tissue engineering studies. When the results of 3 different gels produced for non-ionizing radiation tri-als were examined by comparing them with the standard samples (X and Y) (Table 3), the fact that the radiation shielding property of all samples was determined to be around 99% and the fact that with 99.34% shielding rate, the film containing 10% aloe vera gel was at the same value with the standard samples attract attention. It was observed that silver nanoparticles did not increase the gel effect, but rather inhibited somewhat. In terms of standard samples, X was produced from polyester and silver, while Y was produced from cotton, polyester, and stainless steel; both of them were products available commercially. These products are usually pro-duced in Germany, Italy, and Switzerland, and their prices per square me-ter vary between 75-175 Euros. X is produced in our country and sold for 75 euros per square meter. Taking into account the data obtained, it can be said that metals can be protected from non-ionizing radiation through producing natural products, which are cheaper and do not cause environ-mental pollution (because they are recyclable), by using plants (without using various chemicals). In the conducted literature review, studies on non-ionizing radiation were not be encountered much. In their study, Sheikh et al (2013) reported that aloe vera leaves showed a significant increase in current with a slight increase in voltage at first when they exposed to microwave, but then set themselves to their normal value. Studies support each other. As a result of the study, it was determined that the dye produced by adding aloe vera gel was not effective in protection against ionizing radiation since its ion absorption property is low. The absorption property can be increased by adding some different metals to the gel. It was determined that the shielding property of the film, produced by adding Aloe vera gel, against non-ionizing radiation was equivalent to the standards. It is thought that by developing these data, cheap, natural and recyclable glass film, tulle, and fabric can be produced.

References

[1] Ahmadloo, N., Kadkhodaei, B., Omidvari, S., Mosalaei, A., Ansari, M., Nasrollahi, H., Hamedi, S.H., & Mohammadianpanah, M., (2017). Lack of Prophylactic Effects of Aloe Vera Gel on Radiation Induced Dermatitis in Breast Cancer Patients. Asian Pacific Jour-nal of Cancer Prevention, 18, 1139-1143.

[2] Anjum, S., Gupta, A., Sharma, D., Gautam, D., Bhan, Si, Sharma, A,; Kapil, A.,& Gupta, B., (2016). Development of novel wound care systems based on nanosilver nanohydrogels of polymethacrylic acid with aloe vera and curcumin. Mater. Sci. Eng. C , 64, 157– 166.

[3] Bor D. (2015). Radyasyon Nedir? 2015. Çete, S., Arslan, F., & Yaşar, A., (2005). Investigation Of Antimicrobial Ef-fects Against Some Microorganisms Of Aloe Vera And Nerium Oleander Also Examination Of The Effects On The Xanthine Oxi-dase Activity In Liver Tissue Treated With Cyclosporin. G.U. Jour-nal of Science, 18, 375-380.

[4] Çimen, B., Erdoğan, M, & Oğul, R., (2017). İyonlaştırıcı Radyasyon ve Ko-runma Yöntemleri . Selçuk Üniversitesi Fen fakültesi Fen Dergisi, 43 ,139-147

[5] Dönmez, S., (2017). Radyasyon Tespiti ve Ölçümü. Nucl Med Semin, 3,172-177

[6] Esmaeili, A., & Ebrahimzadeh, M., (2015). Preparation of Polyamide Nanocapsules of Aloe vera L. Delivery with In Vivo Studies. AAPS PharmSciTech, 16, 51-63.

[7] Haddad, P., Amouzgar–Hashemi, F., Samsami, S., Chinichian, S., & Oghabian, M.A.,(2013). Aloe vera for prevention of radiation-in-duced dermatitis: a self-controlled clinical trial. Curr Oncol, 20, 345-348.

[8] İnce MZ., (2002). Tanısal Radyolojide Radasyondan Korunma, Türkiye Atom Enerjisi Kurumu Yayınları, 2, 34.

[9] Nada, A.S, Hawas, A.M., . Abd Elmageed, Z.Y., &Amin, N.E., (2013). Pro-tective value of Aloe vera extract against g-irradiation induced some biochemical disorders in rats. Journal of Ra diation Re-search and Applied Sciences, 6, 31-37.

[10] Olsen, DL, Raub W Jr, Bradley C, Johnson M, Macias JL,& Love V, Markoe A., (2001). The effect of aloe vera gel/mild soap versus mild soap alone in preventing skin reactions in patients undergo-ing radiation therapy. Oncol Nurs Forum, 28,543-7.

[11] Pandey,K., Asthana, N., Sanjay, S.S., & Dwivedi, M.M., (2016). Study of Aloe Vera as a Natural Plasticizer in PEO based Polymeric Elec-trolyte. European Journal of Advances in Engineering and Technol-ogy, 3, 21-25

[12] Pereira, G.G., Guterres, S.S., Balducci, A.G., Colombo,P., &Sonvico, F., (2014). Polymeric Films Loaded with Vitamin E and Aloe vera for Topical Application in the Treatment of Burn Wounds. BioMed Re-search International, 1, 1-9.

[13] Pereira, R., Mendes, A., & Bártolo, P., (2013). Alginate/Aloe vera hydrogel films for biomedical applications. Procedia CIRP, 5, 210 – 215.

[14] Rahman, S., Carter,P., & Bhattarai, N., (2017). Aloe Vera for Tissue Engi-neering Applications. J. Funct. Biomater, 1-17

[15] Rahman, S.M., Mahoney, C., Sankar, J., Marra, K.G., & Bhattarai, N., (2016). Synthesis and characterization of magnesium gluconate contained poly (lactic-co-glycolic acid)/chitosan microspheres. Mater. Sci. Eng. B , 203, 59–66.

[16] Rao, S., Hegde, S.K., Baliga-Rao, M.P., Palatty, P.S., George, T., & Bali-ga, M.S., (2017). An Aloe Vera-Based Cosmeceutical Cream De-lays and Mitigates Ionizing Radiation-Induced Dermatitis in Head and Neck Cancer Patients Undergoing Curative Radiotherapy: A Clinical Study. Medicines, 4, 44- 52.

[17] Sheikh, F.A., Singh, R.P.P, Singh,J.B., & Lehana, P., (2013). Effect Of Mi-crowaves On The Resistance Of Aloe Vera Leaves. International Journal of Engineering Research and Applications, 3(4): 242-247

[18] Silva, S.S., Caridade, S.G., Mano, J.F., & Reis, R.L., (2013). Effect of crosslinking in chitosan/aloe vera-based membranes for bio-medical applications. Carbohydr. Polym, 98, 581–588.

[19] Sugarman, S.L., Goans, R.E., Garrett, S.A., & Livingsto,n G.K.,(2009). Delayed Effects. In: The Medical Aspects of Radiation Incidents, REAC/ TS. Oak Ridge, US. p. 44-46.

[20] Togay, Y.E., (2002). Radyasyon ve Biz, Türkiye Atom Enerjisi Kurumu Yayınları, 2-12.

[21] Tummalapalli, M., Berthet, M., Verrier, B., Deopura, B.L., Alam, M.S., & Gupta, B., (2016). Composite wound dressings of pectin and gelatin with aloe vera and curcumin as bioactive agents. Int. J. Biol. Macromol., 82, 104–113

[22] Uslu, İ., Keskin, S., Gül, A., Karabulut, T.C., &Aksu, M.L., (2010). Prepara-tion and Properties of Electrospun Poly(vinyl alcohol) Blended Hy-brid Polymer with Aloe vera and HPMC as Wound Dress-ing. Hacettepe J. Biol. & Chem., 38, 19-25. Ünlü, A., Nayır, H., Ay, H., Kırca, Ö., &Özdoğan, M., (2016) . Aloe Vera and Cancer. Turk J Oncol, 31, 68-72.

[23] Yılmaz, E., Çoban, D., Kırım, B., & Güler, M., (2019). Effects of Ex-tracts of Feed Additives Including Rosemary (Rosmarinus offici-nalis) and Aloe Vera (Aloe barbadensis) on the Growth Performance and Feed Utility of Nile Tilapia (Oreochromis niloticus). Turkish Journal of Agriculture - Food Sci-ence and Technology, 7,866-870.

Ariaian Young Innovative Minds Institute, AYIMI
Unit 14, No. 32, Malek Ave., Shariati St.
Post Code: 1565843537
Tel - Fax: +9821-77522395, 77507013
Tehran/ Iran
URL: http://www.ayimi.org
http://journal.ayimi.org
Email: info@ayimi.org